Matrix Metalloproteinase Remodelling of the Extracellular Matrix

The Larval Requirement for Matrix Metalloproteinase-Mediated Remodelling of the Cardiac Extracellular Matrix in *Drosophila melanogaster*

By:

Chris Hughes, Honours B.Sc., B.A.

A thesis

Submitted to the School of Graduate Studies

In Partial Fulfilment of the Requirements

For the Degree

Master of Science

McMaster University

McMaster University, Master of Science (2018) Hamilton, Ontario (Biology)

Title: The Larval Requirement for Matrix Metalloproteinase-Mediated Remodelling of the Cardiac Extracellular Matrix in *Drosophila melanogaster*

Author: Chris Hughes, Honours B.Sc., Concordia University and B.A., McGill University

Supervisor: J. Roger Jacobs, Ph.D., Professor, McMaster University

Number of Pages: xiii, 180

Lay Abstract

The fruit fly (*Drosophila*) heart undergoes significant changes in organisation and size throughout development and growth. The heart is surrounded and supported by a network of extracellular matrix (ECM) proteins, which is regulated by proteases, including matrix metalloproteinases (MMPs). Previous research has shown that MMPs are required for normal heart formation. I demonstrate that a reduction in MMP activity during embryonic development results in larval heart defects and an increase in the disorganisation of ECM proteins around the heart, whereas reduction during larval development results in less pronounced protein mislocalisation. These findings are corroborated via over-expression of an MMP inhibitor.

Abstract

The *Drosophila* heart is a tubular vessel surrounded by a dynamic scaffold of extracellular matrix (ECM) proteins. Heart development and function rely upon protease-mediated remodelling and turnover of the ECM, and changes in ECM composition correlate with age and cardiac disease. Previous research has shown that a family of proteases called matrix metalloproteinases (MMPs), and their inhibitors (TIMPs), are necessary for normal cardiac cell migration and lumenogenesis. The *Drosophila* heart expands considerably throughout growth, but the role of MMP activity has not been elucidated at this time. I examine the role of the two *Drosophila* MMPs, MMP1 and MMP2, as well as TIMP, in defining larval heart structure and ECM protein distribution. I observe heart phenotypes via immunofluorescence labelling and confocal microscopy using loss-of-function mutants, gene over-expression, and gene knock-down techniques. Reduced MMP1 function during embryogenesis correlates with myofibrillar disorganisation, whereas reduced MMP2 function or TIMP over-expression both result in cardia bifida as well as increased density and ectopic localisation of Collagen-IV and Pericardin. Post-embryonic MMP reduction compromises cardiac structural integrity but does not affect Pericardin localisation. Live imaging of the larval heart with optical coherence tomography (OCT) and light microscopy reveals that reduced MMP2 function correlates with decreased heart rate but not impaired dilation or contraction. These data suggest that MMP2 activity during embryogenesis is critical for larval heart development.

In contrast, post-embryonic protease function appears to have a less pronounced effect on ECM protein distribution throughout larval development.

Acknowledgements

I wish to extend my heartfelt gratitude to Dr. Roger Jacobs. In your role as a supervisor and mentor you have shown me encouragement and patience. You have taught me a great deal, not least the importance of keeping perspective of the whole amidst the noise of the details (a lesson perhaps one day I'll have successfully taken to heart).

I would also like to express thanks to Dr. Ana Campos. You have always provided sage advice and indispensable feedback during our meetings, pressing me to think critically and communicate precisely.

Thank you also Dr. Ian Dworkin for all you have taught me about *Drosophila* genetics and maintenance, and for agreeing to chair this defense.

Finally, I want to express my appreciation for the knowledge and friendship provided by all the members of the Jacobs lab, past and present. To Dr. Qanber Raza, thank you for teaching me so many things that proved indispensable in my research. To Duygu and Meryl, thank you for being my role models in the lab, for training me in that ancient art of Fly Pushing, and for your unfailing support and friendship. To Rachel, thank you for your valuable edits (and colourful commentary). To Hasan and Balpreet, thank you for taking care of my flies. To Heather, Mahan, Pouya, Ana, Aaron, and Sam, thank you for all your help, and for providing me with such fond memories of my time at McMaster.

Table of Contents

List of Figures

Abbreviations and Symbols

+	Wildtype chromosome
βPS	βPS1-Integrin
µm	Micron (micrometre)
µl	Microlitre
A7	Abdominal segment 7
ADAM	A disintegrin and metalloproteinase
ADAMTS	ADAM with a thrombospondin motif
CB	Cardioblast
Cg25C	Collagen at 25C
CM	Cardiomyocyte
da	Daughterless
DV	Dorsal vessel
ECM	Extracellular matrix
GFP	Green fluorescent protein
MMP	Matrix metalloproteinase
PBS	Phosphate Buffered Saline
PBT	PSB + 0 .3% Triton
PC	Pericardial cell
ROI	Region of interest
Prc	Pericardin
RECK	Reversion-inducing cysteine-rich protein with Kazal motifs
RFP	Red fluorescent protein
SEM	Standard error of the mean
TIMP	Tissue inhibitor of metalloproteinases
UAS	Upstream activation sequence
Vkg	Viking (Collagen-IV gene)
WT	Wildtype

1.0 Introduction:

My thesis examines cardiac extracellular matrix (ECM) remodelling during *Drosophila* larval development, throughout which significant heart growth occurs. Remodelling is defined in this thesis as the process of synthesis, deposition, and breakdown of ECM constituents, whose net effect is turnover (Stamenkovic 2003). Critically, ECM remodelling need not relate specifically to morphogenesis, as it is also considered a function of tissue homeostasis and growth (Streuli 1999).

Of specific interest is the role of matrix metalloproteinases (MMPs) and their inhibitors in mediating these events. Studies involving various model organisms show that changes in cardiac ECM composition occur naturally with age, and that the disruption of ECM homeostasis is correlated with multiple diseases states (Biernacka and Frangogiannis 2011; Bonnans *et al.* 2014). Recent headway has been made in elucidating the requirement of MMPs for embryonic heart development in *Drosophila* (Raza *et al.* 2017). However, less well-defined in this model system is the function of MMPs during larval development.

My objective in this thesis is to determine the effects of MMP mis-regulation on the structure and functioning of the larval heart, and its impact on the distribution of essential ECM proteins, namely Collagen-IV (Vkg) and Pericardin (Prc). Here the *Drosophila* model provides a distinct advantage, allowing for spatial and temporal control of gene activity, such that I might specifically examine the post-embryonic requirements of *Drosophila* MMPs within and around the cardiac muscle tissue.

The following introductory section provides a primer on the development and morphology of the *Drosophila* dorsal vessel, as well as the ECM and its core components, including relevant receptors and signalling factors. Discussed in detail is the activity of *Drosophila* MMPs and TIMP.

1.1 The dorsal vessel

The *Drosophila* heart, also termed the dorsal vessel (DV), is a linear tube positioned along the dorsal midline. Though not looped or multichambered as is the vertebrate heart, the *Drosophila* dorsal vessel does still resemble its distant cousin during early development, as both are formed of homologous mesodermal precursors and share many conserved transcription factors and signalling pathways. This makes the *Drosophila* heart a useful system for the study of various developmental processes and disease states (Bodmer 1995; Bodmer and Venkatesh 1998). The vessel is composed of cardiomyocytes, which enclose the lumenal space. These are flanked by non-contractile nephrocyte-like pericardial cells (PCs) that act to filter toxins (Weavers *et al.* 2009). Alary muscles attach to the extracellular matrix (ECM) surrounding the PCs, serving to anchor the DV to the epidermis (Fig. 1.1) (Bodmer 1995; Chartier *et al.* 2002). Cardioblast-derived ostial cells form passive in-flow tracts for hemolymph, which is propelled anteriorly by the contracting heart (Molina and Cripps 2001).

During early embryogenesis, the dorsolateral-most mesodermal cells activate cardiac-specific transcription factors, such as Tinman (Tin), upon receiving signals from

Decapentaplegic and Wingless. Subsequently, the lateral ectoderm, accompanied by the Tin-expressing mesodermal cardiac precursors, expands dorsally to displace the amnioserosa (Reim and Frasch 2005; Bryantsev and Cripps 2009; Haack *et al.* 2014; Raza and Jacobs 2016). Post-mitotic cardioblasts migrate independently towards their contralateral partners, assuming a teardrop shape through the extension of motile filaments at the apical domain, which comprises a leading edge, as seen in Fig. 1.2B (Raza and Jacobs 2016). At stage 16, cardioblasts make contact with their contralateral partners at the dorsal midline. The apical domains meet to form a Cadherin-based dorsal seam (junctional domain). The CBs curve to envelop a lumenal space as a second seam is formed ventrally, as in Fig. 1.2C (Tao and Schulz 2007; Hughes and Jacobs 2017).

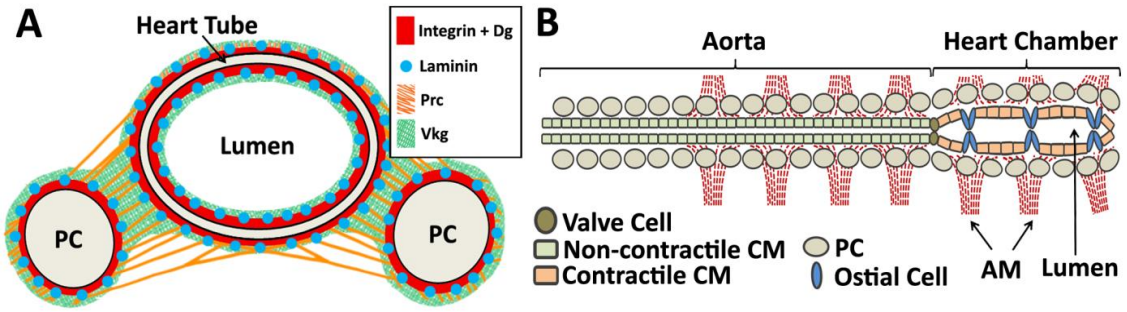

Figure 1.1: Organisation of the larval dorsal vessel. (A) Cross-sectional view of the larval dorsal vessel. The dorsal vessel is flanked by pericardial cells (PCs). Collagen-IV (Vkg) is expressed along the lumenal and ablumenal surfaces of the vessel and envelops the PCs. Pericardin (Prc) is expressed along the ablumenal surface of the vessel and envelops the PCs. βPS1-Integrin is expressed lumenally and ablumenally. **(B)** The dorsal vessel is comprised of an anterior aorta and posterior heart chamber, separated by valve cells. The heart chamber is composed of contractile cardioblasts. The vessel is suspended from the epidermis by seven pairs of alary muscles. Adapted from Hughes and Jacobs (2017) with the authors' permission.

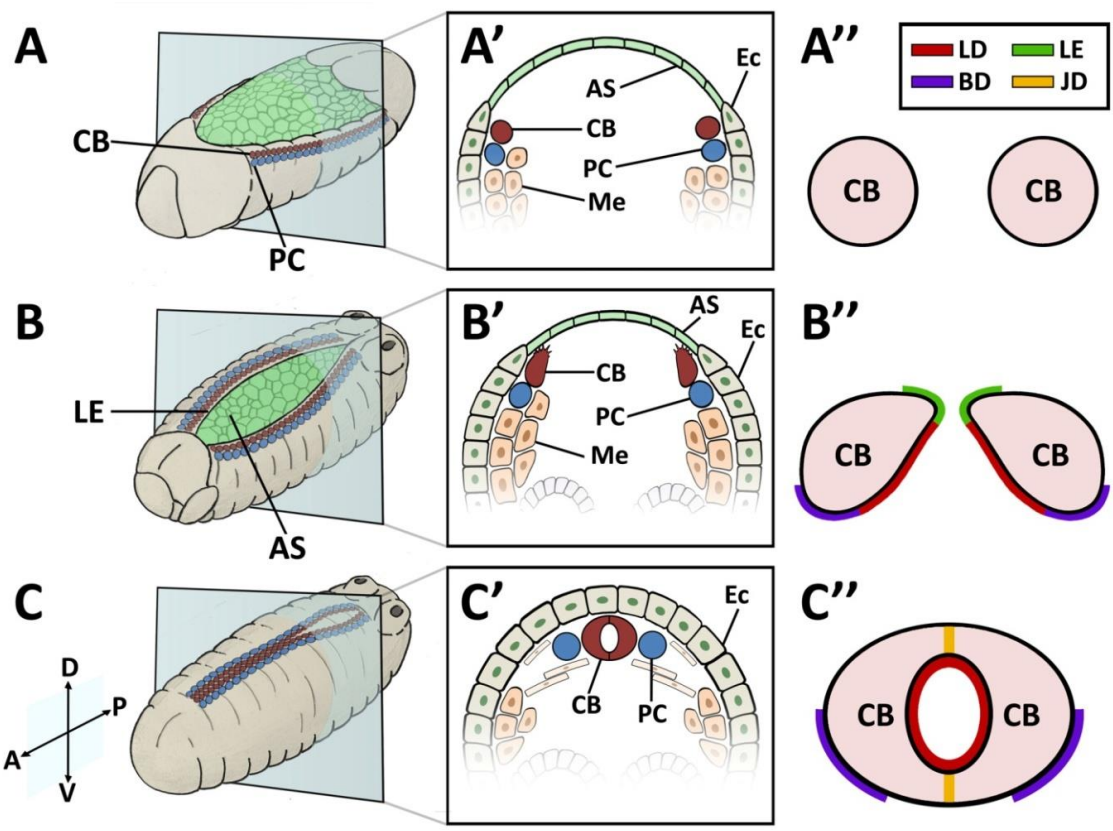

Figure 1.2: Cardioblast migration during embryonic development. (A-A'') Illustration of a stage 12 embryo. Cardioblast and pericardial cell precursors are not yet migratory, and are associated with the ectoderm. **(B-B'')** By stage 14, cardioblasts and pericardial cells have become migratory. Cardioblasts extend filopodia at the apical domain (leading edge). **(C-C'')** At stage 16, cardioblasts fuse with their contralateral partners at the midline. The dorsal junctional domain forms first, and is followed by ventral fusion, resulting in the formation of a singular lumenal space. A: anterior; AS: amnioserosa; BD: basal domain; CB: cardiobalast; D: dorsal; Ec: ectoderm; JD: junctional domain; LE: leading edge; LD: lumenal domain; Me: mesoderm; P: posterior; PC: pericardial cell; V: ventral. Adapted from Hughes and Jacobs (2017) with the authors' permission.

By the end of embryogenesis, and throughout larval development, the dorsal vessel is divided into two regions separated by valve cells: a non-contractile aorta that extends from thoracic segment 2 (T2) to abdominal segment 4 (A4), and a contractile heart chamber comprising segments A5 to A8 (Bodmer 1995). The former is specified by *Ultrabithorax,* and the latter by *abdominal-A* (Lo and Frasch 2003). Seven pairs of alary muscles, positioned along segments A1 through A7, anchor the dorsal vessel to the epidermis (Bataillé *et al.* 2015). Paired lymph glands form along the anterior aorta near the ventral ganglion, derived from mesoderm that would otherwise differentiate into pericardial cells (Rodriguez *et al.* 1996; Shah *et al.* 2011). The dorsal vessel experiences lumenal expansion throughout larval development and is observed to increase in length nearly five-fold between first instar and the end of third instar. This increase in cardiac size is due solely to the physical enlargement of existing cardiomyocytes, rather than cell proliferation (Molina and Cripps 2001; Lehmacher *et al.* 2012; Bogatan *et al.* 2015). In fact, no cardiomyocyte generation or replacement occurs throughout the organism's post-embryonic lifespan in response to damage, or depletion of tissues, suggesting that *Drosophila* lacks cardiac stem cells (Drechsler *et al.* 2013; Bogatan *et al.* 2015). During metamorphosis, those cardiac cells comprising segments A6 through A8 undergo apoptosis, such that only 84 of the initial 104 cardiomyocytes are retained in the adult heart (Sellin *et al.* 2006; Tao and Schulz 2007). Further cell differentiation occurs, resulting in the specification of additional valve and ostial cells (Lehmacher *et al.* 2012). Paired myofibrils are uniformly positioned around the dorsal vessel, and in the adult heart

longitudinal fibres are apparent across the ventral surface of the cardiomyocytes (Bogatan *et al.* 2015). These are lymph gland-derived multinucleated longitudinal muscle fibres, possibly arising from the three anterior-most alary muscle pairs (Shah *et al.* 2011; Bataillé *et al.* 2015). Aortal myocytes also become contractile (Lehmacher *et al.* 2012).

1.2 The extracellular matrix

The extracellular matrix (ECM) is a three-dimensional scaffold composed of fibrillar and non-fibrillar structural proteins and proteoglycans (Frantz *et al.* 2010; Bonnans *et al.* 2014). It is divided into the basement membrane (BM) and the interstitial matrix. The former sheathes tissues and forms cell adhesions, where it acts as a stabilising/protective force and also serves a role in signalling (Yurchenco *et al.* 2012). The BM is composed predominantly of Laminin and Collagen-IV (reviewed in greater detail below). The interstitial matrix inhabits the extracellular expanse between tissues. It is formed primarily of gel-like proteoglycans, fibronectin, and fibroblast-secreted fibrous Collagens, particularly Collagen-I and Collagen-III (Frantz *et al.* 2010; Bonnans *et al.* 2014).

The ECM is not homogenous throughout an organism, and its components and organisation vary between tissues and across time (Frantz *et al.* 2010). The ECM in fact undergoes significant structural and chemical remodelling during morphogenesis. Throughout development, ECM components are broken down by proteases, allowing for the release of growth factors and the removal of impediments to cell migration (Bonnans

et al. 2014). The ECM may also act as a stable attachment site for cells and so promotes proliferation and differentiation, while the formation of dynamic focal adhesion complexes may promote cell migration (Kular *et al.* 2014). Throughout growth and aging there must be tight regulation of ECM protein synthesis, deposition, and degradation, which arises from the interplay of molecular signals, post-translational processing, and enzyme activity (Horn 2015). The mis-regulation of these processes has devastating effects, and is correlated with the development of multiple diseases states including cancer invasion and fibrosis (Medioni and Noselli 2005).

1.2.1 The cardiac ECM

ECM surrounds the dorsal vessel, providing structural support and preventing damage arising from mechanical stresses (Drechsler *et al.* 2013). It is linked to the cytoskeleton by Integrins, which act as pathways for tension signalling (Bogatan *et al.* 2015). The basement membrane of the cardiac ECM is an interface of two major protein networks, Laminin and Collagen-IV, both of which are necessary to promote normal cardiac development (Yarnitzky and Volk 1995; Hollfelder *et al.* 2014; Isabella and Horne-Badovinac 2015; Jia *et al.* 2015).

The cardiac ECM experiences carefully-controlled remodelling and turnover throughout an organism's lifespan. The ECM of adult vertebrates and *Drosophila* has been studied in some depth. Aging is associated with the accumulation, increased deposition, and inter-linking of ECM proteins in vertebrates (Burgess *et al.* 2001; Horn *et al.* 2012; Horn 2015) and *Drosophila* (Sessions *et al.* 2017; Vaughan *et al.* 2017), resulting in a

decline in cardiac function. Perturbations to the make-up of the ECM, and the resultant loss of homeostasis, are correlated with diseases such as myocardial infarction, hypertrophy, and dilated cardiomyopathy (Conrad *et al.* 1995; Nishimura *et al.* 2011; Segura *et al.* 2014; Sessions and Engler 2016). However, less well described is the importance of cardiac ECM remodelling and turnover for *Drosophila* larval development and metamorphosis.

1.2.2 Laminin

Laminin (Lan) is a conserved heterotrimeric glycoprotein involved in cell adhesion and cell migration, and forms the basis of the scaffold upon which the basement membrane is built (Yarnitzky and Volk 1995; Colognato and Yurchenco 2000). Laminins are formed of an α, β, and γ chain, which, in *Drosophila*, are encoded by *LanA/wing-blister, LanB1,* and *LanB2*, respectively (Urbano *et al.* 2009; Hollfelder *et al.* 2014). Key Lan receptors are the cell-adhesion receptors Dystroglycan (Dg) and Integrin (Colognato and Yurchenco 2000). Loss of Lan function is responsible for cardiac defects such as muscle and pericardial cell detachment, reduced lumenal expansion, and breakages along the dorsal vessel resulting from the inability to stabilise Collagens and other critical ECM proteins (Urbano *et al.* 2009; Wolfstetter and Holz 2012; Hollfelder *et al.* 2014).

1.2.3 Collagens and Collagen-like proteins of the basement membrane

Drosophila possesses multiple basement membrane Collagens, namely Collagen-IV, encoded by *viking* (*vkg*) and *Cg25C,* and Collagen-XV/XVIII, encoded by *multiplexin*

(*mp*) (Myllyharju and Kivirikko 2004; Kular *et al.* 2014). An additional Collagen-like protein is encoded by *pericardin* (*prc*) (Myllyharju and Kivirikko 2004).

Multiplexin (Mp; orthologous to vertebrate Collagen-XV/XVIII) is a matricellular protein localised to the cardioblast lumenal domain during migration, where it promotes lumenal expansion within the posterior heart chamber (Harpaz *et al.* 2013; Volk *et al.* 2014). Within this thesis greater consideration is given to Collagen-IV and Pericardin (Prc), as these are more abundant constituents of the matrix (Pastor-Pareja and Xu 2011).

Collagen-IV is a heterotrimeric non-fibrillar protein of the basement membrane, formed from one Vkg and two Cg25C chains (Hollfelder *et al.* 2014). During embryogenesis, hemocytes are responsible for secreting the majority of Collagen-IV, whereas this role is assumed by the fat body during larval development (Bunt *et al.* 2010; Pastor-Pareja and Xu 2011; Cevik 2016). Collagen-IV is localised to the lumenal and ablumenal domains of the dorsal vessel, offering support through its association with the Laminin-Nidogen complex (Martinek *et al.* 2008; Hollfelder *et al.* 2014). It has recently been suggested that Collagen-IV accumulates in aged adult *Drosophila*, likely contributing to cardiac stiffening (Vaughan *et al.* 2017).

Prc is a fibrillar cardiac ECM protein that bears some similarity to mammalian Collagen-IV α-chains and *Drosophila* Vkg, but shows dissimilarities with respect to the Collagen-IV-typical $(Gly\text{-}X\text{-}Y)_n$ repeats and its web-like assembly (Chartier *et al.* 2002; Drechsler *et al.* 2013). Prc is produced by pericardial cells during embryogenesis, and by non-cardiac cells such as adipocytes throughout larval development (Drechsler *et al.*

2013). It is recruited to the cardiac ECM by Lonely Heart (loh), a disintegrin and metalloprotease with thrombospondin repeats (ADAMTS)-like protein homologue. Prc is present at high levels after the fusion of the dorsal ectoderm midline, localising to the basal surface of cardioblasts (Drechsler *et al.* 2013; Raza 2015). It is absent from the lumen of the dorsal vessel (Chartier *et al.* 2002). Prc is up-regulated in the embryo and first and second instar larvae, as well as in pupae throughout metamorphosis. Prc is critical for adhesion between pericardial cells and cardiomyocytes. Deficiency in Prc results in aberrant Actin distribution and pericardial cell detachment, causing separation of the dorsal vessel from the alary muscle (Drechsler *et al.* 2013).

1.2.4 Integrins

Integrins are transmembrane receptors formed of α and β subunits that are involved in cell-cell and cell-matrix adhesion (Hynes 1987). Integrins link the Collagen and Laminin-based ECM to the Actin cytoskeleton. They are necessary for the polarisation of migrating cardioblasts through the establishment of the apical ECM, and for the formation of the lumenal domain, through the assembly of structural proteins such as Laminins, Collagens, and Dystroglycans (Vanderploeg *et al.* 2012).

Drosophila encodes three α subunits (αPS1-3) and two β subunits (βPS1 and βV) (Stark *et al.* 1997). The αPS3βPS1 dimer (henceforth βPS1-Integrin) is expressed in tissues undergoing morphogenesis, including cardioblasts (Stark *et al.* 1997). βPS1-Integrin is highly expressed at the leading edge of migrating CBs in stage 15 embryos. By stage 17, βPS1-Integrin is concentrated at the lumenal domain, and weakly expressed at the basal

domain. Loss-of-function mutations in βPS1-Integrin result in reduced leading edge activity (Vanderploeg *et al.* 2012). β-Integrin expression is elevated in aged flies, and up-regulation is associated with increased myocardial stiffness, reduced diastolic diameter, and arrhythmia (Nishimura *et al.* 2014).

1.2.5 Adhesion molecules and morphogens

E-Cadherin is an adhesion molecule encoded by the *Drosophila* gene *shotgun* (Haag *et al.* 1999). It is involved in lumen formation through its role in midline cardioblast adhesion. Cadherin localisation is mediated by repulsive signalling by the morphogen Slit and its transmembrane receptor Roundabout (Robo) (Santiago-Martínez *et al.* 2008). Slit and Robo localise to the cardioblast pre-lumenal domain. They are involved in specifying cell polarity and are required for normal lumen formation in *Drosophila* through the exclusion of Cadherin from the pre-lumenal domain (Qian *et al.* 2005; Santiago-Martínez *et al.* 2008).

1.3 Metalloproteinases and their inhibitors

Turnover and remodelling of the cardiac ECM is mediated by the activity of several families of proteases, including matrix metalloproteinases (MMPs) and Adamalysins, which together form part of the metzincin protease superfamily (Bonnans *et al.* 2014; Yamamoto *et al.* 2015). The activity of these proteases is regulated in turn by specific inhibitors, including the secreted tissue inhibitors of metalloproteinases (TIMPs) and the

membrane-bound reversion-inducing cysteine-rich protein with Kazal motifs (RECK) (Oh *et al.* 2001; Nagase *et al.* 2006; Srivastava *et al.* 2007; Arpino *et al.* 2015; Horn 2015).

1.3.1 Structure and function

MMPs are zinc-dependent multi-domain endopeptidases involved in tissue repair and wound/immune response, remodelling, and morphogenesis (Llano *et al.* 2000; Nagase *et al.* 2006; Page-McCaw *et al.* 2007). The principal role of MMPs is the breakdown of ECM, allowing for the release of bound growth factors (Nagase *et al.* 2006). MMPs are directly inhibited by TIMPs and RECK (Oh *et al.* 2001; Nagase *et al.* 2006; Srivastava *et al.* 2007; Arpino *et al.* 2015; Horn 2015). MMPs are comprised of a catalytic domain and a hemopexin domain connected by a linker peptide (Llano *et al.* 2000, 2002; Glasheen *et al.* 2009). They are initially produced as zymogens, their activity inhibited by the presence of a pro-domain. These pro-MMPs are activated by cysteine-switch-mediated conformational changes or by proteolytic cleavage (Van Wart and Birkedal-Hansen 1990). MMPs can be generally classified as either secreted or transmembrane, however, in mammals six major categories exist: 1) membrane-type MMPs, 2) collagenases, 3) gelatinases, 4) matrilysins, 5) stromelysins, and 6) 'other' (Visse and Nagase 2003; Sternlicht and Werb 2009). Vertebrate collagenases, gelatinases, and stromelysins digest Collagens, including Collagen-IV (Snoek-van Beurden and Von den Hoff 2005). The activity of MMPs is required for normal cardiac function in vertebrates and for normal cardiogenesis in *Drosophila* (Lemaître and D'Armiento 2006; Hughes and Jacobs 2017; Raza *et al.* 2017).

The Adamalysin family is composed of a disintigrin and metalloproteinase (ADAMs) as well as ADAMs with a thrombospondin motif (ADAMTS) (Bonnans *et al.* 2014). ADAMs are transmembrane glycoproteins with a pro-domain, a disintigrin-like domain, and a metalloprotease domain (Meyer *et al.* 2011). They are involved in the release of membrane-bound proteins. ADAMs such as Kuzbanian and TNF-α-converting enzyme (TACE) are required for cardiogenesis in vertebrates and *Drosophila* (Albrecht *et al.* 2006). ADAMTS, on the other hand, are secreted proteinases that may also serve as pro-collagens (Lockhart *et al.* 2011; Bonnans *et al.* 2014). Like MMPs, ADAMTS are produced as zymogens (Yamamoto *et al.* 2015). The ADAMTS-like protein Lonely Heart is critical for *Drosophila* cardiogenesis (Drechsler *et al.* 2013). As with MMPs, ADAMs and ADAMTS are inhibited by TIMPs (Wei *et al.* 2003).

TIMPs are formed of two domains; a C-terminal domain and an N-terminal inhibitory domain, each with a conserved cysteine sequence, stabilised by disulphide bonds (Wei *et al.* 2003; Brew and Nagase 2010). This inhibitory domain binds the active site of the MMP, chelating the catalytic Zn^{2+} ion and removing the Zn-bound H_2O molecule required for peptide bond hydrolysis (Nagase *et al.* 2006; Brew and Nagase 2010).

RECK is a transmembrane glycoprotein with a Serine protease inhibitor-like domain (Oh *et al.* 2001). It is believed to inhibit auto-proteolysis, thus preventing the complete processing of the active form of the MMP protein.

1.3.2 *Drosophila* MMPs and TIMP

While mammals possess upwards of 20 MMPs and four TIMPs, *Drosophila* encodes two partially-redundant MMPs, MMP1 and MMP2, and a single TIMP that is capable of inhibiting both (Llano *et al.* 2000, 2002; Page-McCaw *et al.* 2003; Nagase *et al.* 2006).

Both *Drosophila* MMPs are capable of hydrolysing components of the ECM such as Collagens, and thus demonstrate some redundancy through their affinity for similar substrates; however, MMP1, unlike MMP2, is unable to cleave Laminin or Gelatin (Llano *et al.* 2000, 2002; Miller *et al.* 2008; LaFever *et al.* 2017). MMP2 is postulated to have broad substrate affinity due to the conformation of its substrate specifying S1' channel (Llano *et al.* 2002). MMP2 has also been found to target elements of the basement membrane, whereas MMP1 targets cell-cell junctions (Jia *et al.* 2015). Although *Drosophila* MMP2 lacks certain conserved sequences found in vertebrate collagenases and stromelysins, *in vitro* fluorescence-based analysis of enzymatic activity shows hydrolysis of collagenase, gelatinase, and stromelysin substrates by MMP2 (Llano *et al.* 2002). Additionally, Collagen-IV protein levels are shown via immunohistochemistry to vary with altered MMP2 (Guha *et al.* 2009; Raza *et al.* 2017), suggesting that this protease either directly or indirectly regulates Collagen-IV.

It was previously believed that MMP1 was exclusively secreted and MMP2 anchored to the membrane; however, recent *in vitro* evidence suggests that alternate splicing of *Mmp1* or *Mmp2* might result in the generation of secreted and membrane-

bound isoforms of both proteins (LaFever *et al.* 2017). It is as yet unknown whether such isoforms might be produced *in vivo*.

Drosophila TIMP is orthologous to the mammalian TIMPs, and is capable of inhibiting mammalian MMPs with varying effectiveness; it is a weak inhibitor of collagenases (e.g. MMP-1), and a stronger inhibitor of stromelysins (e.g. MMP-3) (Wei *et al.* 2003). *Drosophila* TIMP resembles most closely mammalian TIMP-3 with respect to charge distribution and function; both are capable of inhibiting human TACE and other proteins of the ADAM and ADAMTS families such as ADAM10 (orthologous to Kuzbanian). However, *Drosophila* TIMP lacks one of the three conserved disulphide bonds found within the N-terminal inhibitory domain of the mammalian TIMPs (Wei *et al.* 2003).

1.3.3 MMP expression and localisation

The spatial expression patterns of the two *Drosophila* MMPs are not identical; for instance, although both MMP1 and MMP2 are expressed within the central nervous system (CNS), MMP1 is localised to the CNS midline whereas MMP2 shows diffuse CNS expression (Lee *et al.* 2012). During cardiogenesis, MMP1 is localised to the pre-lumenal domain of the migrating cardioblast, where it limits the expansion of junctional domain proteins such as Cadherin (Raza *et al.* 2017). MMP2 is localised to the cardioblast leading edge, where it restricts pre-lumenal Collagen, Dystroglycan, and Slit. Both MMPs promote collective cell migration, and are required for specifying cardioblast polarity (Raza *et al.* 2017).

Temporal expression is likewise dissimilar; MMP1 is expressed primarily during embryogenesis and larval development, but is largely absent from the adult organism. MMP2 is expressed throughout early development and persists through adulthood (Llano *et al.* 2000, 2002; Page-McCaw *et al.* 2003). Expression of both MMPs is elevated during metamorphosis (Page-McCaw *et al.* 2003). TIMP is expressed from late embryogenesis, at the point of earliest MMP expression from approximately stage 13, onwards (Page-McCaw *et al.* 2003).

1.3.4 MMP mutants

Though dispensable during embryogenesis, *Drosophila* MMPs are necessary for tissue remodelling at later developmental stages. Homozygous phenotypic null mutants for *Mmp1* (e.g. $mmp1^{q112}$) or *Mmp2* (e.g. $mmp2^{w307}$) have a high hatching success rate comparable to that of the wild-type (>92%), based on the findings of Page-McCaw *et al.* (2003) and the first chapter of my thesis. However, $mmp1^{q112}$ mutant larvae are reduced in size and display shortened or broken trachea, and have decreased survival to pupariation (16%). $mmp2^{w307}$ mutants show relatively improved survival to pupariation (79%), with death occurring during the pupal stage, prior to eclosion (Page-McCaw *et al.* 2003; Raza 2015). Trans-heterozygous *mmp1,mmp2* double mutants complete embryogenesis, indicating that MMP1 and MMP2 do not play redundant roles in embryonic survival (Page-McCaw *et al.* 2003). Maternal-zygotic *mmp1,mmp2* double mutants show an identical phenotype to double mutants lacking only zygotic *Mmp* contributions, suggesting an absence of maternal effects. Ubiquitous over-expression of

Timp similarly allows for embryogenesis, with larvae resembling *mmp1*^{q112} or *mmp1*^{q112}*,mmp2*^{w307} double mutants (Page-McCaw *et al.* 2003).

1.3.5 MMP-mediated remodelling of the cardiac ECM

It has been shown in multiple organisms that myocardial stiffness increases with age (Horn *et al.* 2012). In mice and other mammals, accumulation of Collagen and the onset of fibrosis during the aging process results in reduced heart contractility and impaired diastolic function (Cieslik *et al.* 2012). MMP expression is closely regulated throughout morphogenesis, growth, and aging. The loss of certain MMPs, or the loss of MMP inhibition, is correlated with heart failure or dysfunction in vertebrates (Spinale 2002; Nagase *et al.* 2006). For instance, mice deficient for the MMP inducer cd147 show reduced membrane-type MMP-1 expression and increased diastolic and systolic ventricular volume but unchanged heart rate, whereas over-expression of MMP1 induces fibrosis and accumulation of Collagen (Huet *et al.* 2015; Horn and Trafford 2016). Heart failure in old-age sheep has been correlated with an increase in MMP-2 activity and a decrease in TIMP levels (Horn *et al.* 2012). In chicken and rat models, ectopic inhibition of MMPs, especially MMP-2, results in heart defects (Ali *et al.* 2011).

The part played by MMPs in defining the cardiac ECM is a complex one. Mammalian MMPs, such as the Gelatinases MMP-2 and MMP-9, and the membrane-tethered MMP-14, are variably expressed in aged and diseased organisms, and their contributions to the mitigation or worsening of cardiac pathologies are very much context-dependent (Sessions and Engler 2016). For instance, a reduction in MMP-2

function might promote fibrosis in aged organisms yet reduce fibrosis during pressure overload (Sessions and Engler 2016).

The role of MMPs in *Drosophila* heart development and maintenance has, until recently, been largely unexplored. New studies by Raza *et al.* (2015, 2017) have demonstrated the importance of MMPs for heart morphogenesis. Loss of *Mmp1* or *Mmp2* expression compromises the organised migration of cardioblasts to the midline, resulting in irregular or delayed migratory patterns. Both *Drosophila* MMPs are necessary for normal lumen formation, and MMP2 is also required for apical adhesion of cardioblasts. Homozygous *mmp1* mutant embryos have a reduced lumen, arising from the expansion of the Cadherin-based junctional domain. Homozygous *mmp2* null mutants and *mmp1,mmp2* double mutants do not form a continuous lumen due to the failed midline attachment of some contralateral cardioblasts. Mutants lacking MMP2 function also exhibit mis-localised Pericardin along the medial surface and mis-localised Integrin along the cardioblast apical region (Raza *et al.* 2017).

1.4 Advantages of the *Drosophila* model

Drosophila is a powerful system for studying cardiac development and ECM remodelling, owing to the low number of MMPs and the presence of a singular TIMP. The smaller genome and lower number of protein variants in *Drosophila* renders genetic manipulation a much simpler affair than in vertebrate models (Mark D. Adams, Susan E.

Celniker, Robert A. Holt, Cheryl A. Evans *et al.* 2000; Gu *et al.* 2005; Brown *et al.* 2014). Myriad tools are readily exploitable to generate mutants and genetic mosaics. Amongst these is the yeast-derived Gal4-UAS system, which, with the addition of the temperature-sensitive *Gal80^{TS}* allele, enables both spatial and temporal control of gene expression through RNA interference (RNAi) or activation of transgenes (Fig. 1.3) (Duffy 2002; Suster *et al.* 2004). Gal4-UAS is a critical tool of this research, as such control is invaluable when examining essential genes and pathways whose ubiquitous knock-down might otherwise prove lethal during early development, or when purely post-embryonic phenotypes are of interest.

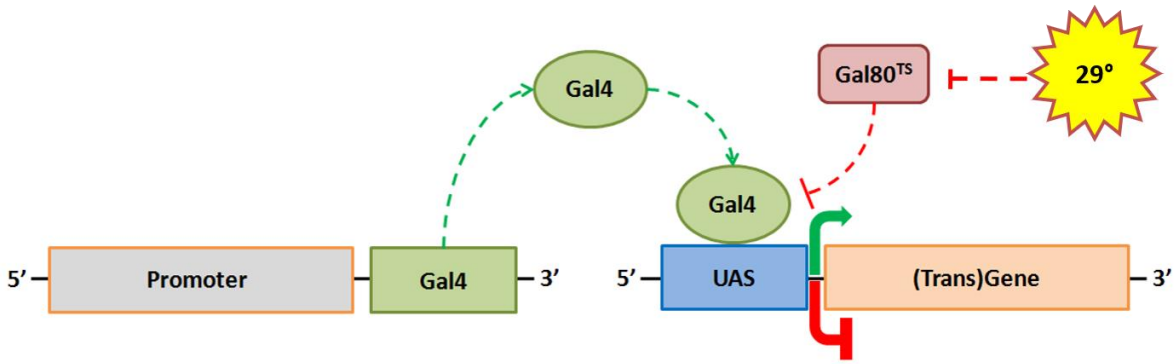

Figure 1.3: Model of the yeast-based Gal4-UAS system with the temperature-sensitive *Gal80^{TS}*. The Gal4-UAS system is used to drive gene expression within specific cells or tissues. The system is composed of a Gal4 transcription activator driven by a promoter, and an upstream activation sequence (UAS) that acts as an enhancer for an endogenous gene or transgene. Gal80^{TS} is a temperature-sensitive repressor of Gal4 that functions as a genetic switch; at permissive temperatures (18°C) it inhibits Gal4 through the binding of the transcriptional activation domain, but Gal80^{TS} activity is itself inhibited at non-permissive temperatures (29°C), allowing Gal4 to bind the UAS and activate gene transcription (Suster *et al.* 2004).

1.5 Project outline and objectives

Objective: The primary objective of this research is to discern the role of MMPs and their inhibitor TIMP in larval heart development. Heart morphogenesis and growth are determined in large part by ECM remodelling; changes in the levels of ECM proteins and MMPs are observed in older or diseased vertebrate hearts (Bonnema *et al.* 2007; Raza 2015; Hughes and Jacobs 2017). Of interest, therefore, is the effect of MMP mis-regulation on cardiac morphology and the distribution of ECM structural and receptor proteins, particularly Collagen-IV (Vkg), Pericardin (Prc), and βPS1-Integrin. Here I examine the requirements of the two *Drosophila* MMPs, MMP1 and MMP2, for proper cardiac development and cardiac functioning in third instar larvae.

1.1 Examine homozygous and heterozygous *mmp1* and *mmp2* mutants at early and late third instar to determine the resulting cardiac phenotypes and the impact on Vkg and Prc expression.

1.2 Inhibit the function of multiple proteases by temperature- and cell-specific over-expression of *Timp* to determine the resulting cardiac phenotypes and the impact on the expression of Vkg and Prc.

1.3 Ascertain the spatial and temporal requirements of MMP2 activity for heart development and Vkg and Prc expression by knocking down the expression of *Mmp2* or over-expressing *Mmp2* at different stages of development using cell-specific promoters.

Hypothesis 1: Cardiac development relies upon proper ECM localisation. Cardiac vessel size and structure will be compromised in larvae with reduced MMP function due to impaired lumenogenesis (noted by Raza *et al.* 2017).

1.1 Dissections of *mmp1, mmp2,* and *mmp1,mmp2* (double) heterozygous and homozygous mutants at both early and late third instar were performed alongside one wildtype control group.

1.2 Dissected larvae from 1.1 were immunolabelled with anti-βPS-Integrin and conjugated Phalloidin (Actin), and were examined under the confocal microscope to compare the severity of gross structural defects and cardiac muscle arrangement.

Hypothesis 2: Normal distribution of ECM structural proteins at the larval heart relies upon the proper functioning of MMPs.

2.1 *mmp1, mmp2,* and *mmp1,mmp2* (double) heterozygous and homozygous mutants were dissected at early and late third instar, alongside one wildtype control group.

2.2 Inducible over-expression of *Timp* was performed using temperature-sensitive versions cell-specific drivers. Over-expression was induced ubiquitously (*daGal4*) or locally within cardiac cells (*HandGal4*). *Timp* was over-expressed following four temperature regimens: 1) expression throughout embryonic and larval development (29°C) to determine the maximal severity of the mis-expression phenotype; 2) expression throughout embryonic but not larval development (29°C to 18°C shift at

second instar) to determine if there was recovery when normal MMP activity was restored during heart growth or if early patterning of ECM proteins persisted; 3) expression during larval but not embryonic development (18°C to 29°C shift at second instar) to determine the role of MMPs in promoting ECM remodelling during larval heart growth; 4) no over-expressed (18°C) to provide an internal control.

2.3 Inducible inhibition of *Mmp2* expression by dsRNA was performed using temperature-sensitive versions of cell-specific drivers. Reduced expression was induced ubiquitously (*daGal4*) or locally within cardiac cells (*HandGal4*) following the four temperature regimes outlined in 2.2.

2.4 Inducible over-expression of *Mmp2* was performed using temperature-sensitive versions cell-specific drivers. Over-expression was induced ubiquitously (*daGal4*) or locally within cardiac cells (*HandGal4*) following the four temperature regimes outlined in 2.2.

2.5 Dissections of early and late third instar larvae from 2.1, 2.2, 2.3, and 2.4, alongside the relevant control group(s), were labelled with αPrc and conjugated Phalloidin. Larvae endogenously expressed Vkg-GFP.

2.6 Dissections from 2.5 were imaged under the confocal microscope. Prc and Vkg fluorescence signals were quantified (mean fluorescence intensity). Mutant and Gal4-UAS larvae were considered separately due to differences in genetic background and imaging settings.

Hypothesis 3**:** Normal heart function in early and late third instar larvae relies upon normal *Mmp2* expression.

3.1 Heart rates of live heterozygous and homozygous *mmp2* mutants and one wildtype control group were measured at early and late third instar using a light microscope.

3.2 OCT live imaging was performed on homozygous *mmp2* mutants and one wildtype control at late third instar. Quantification of heart dilation and contractility was performed.

2.0 Methods:

Drosophila stocks: Stocks are as follows:

Stock	Source	Number	Notes
yw^{1118}	Bowling Green		Lab wildtype
vkg^{cc00791}	M. Buszczak	FBti0099948	GFP trap construct for Collagen-IV
tupGal80^{TS}	Bloomington	7108	Temperature-sensitive *Gal80* on II
tupGal80^{TS}	Bloomington	7018	Temperature-sensitive *Gal80* on III
mmp1^{q112}	A. Page-McCaw		
mmp1^{q112},vkg-GFP	Q. Raza	N/A	Generated from 00791 and *mmp1^{q112}*
mmp2^{w307}	A. Page-McCaw		
mmp2^{w307},vkg-GFP	Q. Raza	N/A	Generated from 00791 and *mmp2^{w307}*
mmp1^{q112},mmp2^{w307}	A. Page-McCaw		
mmp1^{q112},mmp2^{w307},vkg-GFP	Q. Raza	N/A	Generated from 00791 and *mmp1,mmp2*
daGal4	Bloomington	55851	Ubiquitous driver
tupGal80^{TS};daGal4	C. Hughes	N/A	Generated from 7108 and 55851
HandGal4	R. A. Schulz		Cardiac cell driver
HandGal4;tupGal80^{TS}	C. Hughes	N/A	Generated from 7018 and
R4Gal4	Bloomington	33832	Fat body driver
UAS-CD8::RFP	Bloomington	32218	RFP reporter
UAS-mmp1RNAi	A. Page-McCaw	APM3175	dsRNA on III
UAS-mmp2	A. Page-McCaw	APM3085	Over-expression of MMP2 on II
UAS-mmp2,vkg-GFP	C. Hughes	N/A	Generated from 00791 and APM3085
UAS-mmp2RNAi	Bloomington	61309	dsRNA on II
UAS-mmp2RNAi	Bloomington	31371	dsRNA on III
vkg-GFP;UAS-mmp2RNAi	C. Hughes	N/A	Generated from 00791 and 31371
UAS-TIMP	A. Page-McCaw	APM3019	Over-expression of TIMP on III
vkg-GFP;UAS-TIMP	C. Hughes	N/A	Generated from 00791 and APM3019

Controls:

yw was used as a control for non-recombined *mmp* mutants. *yw*;*vkg-GFP/+* was used as a control for those *mmp* mutants and UAS lines recombined with *Vkg-GFP*. *yw;UAS-mmp2,vkg-GFP/+*, *yw*;*vkg-GFP/+;UAS-TIMP/+*, or *yw*;*vkg-GFP/+;UAS-mmp2RNAi/+* were used as controls for UAS-Gal4 crosses. In all cases, only a single copy of the GFP trap construct was present. All controls for the *mmp* mutants were reared at 25°C. All controls for the *UAS-Gal4* crosses were reared at 29°C.

Larval collections:

Fly houses containing 50 to 150 flies (3:1 ratio of females to males) were used for collections. Houses were composed of an inverted 100mL plastic measuring cup with punctured air holes resting atop a plate containing a solid apple-agar substrate (approximately 10mL) with a dollop of yeast paste (yeast and H_2O) added for nourishment. Newly introduced flies were allowed 48 hours at room temperature (23°C) for acclimation before collections were initiated. An egg-laying window of 2.5 to 3 hours at 23°C was used as a standard. Upon removal, the egg plate was immediately transferred to an incubator at a set temperature (18°C, 25°C, or 29°C). Hatching time was calculated for each genotype at the given temperature. Plates were cleared after visual inspection once hatching has begun. At 25°C and 29°C, freshly-hatched first instar larvae were collected within a window of 60 minutes, after which the plate was cleared and the time reset for future collections. At 18°C, 3 to 4 hours was allowed, in order to compensate for

slower development. First instar larvae of the desired genotype were identified visually, by selection for or against fluorescence markers, and were removed from the apple-agar substrate with forceps. Larvae were scooped from beneath rather than clasped in order to minimise damage. Larvae were then transferred to a food medium plate (10mL) at a maximum density of 25 larvae per plate (minimum 10 per plate). Experimental and control houses were set up in parallel.

Temperature shifts (18 to 29°C or 29 to 18°C) of Gal4-UAS crosses expressing the temperature-sensitive $Gal80^{TS}$ were performed at early second instar to distinguish between cardiogenesis (embryogenesis and first larval instar) and cardiac growth (second and third larval instar). Shifts were performed based upon the time elapsed since hatching. Different genotypes had slightly differing developmental timing, so shifts were performed based upon each genotype's average time to reach second instar, rounded to the nearest hour. At 29°C this was generally between 22-24 hours, whereas at 18°C, this was typically between 42-44 hours.

Early third instar larvae were identified by branched anterior spiracles. The approximate timing of the moult was determined for each genotype at each temperature, and was set at a point when a majority of larvae revealed branching. Dissections were performed within a three-hour window once branching in multiple individuals has been confirmed. Late third instar larvae were dissected at a point when one or more larvae within the cohort had initiated pupariation. The approximate timing of pupariation was

determined for each genotype at each temperature, and was used as a benchmark. Dissections were performed within a three-hour window.

Dissections:

Larval dissections were performed at early third instar, at the time of anterior spiracle branching, or at late third instar, immediately prior to pupariation. Live larvae were immobilised dorsal-side-down in 1xPBS solution using magnetically-fastened pins. The primary incision was made no less than a third of the body length from the anterior-most extremity to prevent disruption of the anterior fat body and cardiac muscle attachments. Tracheal tubes were left intact to minimise damage to the alary muscles. Individual dissections were performed in less than 10 minutes. When possible, control and experimental samples were reared and dissected concurrently.

Adult dissections were performed using five-day-old females. Adult flies were anaesthetised by exposure to FlyNap; five to 10 females were transferred to a chamber within a specialised externally-sealed container to which was added a sponge carrying a small aliquot of FlyNap. Females were exposed to FlyNap vapours for 15 minutes or until all individuals had ceased moving. The adult flies then were immobilised dorsal-side-down by application of Vaseline to the wings. The head and thoracic segments were removed, whilst preserving the entirety of the dorsal abdomen. Five to 10 individuals were immobilised on the same plate and were dissected in concert. Dissections of each cohort were performed in less than 15 minutes. When possible, control and experimental samples were reared and dissected concurrently.

Immunolabelling:

Dissections were fixed in in 4% Paraformaldehyde for 5 minutes while held in place by magnetic pins (larvae) or Vaseline (adults). Dissections were then transferred to a 24-well plate and agitated at low speed on an orbital rotator at room temperature (23°C). Tissues were fixed in 4% Paraformaldehyde for an additional 20 minutes and were subsequently washed in 1xPBT (3 washes at 10 minutes each). Dissections were then transferred to a 96-well plate and blocked with 10µL normal goat serum (NGS) in 150µL 1xPBT for a period of 30 minutes prior to the addition of 5µL primary antibody (1:30) and left to incubate at 4°C for 12 hours whilst undergoing constant agitation. No more than six dissections were placed in a single well. Samples were then removed from the 4°C fridge and transferred to a 24-well plate and agitated at low speed on an orbital rotator at room temperature (23°C). A second round of washing was performed (3 x 10-minute washes in 1xPBT). Tissues were then transferred to a 96-well plate and blocked with 10µL NGS in 150µL 1xPBT for a period of 30 minutes prior to the addition of 1µL secondary antibody (1:160) and 1µL Phalloidin (1:160). Samples were incubated for 60 minutes and were then transferred to a 24-well plate and re-washed in 1xPBT (3 x 10-minute washes) and 1xPBS (1 x 10-minute wash). Samples were then removed from the orbital rotator and transferred to a bath of 50% glycerol and stored at 4°C without agitation until imaging (12-18 hours post-staining).

The antibodies used are as follows:

Primary antibodies: mouse anti-βPS (βPS1-Integrin, DF.6g11-s, DSHB, monoclonal primary antibody), mouse anti-Prc (Pericardin, EC11, DSHB, monoclonal primary antibody).

Secondary antibodies: Alexa Fluor 543 anti-mouse conjugated phalloidin (A22283, LifeTechnologies, Burlington ON, Canada), Alexa Fluor 647 anti-mouse (A21236, LifeTechnologies, Burlington ON, Canada)

Slide preparation:

Tissues were mounted on glass microscope slides in a 70% glycerol medium immediately prior to imaging. Dissections were braced between two coverslips, which support the central overlying coverslip and prevent the introduction of compression-induced damage or aberration. To ensure minimal diffraction and image aberration, number 1.5 (0.16-0.19mm thickness) glass coverslips were employed.

Confocal imaging:

Fluorescence imaging was performed using a Leica SP5 confocal microscope. Coronal Z-stacks and cross-sectional Y-stacks were captured at 1.3µm intervals at a native resolution of 1024x512 pixels. Settings were held constant across samples. Sequential scanning by frame was used to minimise cross-talk; the 488nm and 647nm lasers were active in the first scan and the 543nm laser was active in the second. Post image capture, coronal Z-stacks were blurred (5 pixels) and projected (max projection) to form a false 3D

impression using the native Leica software (LAS AF). Cross-sections were blurred but not projected.

Assessment of cardia bifida:

The prevalence of cardia bifida was quantified using a binary system of presence versus absence. Cardia bifida was ascertained by the presence of fenestrations within the cardiac tube, as determined by the distribution of cytoskeletal Actin fibrils. Individual Z-stacks from confocal image captures were examined sequentially from the ventral surface of the heart chamber (sections A6-A7) through to the mid-section using Leica software (LAS AF Lite). Hearts were scored as demonstrating the bifida phenotype only if two discrete myofibrillar envelopes (Phalloidin-labelled Actin) persisted throughout the entire depth of the vessel. The size of the bifurcated region was not considered.

Fluorescence quantification:

Collagen-IV expression was quantified via analysis of the fluorescence intensity of endogenously expressed Vkg-GFP. *mmp2* mutants with conspicuous Vkg aggregates were used as a benchmark for confocal settings to ensure against pixel saturation. Confocal Z-stacks of dissected late third instar larvae were imported into ImageJ and converted into RGB images. These stacks were subsequently cropped to include only the volume of the dorsal vessel, from the ventral to dorsal surface, and then projected (max projection) into a single plane. The ROI was defined as the entirety of segment A7, which was delineated from adjacent segments by the ostial inlets. A trace was formed using the Phalloidin-labelled Actin cytoskeleton as a guide. Collagen aggregates were included when tracing

the ROI, but not the intervening spaces between bifurcated vessels or overlying fat body (where applicable). The mean fluorescence signal of the ROI was calculated natively in ImageJ. Mean fluorescence values were calibrated by subtracting the mean background signal.

Pericardin expression was quantified via analysis of the fluorescence intensity of immuno-labelled Prc (mouse anti-Prc primary antibody with 647nm goat anti-mouse secondary antibody). Confocal Z-stacks of dissected early and late third instar larvae were imported into ImageJ as per the above protocol. The ROI was defined as the entirety of segment A7, which was delineated from adjacent segments by the ostial inlets. A rectangle was drawn from the midline of the DV to a set distance of 190µm (20x with 1x zoom) or 80µm (20x with 2x zoom) on either side of the vessel. Those projections analysed were of a consistent magnification and zoom for each genotype. The mean fluorescence signal of the ROI was calculated natively in ImageJ. Mean fluorescence values were calibrated by subtracting the mean background signal.

Anaesthetisation with chloroform:

Third instar larvae were anaesthetised with chloroform and secured on double-sided tape to limit mobility during OCT imaging. A 500µL dose of chloroform was transferred via pipette onto a fragment of rayon pharmaceutical coil (‘cotton’) inserted into one end of a glass cylinder or bottomless vial. The cotton was pushed down to the midpoint of the cylinder to ensure the spatial volume beneath remained consistent. Five third instar larvae were arrayed on a glass slide. The glass cylinder was placed over the

larvae for a period of 25 seconds, removed for three seconds, and then placed again over the larvae for 25 seconds as per the protocol devised by Duygu Cevik (personal communication). Larvae were then immediately transferred to double-sided tape, dorsal side up. A new rayon fragment with freshly applied chloroform was used for each batch of larvae. Complete sedation persisted for approximately 30 minutes, after which larvae slowly regained motor function.

OCT live imaging:

OCT imaging was performed on anaesthetised late third instar larvae using a custom-designed apparatus and in-house softwares provided by the Vitkin lab at the University of Toronto (Bogatan *et al.* 2015; Matveev *et al.* 2015). Cross-sections were captured via B-scans, which penetrate to the approximate midpoint of the larva. Early third instar larvae were not imaged due to issues resolving the smaller dorsal vessel lumens. Larvae were secured with double-sided tape to a glass microscope slide, which was mounted on an angled stage (7° to the imaging plane, anterior at top). Image sequences were captured at approximately 70 frames per second for a period of 7.1 seconds (14µs per frame) at a resolution of 512x512 pixels, with an X-axis amplitude of 1mm, and a Y-axis amplitude of 0mm for cross-sections and 1mm for 3D sections. Larvae were imaged at segment A6. Data were exported in .avi video format, and individual frames were exported as .bmp image files.

Heart dilation:

Dilation was measured as the area in μm^2 at diastole (i.e. maximal heart chamber expansion). Measures were taken from 2D cross-sectional videos of anaesthetised third instar larvae (see OCT live imaging protocol). Video sequences were examined frame-by-frame using ImageJ software. Image sizes were corrected to account for the elongated Z-axis caused by tissue interference, assuming a refractive index of 1.33 for the cuticle and underlying tissues (Nienhaus *et al.* 2012; Zhou *et al.* 2013). Therefore, 512x700 pixel cross-sections were resized to 512x248, assuming 1 pixel is 0.692µm in water along the Z-axis (0.692µm/pixel x 700 pixels = 0.484mm; 0.484mm x 512 = 248 pixels to correct the aspect ratio). The first five confirmed consecutive diastoles within the set were used for analysis. The wall of the diastolic lumen was traced by hand using the ImageJ pencil tool. The area of the enclosed space was measured. This was repeated for each of the five selected frames. Measurements were then averaged.

Heart contractility:

Contractility was measured as the ratio of diastolic area to systolic area, and was calculated by dividing the area at diastole by the area at systole. Measures were taken from 2D cross-sectional videos of anaesthetised third instar larvae (see OCT live imaging protocol). Individual area measurements were taken as per the guidelines provided for heart dilation, with the addition of the five concomitant systolic frames (maximal heart chamber contraction). The averaged ratio was used.

Basal heart rate:

Heart rate analysis was performed using non-anaesthetised third instar larvae. Larvae were immobilised on a glass microscope slide with double-sided tape, dorsal side up. Once secured beneath the objective, the larvae were left to acclimate for 5 minutes or until a regular heart rate is established. 12- to 15-second image captures were taken using a Zeiss Axioskop light microscope at a minimum of 60 frames per second (FPS). If this sequence was interrupted by intermittent arrhythmia or slowing of contraction, or by peristalsis, the video was re-captured. Cases of extended arrhythmias without peristalsis were logged. Videos were then played back and the number of full contractions was counted in triplicate using a mechanical counter. The median of the three counts was used. The number of frames was divided by the average FPS to determine the length of the video. This value, in conjunction with the beat count, was used to calculate beats per minute (BPM). The median BPM for each genotype was calculated. Potential outliers were identified as those values 1.5 inter-quartile ranges (1.5 IQR) beyond the first and third quartiles, but these were not removed from the dataset.

Hatching success and larval survivorship assay:

mmp mutants and relevant controls were reared at 25°C. Gal4-UAS lines with the temperature-sensitive $Gal80^{TS}$ allele were subjected to four temperature regimes; 1) 18°C, 2) 18 to 29°C, 3) 29 to 18°C, 4) 29°C. Eggs were selected prior to hatching once fluorescence-based genotyping was possible. Eggs were transferred to an apple agar plate at a maximum density of 35 eggs per plate with the assumption that some eggs would be

dead or unfertilised. A small dollop of yeast paste was placed at its centre to provide nutrition. Eggs were migrated with forceps using a scooping motion to minimise damage during transfer. Plates were then moved to an incubator at 18°C, 25°C, or 29°C. The number of hatched and dead eggs was counted, and unfertilised eggs were subtracted from the total count. Dead larvae were counted and removed each day. When larvae reached third instar, they were migrated to a fresh apple agar plate with yeast to allow for easier counting and to ensure an adequate food supply. Mortality was determined for each of the following developmental stages: 1) L1 to early L3, 2) early L3 to late L3, 3) late L3 to pupariation, 4) pupariation to adulthood. Mortality during first and second instar was combined due to the difficulty of performing precise counts during this period without inflicting accidental damage. This figure was calculated by subtracting the number of early third instar larvae from the number of hatched eggs. Survival to adulthood (eclosion) was determined by counting the number of empty pupal cases. Once the first adult had emerged, a grace period of four days was allotted, after which all non-eclosed pupae were considered dead. Had no eclosion appeared imminent after the expected time for the specified temperature, a grace period of four days was observed. Should no eclosion have occured within this period, all pupae were considered dead. Eclosion was considered successful if the pupal case was fully evacuated or if the adult organism was fully formed but had only partially emerged.

Back-crossing, validation, and recombination/double-balancing of *Vkg-GFP* or *Gal80^{TS}*:

UAS and Gal4 lines were back-crossed to *yw* (laboratory wildtype) for five generation before being crossed to a fluorescently-tagged balancer. Gal4 lines were validated via fluorescence microscopy after crossing males to *UAS-CD8-RFP* females. UAS lines were validated by crossing males to *daGal4/TM6-tb* females and examining lethality of the non-tubby progeny. UAS lines were then recombined or double-balanced with *vkg-GFP*. Gal4 lines were recombined or double-balanced with *Gal80^{TS}*.

Microbial infection:

An as yet unidentified microbial agent contaminated a majority of fly stocks. This infection manifested as a thick film on yeast food plates, resulting in occasional drowning. The infection was exacerbated at higher temperatures (29°C). Initially, chloramphenicol was added to fly food used for plates at a concentration of 25µg/mL, and an additional 100mL of 25µg/mL solution was added to the top of the yeast food plate prior to the transfer of first instar larvae. Stock chloramphenicol solutions were produced according to the protocol used by Cevik (2016). All crosses were raised on chloramphenicol-treated plates, regardless of temperature treatment. This regime was abandoned due to the emergence of resistance. The agent is currently being sequenced.

Stock maintenance:

Fly stocks were reared on yeast-based food in 28.5x95mm wide-mouth polystyrene vials at room temperature (22 to 23°C). All stocks were maintained in duplicate vials. Adult flies were transferred to fresh food vials every 12 to 14 days. Duplicate vials were developmentally staggered by seven days, such that one copy was transferred each week. Stock maintenance and food preparation were performed by Hasan Hawilo, Balpreet Panesar, and Samantha Turner.

3.0 Results:

3.1 Survivorship of larvae with altered MMP function

The objective of my research was to elucidate the larval requirement for ECM proteases during cardiac growth. I therefore began my investigation by establishing when MMP function is required to ensure larval survival.

It has previously been demonstrated with phenotypic null mutants for *Mmp1* (*mmp1*^{q112}) and *Mmp2* (*mmp2*^{w307}) that functioning MMP1 and MMP2 are not required to complete embryogenesis, though they are required for successful eclosion (Page-McCaw *et al.* 2003; Raza 2015). However, not described is the precise spatial and temporal requirements for MMP activity to ensure normal heart development.

I used the Gal4-UAS system to alter gene expression in specific tissues to elucidate the effects of altered MMP function during larval development, and altered MMP function specifically within the heart. Reduced MMP function was induced by the over-expression of the protease inhibitor TIMP using *UAS-TIMP* (Page-McCaw *et al.* 2003). However, TIMP is also capable of inhibiting numerous other proteases of the ADAM and ADAMTS families (Wei *et al.* 2003), which may also be involved in cardiac ECM remodelling. To better characterise the role of MMP2 specifically, I altered *Mmp2* activity by expressing dsRNA using *UAS-mmp2RNAi* or by over-expressing it using *UAS-mmp2* (Raza *et al.* 2017). These UAS constructs were driven ubiquitously with *daGal4* or specifically within cardiomyocytes and pericardial cells with *HandGal4*. The introduction of the temperature-sensitive *Gal80*^{TS}

allele into *daGal4* lines (henceforth *daGal80*) permitted temporal control of gene expression. Transcription of the (trans)gene was inhibited by $Gal80^{TS}$ (del Valle Rodríguez *et al.* 2011) when organisms were reared at the permissive temperature (18°C), whereas transcription was enabled once organisms were shifted to the non-permissive temperature (29°C). The spatial expression pattern of both Gal4s was verified with a UAS-RFP reporter. This revealed organism-wide fluorescence with *daGal80* and localised fluorescence with *HandGal4* in cardiomyocytes, pericardial cells, and the lymph glands.

The dorsal vessel is fully formed and competent (contractile) by the time of hatching (Tao and Schulz 2007) though it is not required for larval survival (Medioni *et al.* 2009). However, additional differentiation of the cardiomyocytes/lymph glands continues into first instar (Sellin *et al.* 2006) so all temperature shifts were performed at the start of second instar. This ensured a clean separation between cardiogenesis (mid embryonic stages into the first larval instar) and subsequent cardiac growth (second through third larval instar). Survivorship assays also functioned to validate the activity of the UAS inserts and Gal4 drivers. A complete overview is provided in supplementary figure S4.

3.1.1 Survivorship of *mmp* mutant larvae

Considerable mortality was observed in homozygous $mmp1^{q112}$ mutants and $mmp2^{w307}$ mutants (henceforth *mmp1* and *mmp2,* respectively) throughout larval development, and neither survived to eclosion (Fig. 3.1). 75% of *mmp1* mutants expired before reaching late third instar and 84% expired prior to pupariation. Third instar larvae often possessed broken and necrotic trachea, described previously by Page-McCaw *et al*.

(2003), which was likely a contributor to the high levels of larval mortality. *mmp2* mutants did not experience significant mortality until the pupal stage, with 79% surviving to pupariation. Heterozygous *mmp2* mutants had similar survivorship to the wildtype control, and successfully eclosed. Heterozygous *mmp1* mutants displayed a modest but significant improvement in survival over the wildtype control throughout the observed period, and successfully eclosed. It is unclear if a mild reduction in MMP1 function had some protective effect. *mmp1,mmp2* double mutants were not included in this analysis, but personal observations suggest hetero- and homozygotes show similar survival to their *mmp1* mutant counterparts. This is corroborated by the findings of Page-McCaw *et al.* (2003).

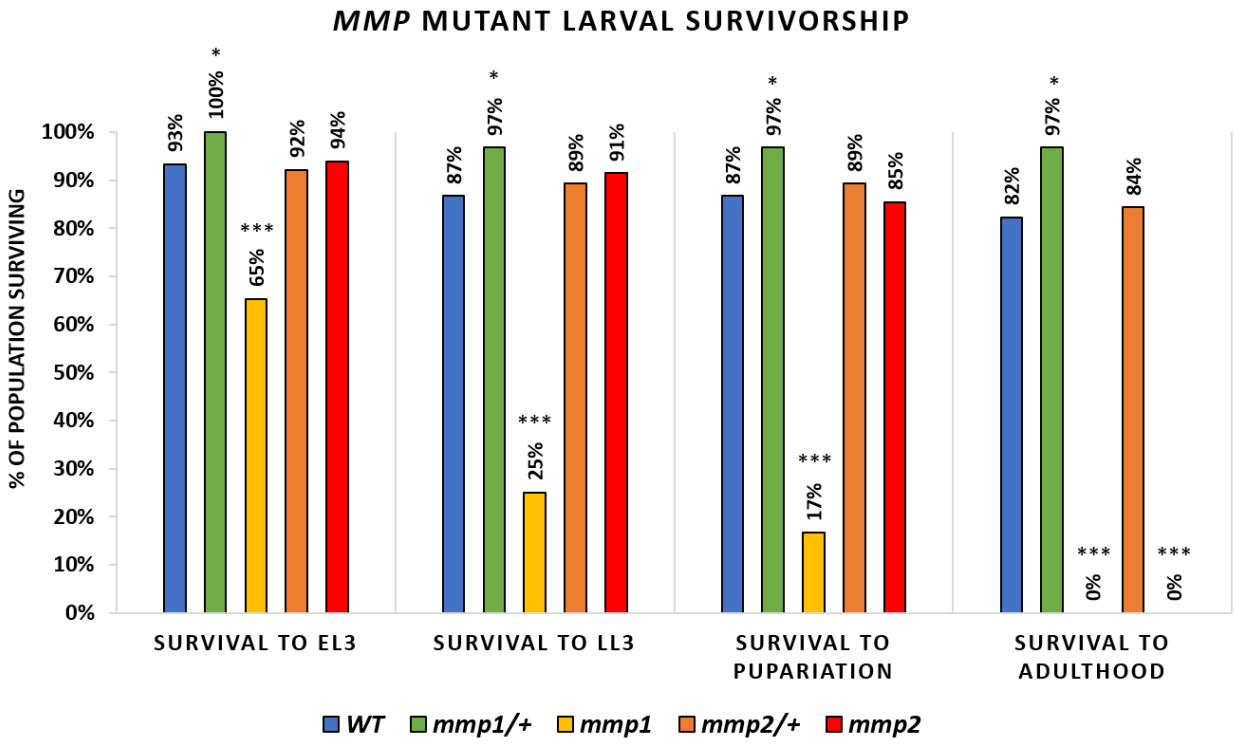

Figure 3.1: Homozygous *mmp* mutants experience significant mortality throughout larval and pupal stages. Specimens were reared at 25°C throughout all life stages. Homozygous *mmp1* mutants (**yellow**) experience a significant reduction in survival prior to early third instar; 35% of first instar larvae fail to reach third instar. Homozygous *mmp2* mutants (**red**) do not experience a significant reduction in survival until post-pupariation (a drop from 85% to 0% survival prior to eclosion). Heterozygous *mmp1* mutants (**green**) show improved survival when compared to wildtype (**blue**). Heterozygous *mmp2* mutants (**orange**) show similar survival to wildtype. The wildtype is *yw*. Chi-square test. * $p \leq 0.05$ ** $p \leq 0.01$ *** $p \leq 0.005$.

3.1.2 Survivorship of larvae over-expressing TIMP

Over-expression of TIMP was driven either ubiquitously (*daGal80*) or locally within cardiac cells (*HandGal4*) throughout embryonic and larval development (29°C), encompassing both heart morphogenesis and heart growth (Fig. 3.2). The driverless *UAS-TIMP* control showed similar larval survival to the wildtype until pupation, at which point an anomalous increase in mortality was observed. Cardiac-specific over-expression of TIMP throughout embryonic and larval development was not correlated with dramatically reduced survival, and did not prevent eclosion. Constitutive ubiquitous over-expression of TIMP was correlated with a pronounced reduction in survival throughout larval development, with low survival past eclosion. Over-expression of TIMP throughout embryogenesis alone did not prevent survival to adulthood (Fig. 3.3). Larvae over-expressing TIMP from embryogenesis to second instar (i.e. throughout cardiogenesis but not later cardiac growth) showed reduced survival at early third instar even when compared to larvae constitutively over-expressing TIMP, but survival plateaued thereafter. This suggests that mortality is correlated with the shift to the lower temperature. Larvae over-expressing TIMP from second instar onwards (i.e. throughout cardiac growth but not cardiogenesis) showed a similar pattern of survival to larvae constitutively over-expressing TIMP. Internal *UAS-TIMP/daGal80* controls reared at 18°C showed similar survival to the wildtype and driverless controls reared at 29°C, indicating a negligible effect of temperature on survival and some leaky expression of the UAS or Gal4.

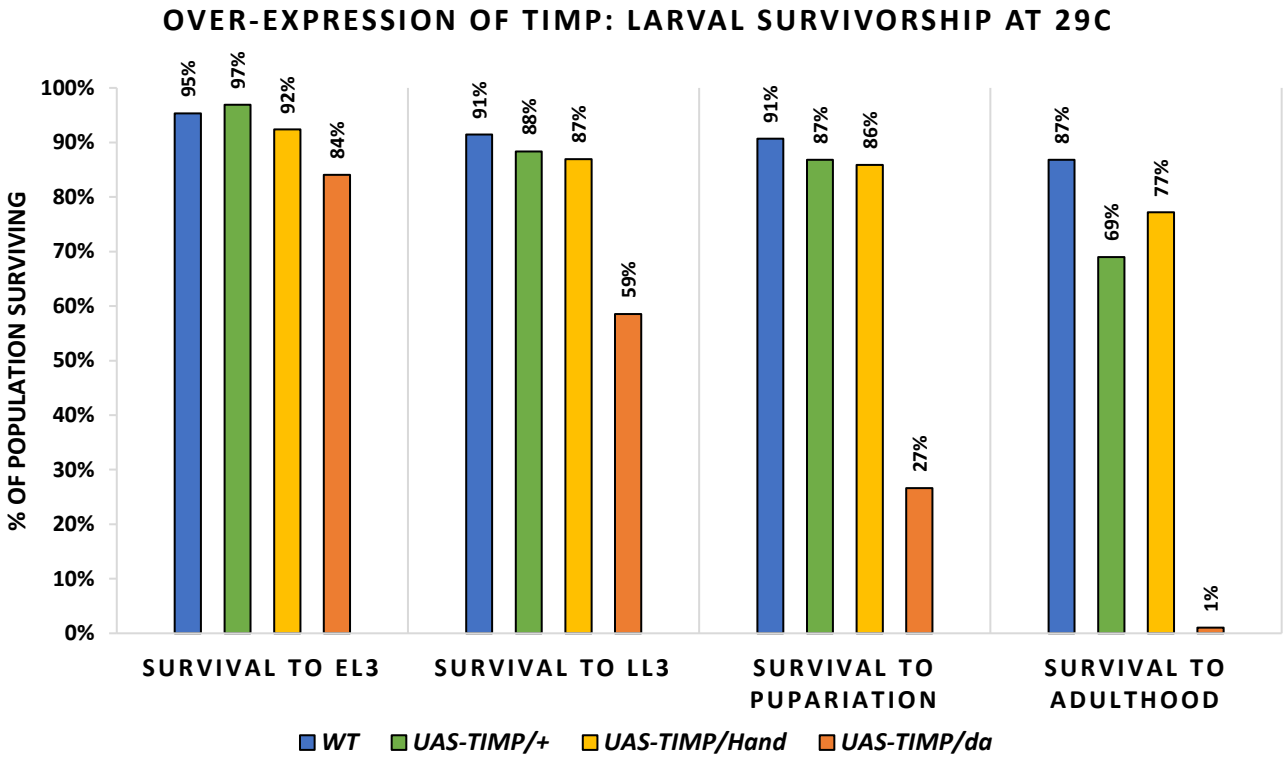

Figure 3.2: Larval survival is compromised upon up-regulation of *Timp*. Specimens were reared at 29°C throughout all life stages. Driverless *UAS-TIMP* controls (**green**) show similar survival to wildtype controls (**blue**), except at eclosion. Localised over-expression of *Timp* within the cardiac cells with *HandGal4* (**yellow**) does not result in significant mortality compared to controls, even at later stages of development; 77% of such individuals survive to adulthood. Ubiquitous over-expression of *Timp* with *daGal80^{TS}* (**orange**) results in considerable mortality from third instar onwards, with low survival to adulthood (1%). The wildtype control is *yw;vkg-GFP/+*.

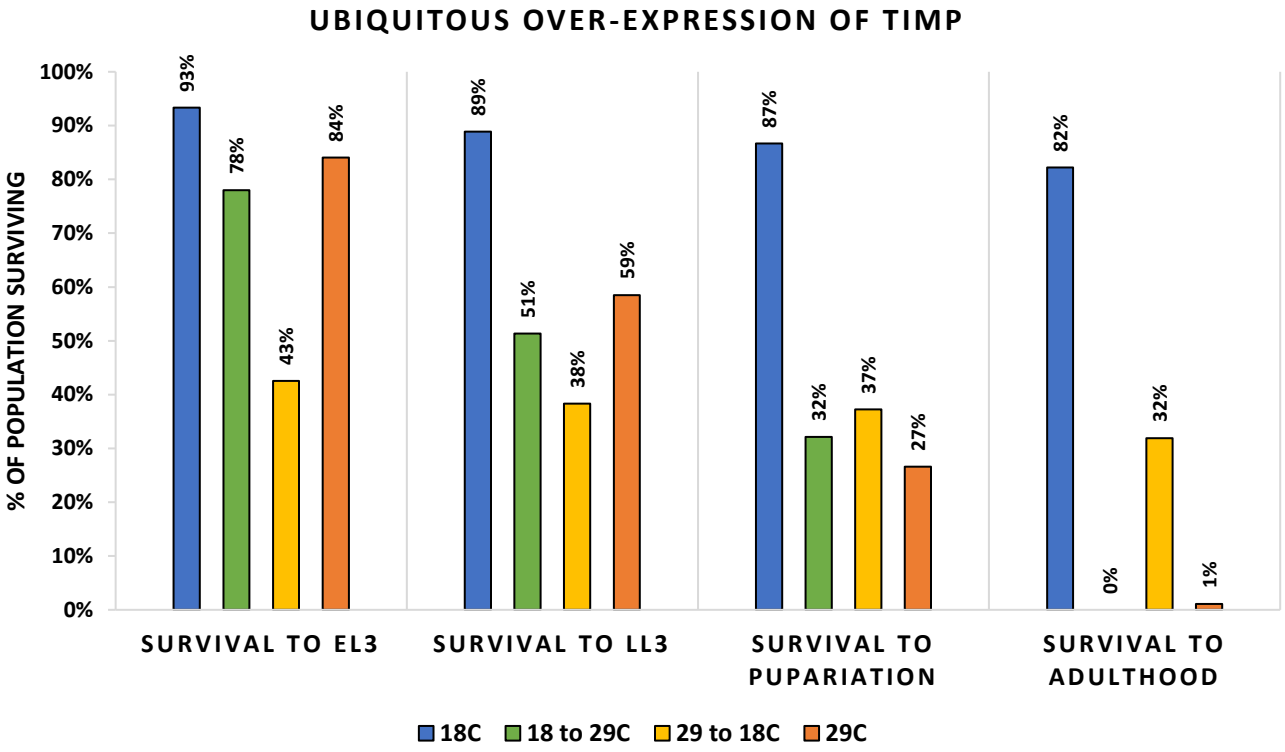

Figure 3.3: Larval survival varies with temporally-regulated over-expression of *Timp*. Over-expression of *Timp* throughout embryonic and larval development (29°C), or upon reaching second instar (18 to 29°C) results in considerable mortality from third instar onwards, with low survival to adulthood (1% and 0%, respectively). Over-expression throughout embryogenesis and first instar (29 to 18°C) results in increased mortality immediately following the temperature shift at second instar, but surviving individuals are capable of successful eclosion.

3.1.3 Survivorship of larvae expressing *Mmp2* dsRNA

The specific requirement of MMP2 function was examined using two *Mmp2* dsRNA inserts; TRiP line 61309 (chromosome II; henceforth *mmp2RNAi*) and TRiP line 31371 (chromosome III; henceforth *mmp2RNAi(III)*) Expression of the *Mmp2* dsRNA insert on chromosome II was driven ubiquitously (*daGal80*) or locally within cardiac cells (*HandGal4*) throughout embryonic and larval development (Fig. 3.4). The driverless dsRNA control showed similar larval survival to the wildtype. Cardiac-specific expression of *Mmp2* dsRNA throughout embryogenic and larval development did not correlate with lower survival, nor did this reduce eclosion. Ubiquitous expression of the dsRNA was correlated with a reduction in survival throughout larval development; this pattern was similar to that of *mmp1* mutants and larvae constitutively over-expressing TIMP. Temporal regulation of *Mmp2* dsRNA revealed that normal expression of MMP2 throughout larval development and pupation was sufficient for successful eclosion, though survival to adulthood was reduced compared to controls (Fig. 3.5). This might suggest leaky expression of the dsRNA as internal controls reared at 18°C also showed consistently lower survival (by >10%) than the wildtype and driverless dsRNA controls reared at 29°C. Larvae expressing *Mmp2* dsRNA from second instar onwards showed a similar pattern of survival to *mmp2* mutants (low mortality until pupation), but better larval survival than those constitutively expressing the dsRNA.

Expression of the *Mmp2* dsRNA insert on chromosome III was driven ubiquitously (*daGal80*) throughout embryonic and larval development (Fig. 3.6). The driverless dsRNA

control exhibited comparable larval survival to the wildtype. Constitutive expression of the dsRNA with *daGal80* at 29°C was correlated with a reduction in survival after pupariation and was similar to the pattern of survival of the homozygous *mmp2* mutant. However, a not-insignificant percentage (12%) of individuals survived to eclosion, suggesting that the reduction of MMP2 was weaker than with the mutant allele or the *Mmp2* dsRNA insert on chromosome II.

3.1.4 Survivorship of larvae over-expressing MMP2

Over-expression of MMP2 was driven ubiquitously (*daGal80*) or locally within cardiac cells (*HandGal4*) throughout embryonic and larval development (Fig. 3.7). The driverless control was not different from the wildtype with respect to larval survival. Cardiac-specific expression of MMP2 throughout embryonic and larval development was correlated with a dramatic reduction in larval survival; only 33% of specimens survived to early third instar and just 1% reached the pupal stage. Ubiquitous expression of MMP2 during embryogenesis resulted in 100% mortality before second instar. Larval but not embryonic over-expression of MMP2 resulted in 100% mortality within several hours of transfer to the non-permissive temperature (Fig. S1). Internal *daGal80* controls reared at 18°C survived to eclosion, but experienced lower overall survival than the wildtype and driverless controls reared at 29°C, perhaps indicating some leakiness in the expression of the insert.

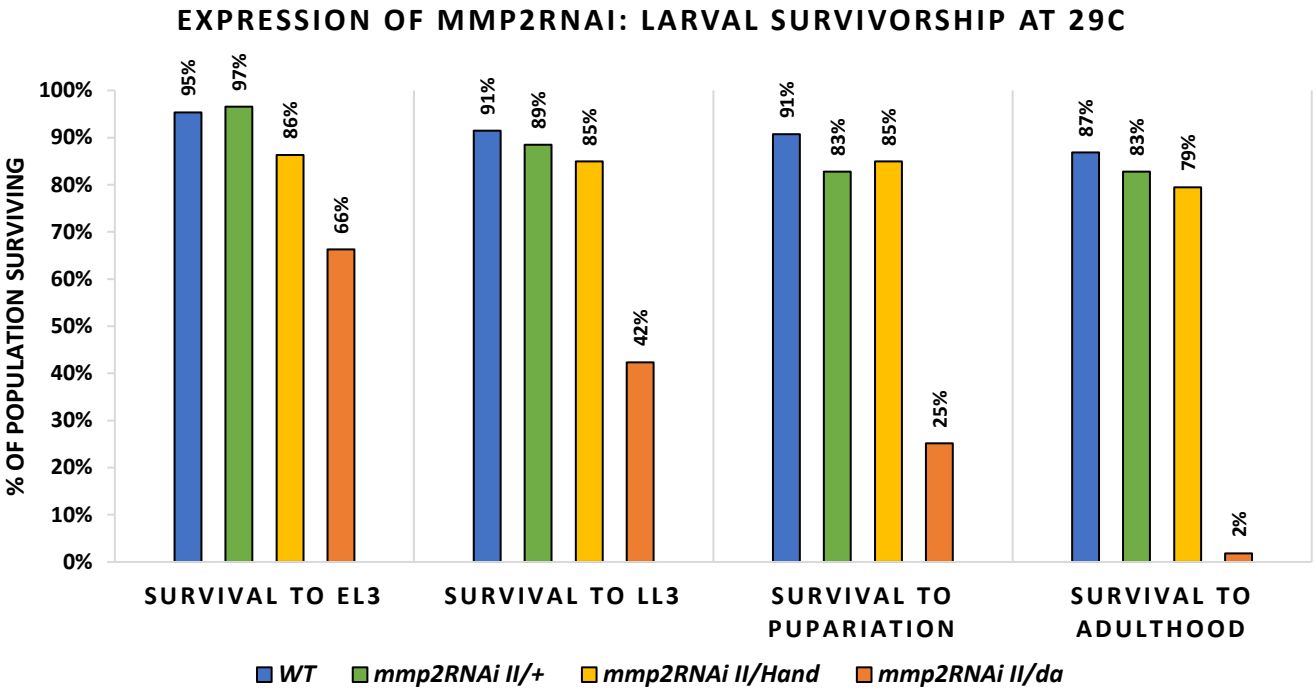

Figure 3.4: Larval survival is compromised upon expression of *Mmp2* dsRNA. Specimens were reared at 29°C throughout all life stages. Driverless *mmp2RNAi* controls (**green**) show similar survival to wildtype controls (**blue**). Localised down-regulation of *Mmp2* within the cardiac cells with *HandGal4* (**yellow**) does not result in significant mortality compared to controls, even at later stages of development; 79% of these individuals survived to adulthood. Ubiquitous down-regulation of *Mmp2* with *daGal80^{TS}* (**orange**) results in considerable mortality from third instar onwards, with low survival to adulthood (2%). The wildtype control is *yw;vkg-GFP/+*.

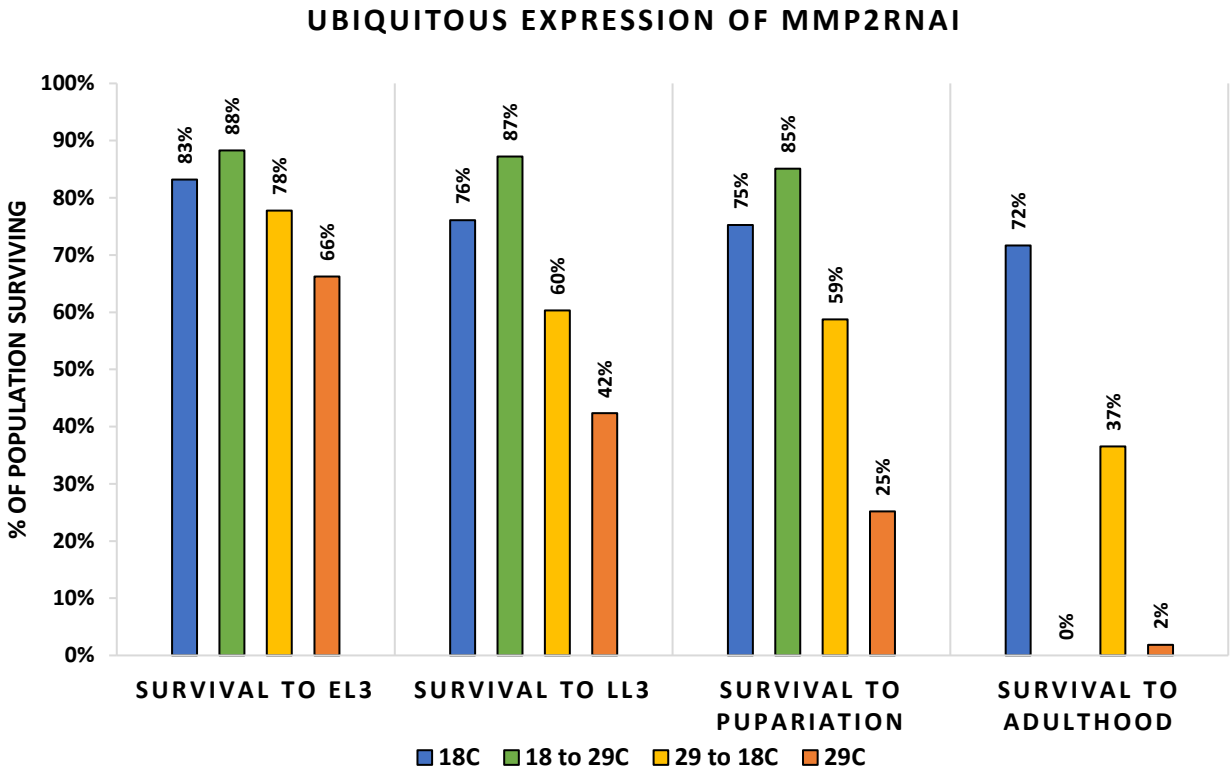

Figure 3.5: Larval survival varies with temporally-regulated reduction of *Mmp2*. Down-regulation of *Mmp2* throughout embryonic and larval development (29°C), and upon reaching second instar (18 to 29°C) results in considerable mortality from third instar onwards, with low survival to adulthood (2% and 0%, respectively). Down-regulation of *Mmp2* throughout embryogenesis and first instar (29 to 18°C) does not drastically reduce survival through larval development and pupariation. A reduction in survival is observed during pupation, with 37% of individuals capable of successful eclosion.

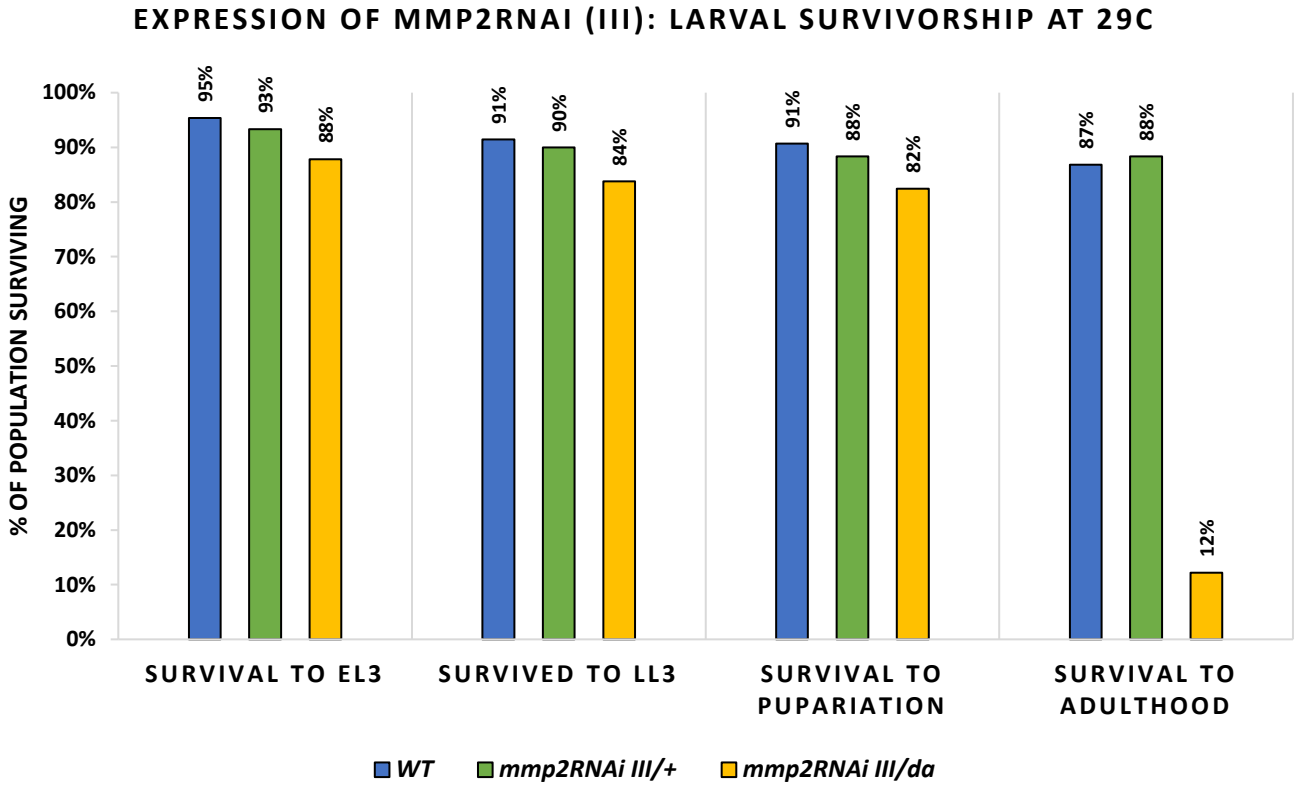

Figure 3.6: Larval survival is compromised upon ubiquitous expression of *Mmp2* dsRNA on chromosome III. Specimens were reared at 29°C throughout all life stages. Driverless *mmp2RNAi* controls (**green**) show similar survival to wildtype controls (**blue**). Ubiquitous down-regulation of *Mmp2* with *daGal80^{TS}* (**yellow**) does not result in significant mortality prior to pupation, with low survivorship to adulthood (12%). The wildtype control is *yw;vkg-GFP/+*.

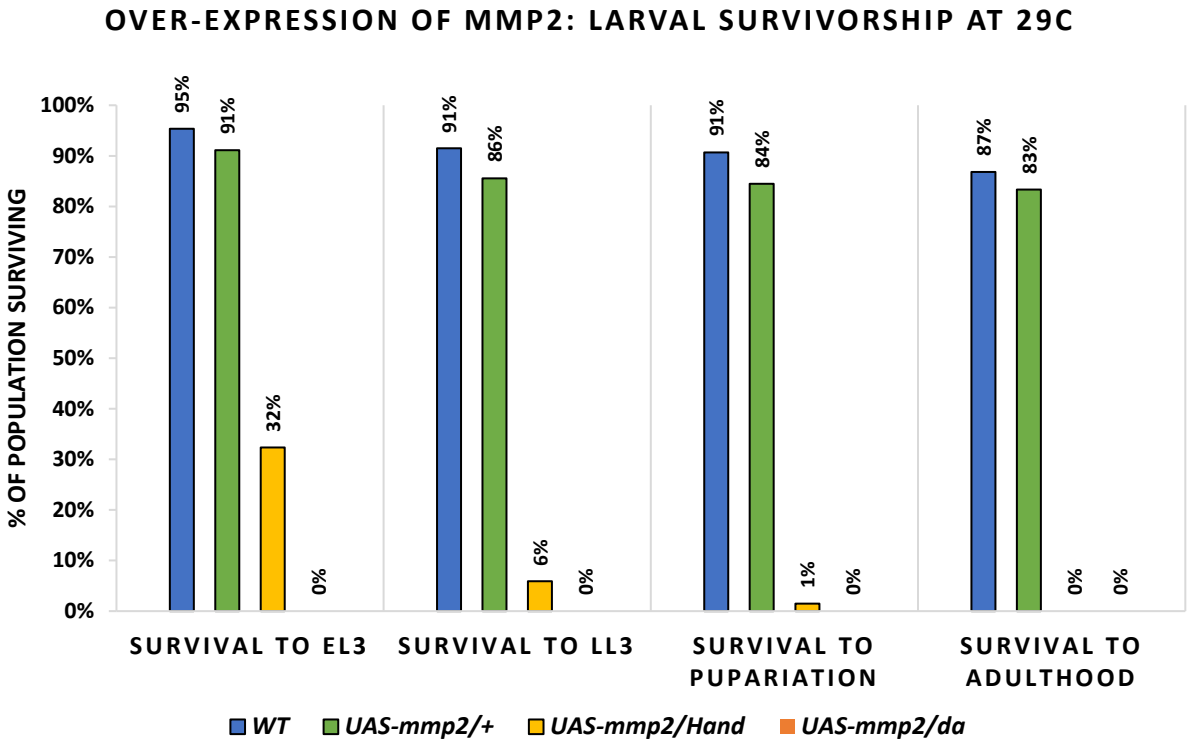

Figure 3.7: Embryonic and larval survival is compromised upon over-expression of *Mmp2*. Specimens were reared at 29°C throughout all life stages. Driverless *UAS-mmp2* controls (**green**) show similar survival to wildtype controls (**blue**). Cardiac-specific over-expression of *Mmp2* with *HandGal4* (**yellow**) is correlated with high mortality through larval development (68% of specimens die before reaching early third instar and 1% pupariate), with no survival to adulthood. Ubiquitous over-expression of *Mmp2* with *daGal80^{TS}* (**orange**) is correlated with high mortality through early larval development (100% of specimens die before reaching early third instar). The wildtype control is *yw;vkg-GFP/+*.

3.1.5 Summary of survivorship

These data suggest that MMP1 function is required for larval survival, and that both MMP1 and MMP2 are required for eclosion. However, normal MMP2 function in the heart appears to be dispensable for larval survival, as no increase in mortality was observed during larval development or metamorphosis upon the cardiac cell-specific reduction of MMP2 or over-expression of the MMP inhibitor TIMP. Ubiquitous over-expression of TIMP resulted in a decline in survival similar to that experienced by larvae with reduced MMP1 function. Over-expression of MMP2, either ubiquitously or specifically in the heart, caused mortality by third instar.

3.2 Effect of *Mmp2* loss of function on cardiac ECM remodelling

I examined mutants to gain insight into the role played by MMP1 and MMP2 during cardiogenesis, and ascertain how embryonic defects manifest throughout larval development. This granted an appreciation for the phenotypes that could be expected from the inhibition of MMP1, MMP2, or MMP1 and MMP2 concurrently. I examined both hetero- and homozygous mutants to determine *Mmp* haplosufficiency. However, it must be noted that this experiment was limited in its explanatory value; it was impossible to determine the specific role of MMP-mediated remodelling during larval development because cardiac structure was compromised during embryogenesis.

3.2.1 Characterisation of dorsal vessel architecture in *mmp* mutant larvae

Cardiogenesis arises through a carefully regulated process of collective cell migration, cell polarisation, guidance signalling, and matrix remodelling that is known to rely upon the activity of MMP1 and MMP2 (Raza 2015; Raza *et al.* 2017). The larval *Drosophila* heart experiences considerable growth between first and third instar (Bogatan *et al.* 2015), and normal cardiac growth and function are likewise expected to depend upon the regulation of protein deposition and degradation by MMPs.

Amongst wildtype individuals, a singular cardiac vessel formed, flanked by pericardial cells (Fig. 3.8). Parallel myofibrils enveloped the circumference of the vessel in a uniform pattern, though occasional gaps were observable amongst wildtype specimens. Alary muscles were positioned near the segmental boundaries; these occasionally showed

longitudinal distribution along the perimeter of the vessel, and singular fibres were in places nearly continuous between the primary attachment sites. Actin intensity was manipulated in confocal projections to ease viewing, and so is not representative of protein levels.

Cardioblast migration and lumenogenesis are compromised with altered MMP1 and MMP2 function. Upon loss of MMP2 function, Raza *et al*. (2017) note the presence of gaps between cardioblasts, which appear rounded and fail to make contralateral contact. In order to detect any changes in cardiac muscle structure, I visualised Actin myofibrils in dissected early and late third instar larvae using fluorescently-tagged Phalloidin.

Lumenal defects persisted through post-embryonic development, as larval *mmp* mutants also exhibited conspicuous cardiac defects, but these defects appeared less severe than their embryonic precursors (Fig. 3.8). Examination of early third instar larvae homozygous for the $mmp1^{q112}$ loss-of-function allele (*mmp1*) revealed disorganisation of the Actin cytoskeleton in the form of gaps between adjacent myofibrils and uneven midline connections (terminal junctions) (Fig. 3.8B). However, *mmp1* mutant dorsal vessels did not exhibit any gross structural/lumenal defects. Direct comparisons of heart size were not performed because *mmp1* mutants were smaller than the wildtype at any given stage, and it was unclear whether there was any difference in heart size relative to body size. *mmp1* heterozygotes did not appear distinct from wildtype with regards to heart morphology.

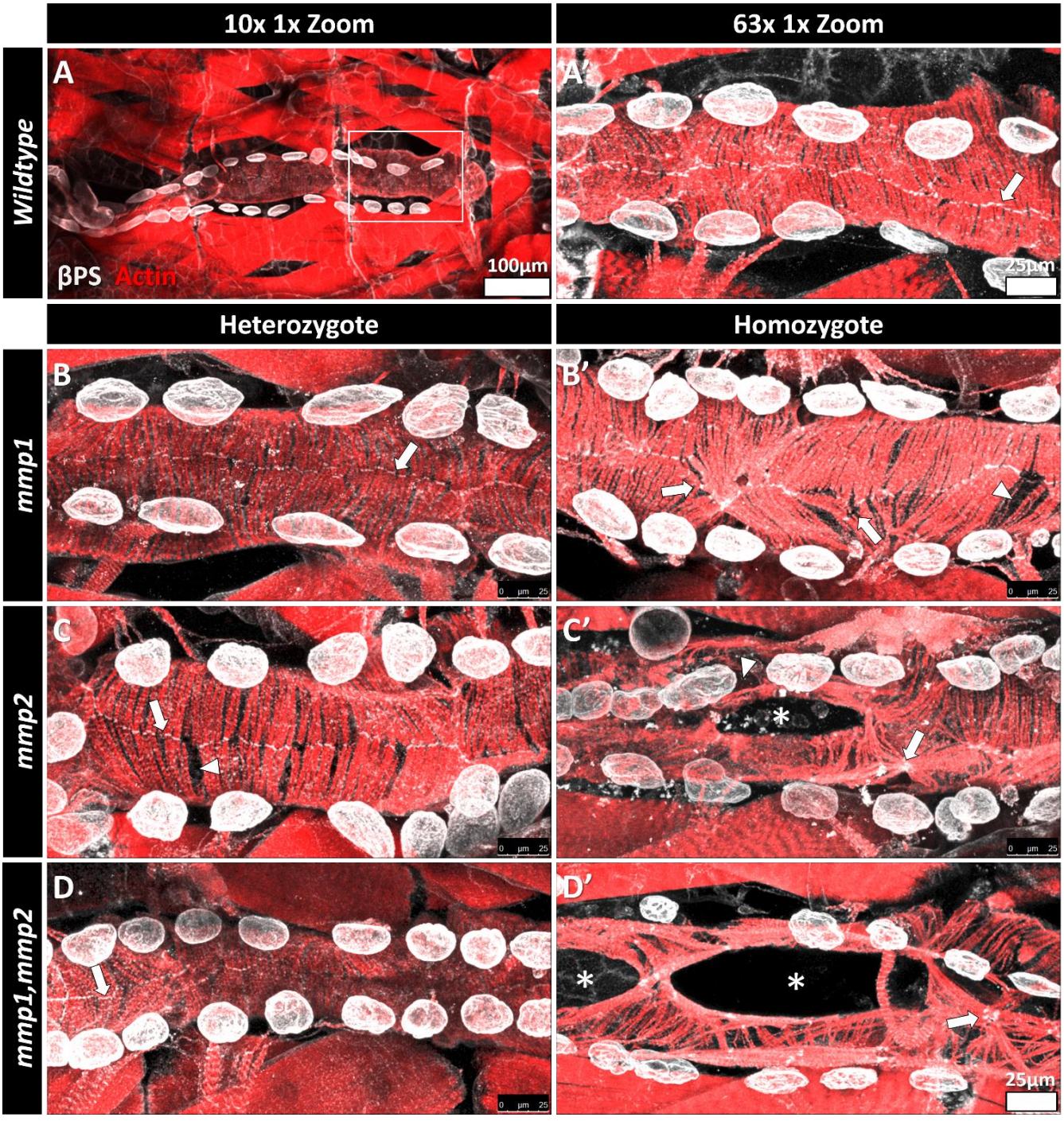
10x 1x Zoom
63x 1x Zoom
Wildtype
A
βPS Actin
100µm
A'
25µm
Heterozygote
Homozygote
mmp1
B
B'
mmp2
C
C'
mmp1,mmp2
D
D'
25µm

Figure 3.8: Dorsal vessels of early third instar *mmp* mutant larvae exhibit structural defects. Coronal projections of DV segments A6 and A7 (posterior at right). Monoclonal βPS antibody (**grey**) is used to visualise Integrin. βPS intensity is manipulated to ease viewing. Conjugated Phalloidin (**red**) is used to visualise the dorsal vessel muscle fibres. **(A-A')** Wildtype larval hearts. **(A)** The DV is a single continuous vessel flanked by PCs along its entire length. White box defines segment A7. **(A')** The DV is enveloped by parallel circumferential Actin myofibrils. βPS-Integrin is expressed at the midline at the location of the adhesion junctions (arrow). The midline is uniform along the length of the vessel. **(B-B')** *mmp1*^{q112} mutants. **(B)** Heterozygous *mmp1* mutants are not observably different from wildtype. **(B')** Homozygous *mmp1* mutants show some disorganisation of cytoskeletal Actin in the form of gaps between myofibrils (arrowhead). The adhesion junctions are not uniform; the midline attachment sites show oscillation in their positioning (arrows). **(C-C')** *mmp2*^{w307} mutants. **(C)** Heterozygous *mmp2* mutants are not observably different from wildtype, save for the presence of some small cytoskeletal gaps. **(C')** Cardia bifida is apparent in *mmp2* homozygotes; the singular dorsal vessel splits into two discrete vessels over a portion of its length (asterisks). Gaps are present between myofibrils and midline adhesion junctions do not form a consistent midline. **(D-D')** *mmp1,mmp2* double mutants. **(D)** Heterozygous *mmp1,mmp2* mutants are not observably different from wildtype. **(D')** The cardiac phenotype of *mmp1mmp2* double mutants is similar to that of *mmp2* mutants. The wildtype is *yw;vkg-GFP/+*.

Larvae homozygous for the *mmp2*^{w307} loss-of-function allele (*mmp2*) exhibited a striking cardiac phenotype in the form of cardia bifida, where one or more regions of the heart chamber was bifurcated to form two discrete vessels. Bifurcated regions varied in size, from less than 25µm in length to spanning multiple segments. Cardia bifida was observed in 48% (21/44) of early third instar larvae and 65% (20/31) of late third instar larvae (Fig. 3.9). Cardiomyocytes enclosed a lumen along the entire length or only a portion of the bifurcated region. When lumenogenesis did not occur, the affected cardiomyocytes appeared to be filled with Actin (Fig. 3.10C”). Cardia bifida was observed in late second instar *mmp2* mutant larvae, suggesting that this phenotype arises relatively early in development, perhaps arising from embryonic defects (Raza 2015; Raza *et al.* 2017), and either persists or worsens throughout larval development. Cytoskeletal arrangement appeared disorganised, with gaps between adjacent myofibrils as well as longitudinal positioning of some fibrils, especially within bifurcated regions of the heart (Fig. 3.8C’). *mmp2* heterozygotes were not distinct from wildtype with regards to heart morphology, with the exception of a single case of cardia bifida (1/49). The observed bifurcation was uniquely asymmetrical and unlike those observed in homozygous mutants, perhaps reflecting a different cause. Larvae homozygous for both loss-of-function alleles (*mmp1,mmp2*) resembled *mmp2* homozygotes with regards to cardiac morphology (fig. 3.8D’), with 55% (11/20) of early third instar larvae exhibiting cardia bifida (Fig. 3.9). *mmp1,mmp2* heterozygotes were not distinct from the wildtype.

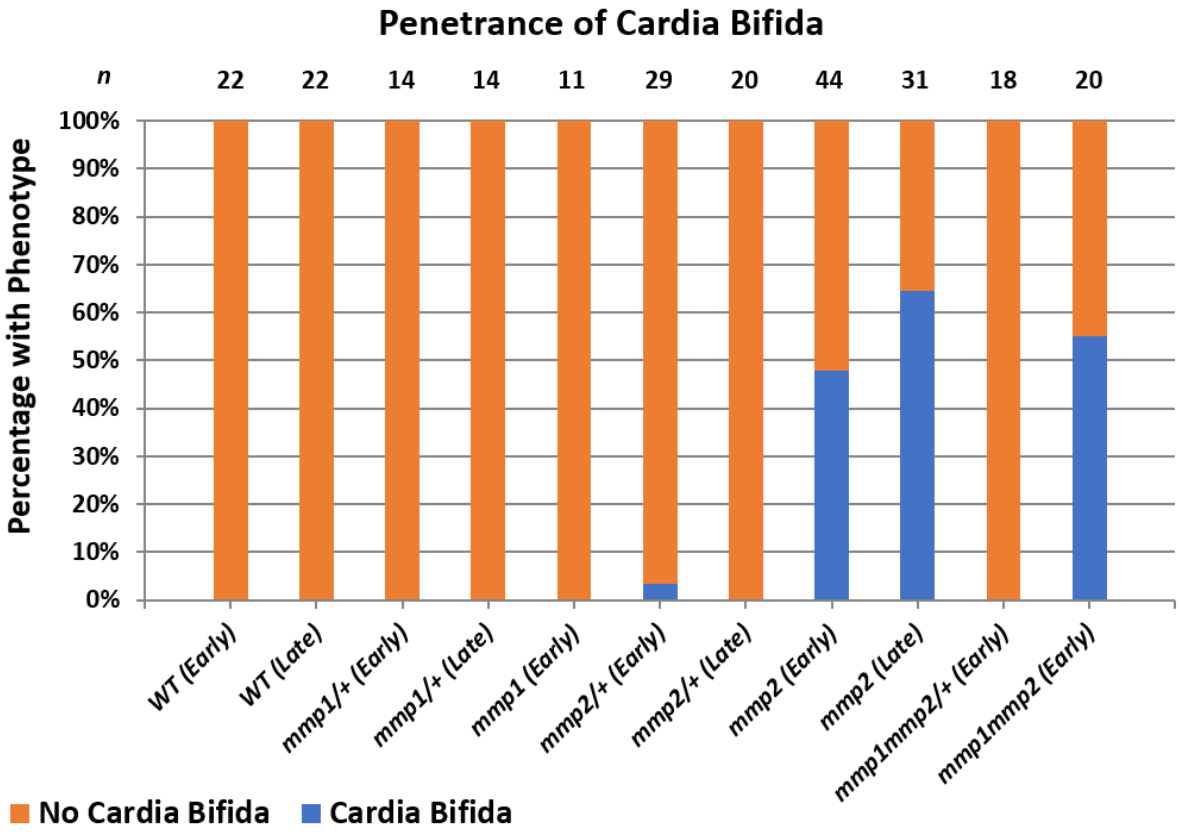

Figure 3.9: Third instar larvae mutant for *mmp2* exhibit cardia bifida. Wildtype organisms, as well as those mutant for *mmp1*, do not reveal any bifurcation along the dorsal vessel. Nor do heterozygous individuals possess this phenotype, with the exception of a small number of *mmp2* heterozygotes (1/29). The incidence of cardia bifida amongst early and late third instar *mmp2* homozygotes is 48% (21/44) and 65% (20/31), respectively. 55% (11/20) of early third instar *mmp1mmp2* homozygotes exhibit cardia bifida. *yw;vkg-GFP/+* is the wildtype.

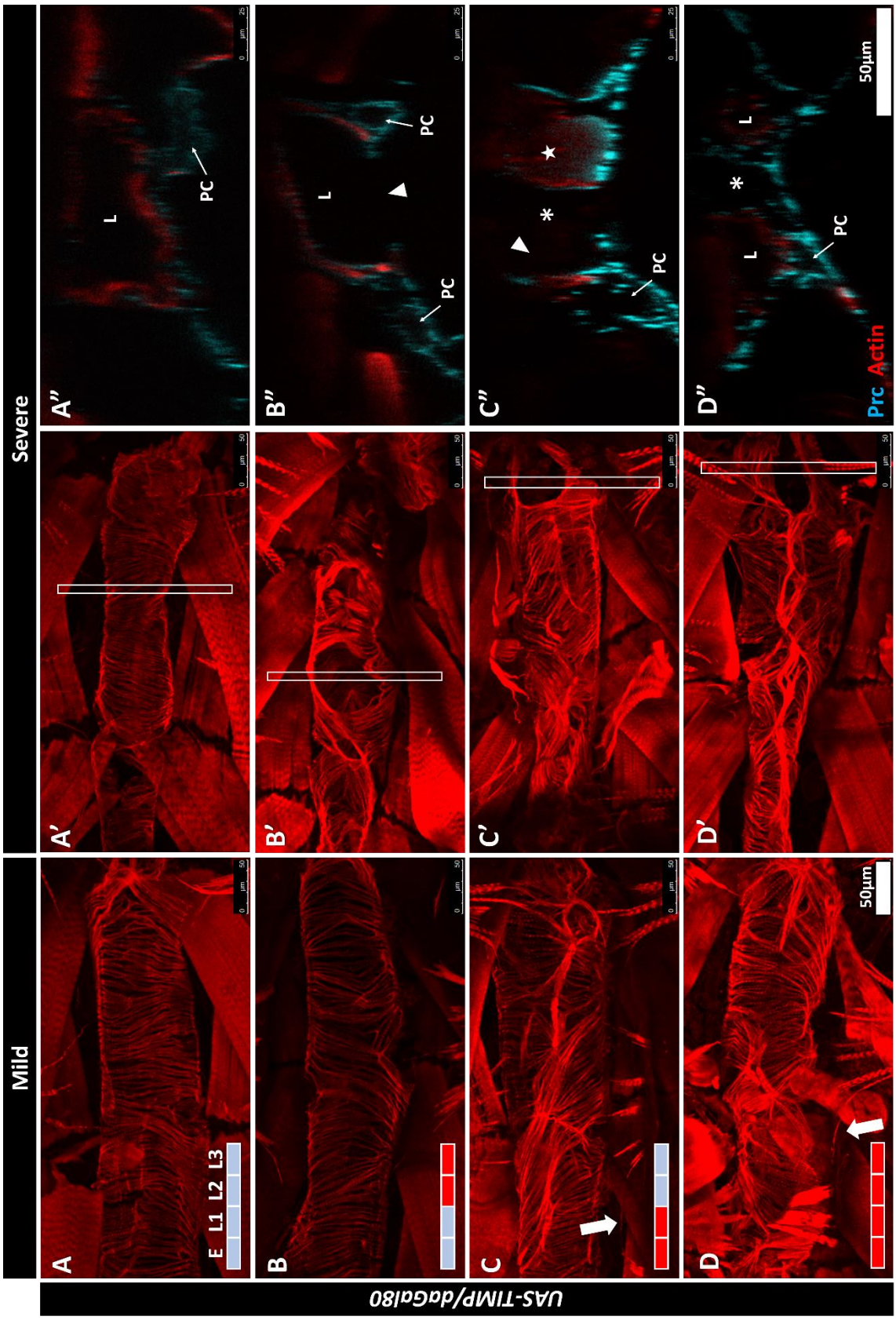
UAS-TIMP/daGal80
Mild
Severe
A
A'
A''
B
B'
B''
C
C'
C''
D
D'
D''
E L1 L2 L3
L
PC
50µm
Prc Actin

Figure 3.10: Ubiquitous over-expression of *Timp* compromises heart architecture in early third instar larvae. DV segments A6 and A7. Larvae were raised at 18°C throughout the grey timeline, and at 29°C throughout the red timeline. Monoclonal Prc antibody (**cyan**) is used to visualise the Prc network. Conjugated Phalloidin (**red**) is used to visualise the dorsal vessel muscle fibres. Over-expression of *Timp* under the regulation of a temperature-sensitive ubiquitous driver (*daGal80^{TS}*). **(A-D)** Mild phenotypes. **(A'-D')** Most severe phenotypes observed. **(A-A")** DVs of organisms raised at the permissive temperature (18°C) throughout embryonic and larval development are enveloped by parallel circumferential Actin myofibrils without conspicuous gaps. **(B-B")** Organisms shifted from the permissive to non-permissive temperature (18 to 29°C) at second instar. **(B'-B")** Lumenal defects are present, such that cardiomyocytes do not fully enclose a lumen along portions of the vessel length (arrowhead marks gap in cytoskeleton). **(C-C")** Organisms shifted from the non-permissive to permissive temperature (29 to 18°C) at second instar. **(C)** Alary muscles are elongated and run parallel to the vessel, stretching between sites of primary attachment (arrow). **(C'-C")** The DV is bifurcated at the posterior end of the heart (asterisk marks gap between vessels). **(C")** One branch shows an incomplete lumen (arrowhead) and the other failed lumenogenesis, where the cardiomyocyte is filled with Actin (star). **(D-D")** Organisms reared entirely at the non-permissive temperature (29°C) show a similar distribution of Vkg to temperature-shifted individuals. White rectangles on the coronal projection designate the region in cross-section. L: lumen; PC: pericardial cell.

The penetrance of the cardia bifida phenotype in homozygous *mmp2* and *mmp1,mmp2* mutants at early third instar (48% and 55%, respectively) was lower than in stage 17 embryos (90% and 80%, respectively, from Raza *et al.* 2017). Given that survival to third instar was 94% for *mmp2* mutants (personal observations) and 35% for *mmp1,mmp2* mutants (from Page-McCaw *et al.* 2003), it is likely that some recovery occurs post-embryonically.

3.2.2 *mmp* mutant phenotypes are recapitulated upon Gal4-UAS-mediated inhibition of MMPs

To ensure that the phenotypes of *mmp* mutants were not related to genetic background effects or unanticipated MMP protein activity, I reduced MMP function using two different methods; directly, via expression of *Mmp* dsRNA, and indirectly, via the over-expression of the endogenous protease inhibitor TIMP.

Cardia bifida was observed in third instar larvae upon inhibition of MMPs and other proteases by ectopically expressed TIMP or upon inhibition of MMP2 specifically by *Mmp2* dsRNA. Larvae ubiquitously over-expressing TIMP also displayed the tracheal defects (broken and necrotic trachea) and small body size observed amongst homozygous *mmp1* and *mmp1,mmp2* double mutants. Ubiquitous reduction of MMP1 by *Mmp1* dsRNA did not result in conspicuous cardiac defects; such larvae resembled similarly aged homozygous *mmp1* mutants, and exhibited tracheal defects as well as high pre-pupal mortality (Fig. S2). A thorough breakdown of the penetrance of lumenal defects is provided in supplementary figure S3.

Actin myofibrils in wildtype organisms were circumferentially distributed along the dorsal vessel in a uniform manner. However, some specimens, including driverless UAS controls (*UAS-TIMP/+* and *UAS-mmp2RNAi/+*), revealed a mild cytoskeletal phenotype of longitudinal bundling of myofibrils along the midline. Terminal βPS1-Integrin connections between longitudinally-arrayed myofibrils did not align with segmental boundaries (data not shown). These bundles were often discontinuous along the length of the vessel and are visible in cross-section as a slight lumenal and ablumenal bulge. In a minority of cases, Phalloidin-labelled Actin extended lumenal intrusions that partially or completely split the vessel along a short length (<5µm; see Fig. 3.11A"). This was only observed in regions of the heart where longitudinal bundles were present both dorsally and ventrally, and did not align with ostial inflow valves. For the purpose of disambiguation, this phenotype is described as a septum, whereas cardia bifida is used to describe cases where the two discrete lumens do not share a vessel wall (i.e. are separated by extracellular space).

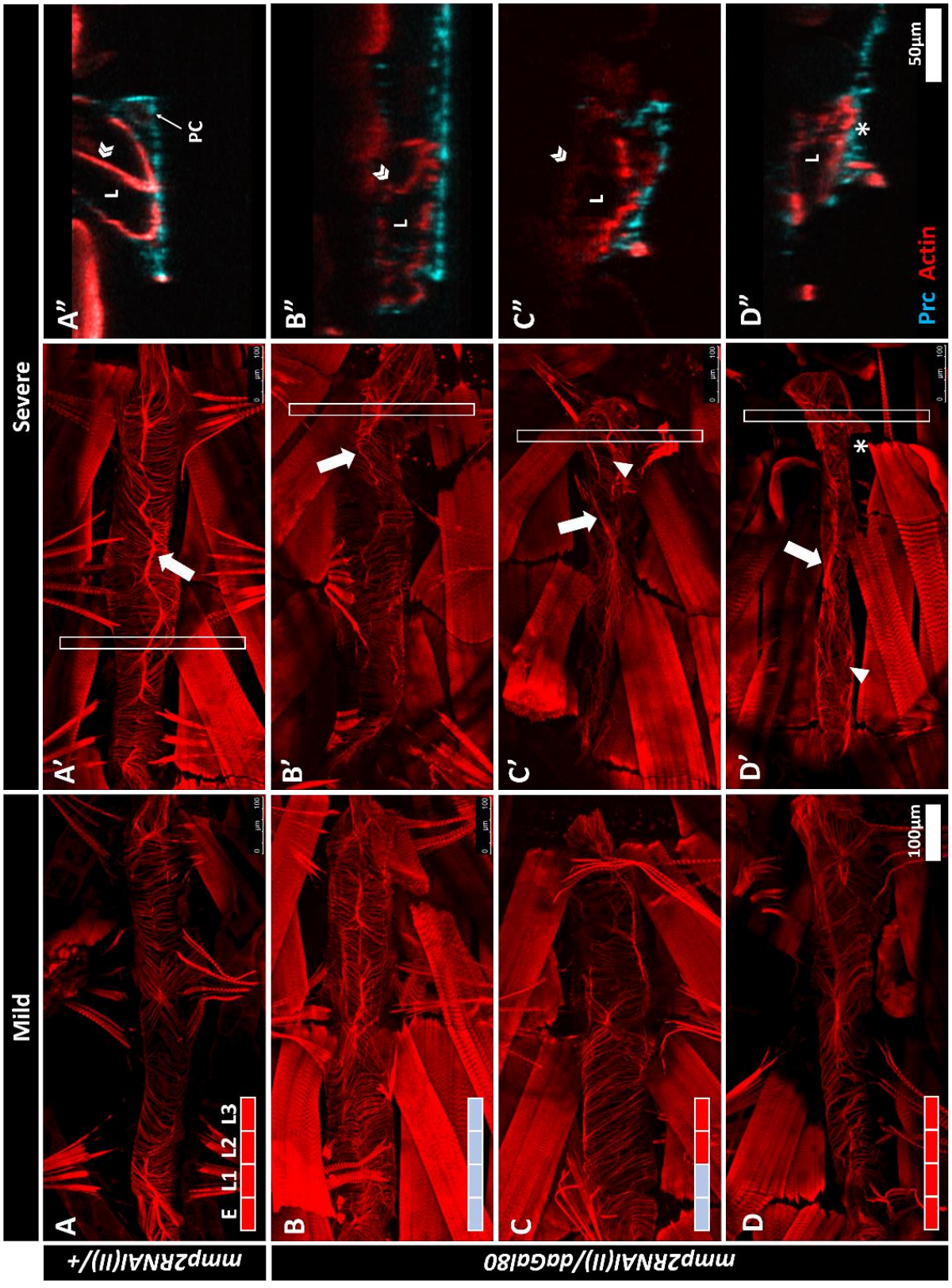
Mild
Severe
mmp2RNAi(II)/+
mmp2RNAi(II)/daGal80
A
A'
A''
B
B'
B''
C
C'
C''
D
D'
D''
E L1 L2 L3
L
PC
100µm
50µm
Prc Actin

Figure 3.11: Ubiquitous expression of *Mmp2* dsRNA in late third instar larvae. DV segments A6 and A7. Expression of *Mmp2* dsRNA under the regulation of a temperature-sensitive ubiquitous driver (*daGal80^{TS}*). **(A-D)** Mild phenotypes. **(A'-D")** Most severe phenotypes observed. **(A-A")** DVs of organisms raised at the permissive temperature (18°C) throughout embryonic and larval development are enveloped by parallel circumferential Actin myofibrils without conspicuous gaps. Longitudinal bundling is observed along the midline (arrow in A'). **(A")** Cross-section shows lumenal extensions of Actin myofibrils (septum) at the site of longitudinal bundling (double chevron). **(B-B")** Organisms shifted from the permissive to non-permissive temperature (18 to 29°C) at second instar. **(B')** Myofibril bundling is less even. **(B")** Dorsal vessel is briefly split at the posterior. **(C-C")** Organisms shifted from the non-permissive to permissive temperature (29 to 18°C) at second instar. **(C')** Actin myofibrils appear disorganised and some gaps are visible (arrowhead). **(C")** Lumenal space is almost completely split along a short length. **(D-D")** Organisms reared entirely at the non-permissive temperature (29°C) **(D'-D")** The dorsal vessel appears narrower and Actin myofibrils are not arrayed uniformly (arrowhead in D'). A posterior spur encloses an offshoot of the lumen (asterisk). White rectangles on the coronal projection designate the region in cross-section. L: lumen; PC: pericardial cell.

Early and late third instar larvae over-expressing TIMP from second instar onwards did not exhibit cardia bifida but did reveal lumenal defects along portions of the vessel length. Cardiomyocytes were attached at the dorsal but not ventral midline (or less commonly the reverse), such that the lumenal space was not completely enveloped and was open to the body cavity (henceforth referred to as an incomplete lumen), possibly as a result of tearing during development (Fig. 3.10B). Early and late third instar larvae over-expressing TIMP from embryogenesis to second instar resembled larvae over-expressing TIMP throughout embryonic and larval development with respect to cardiac phenotype, and exhibited cardia bifida. Such individuals did not, however, display tracheal defects.

Late third instar larvae ubiquitously expressing *Mmp2* dsRNA exhibited milder phenotypes than those over-expressing TIMP; larvae constitutively expressing dsRNA as well as those expressing dsRNA from second instar onwards showed myofibrillar disorganisation but not cardia bifida (Fig. 3.11).

Localised reduction of MMP2 within cardiac cells using the *HandGal4* driver was sufficient to induce cardia bifida (Fig. 3.12). Contrary to results with *daGal80*, cardia bifida was observed amongst larvae locally expressing *Mmp2* dsRNA. It was notable that the penetrance of the bifida phenotype is low (<14%; 3/29) in the presence of the *HandGal4*, and was observed in only one of the two *Mmp2* dsRNA stocks; *mmp2RNAi* (chromosome II) exhibited cardia bifida whereas *mmp2RNAi(III)* (chromosome III) did not. Both inserts appeared to have some activity, based on the results of the survivorship assay.

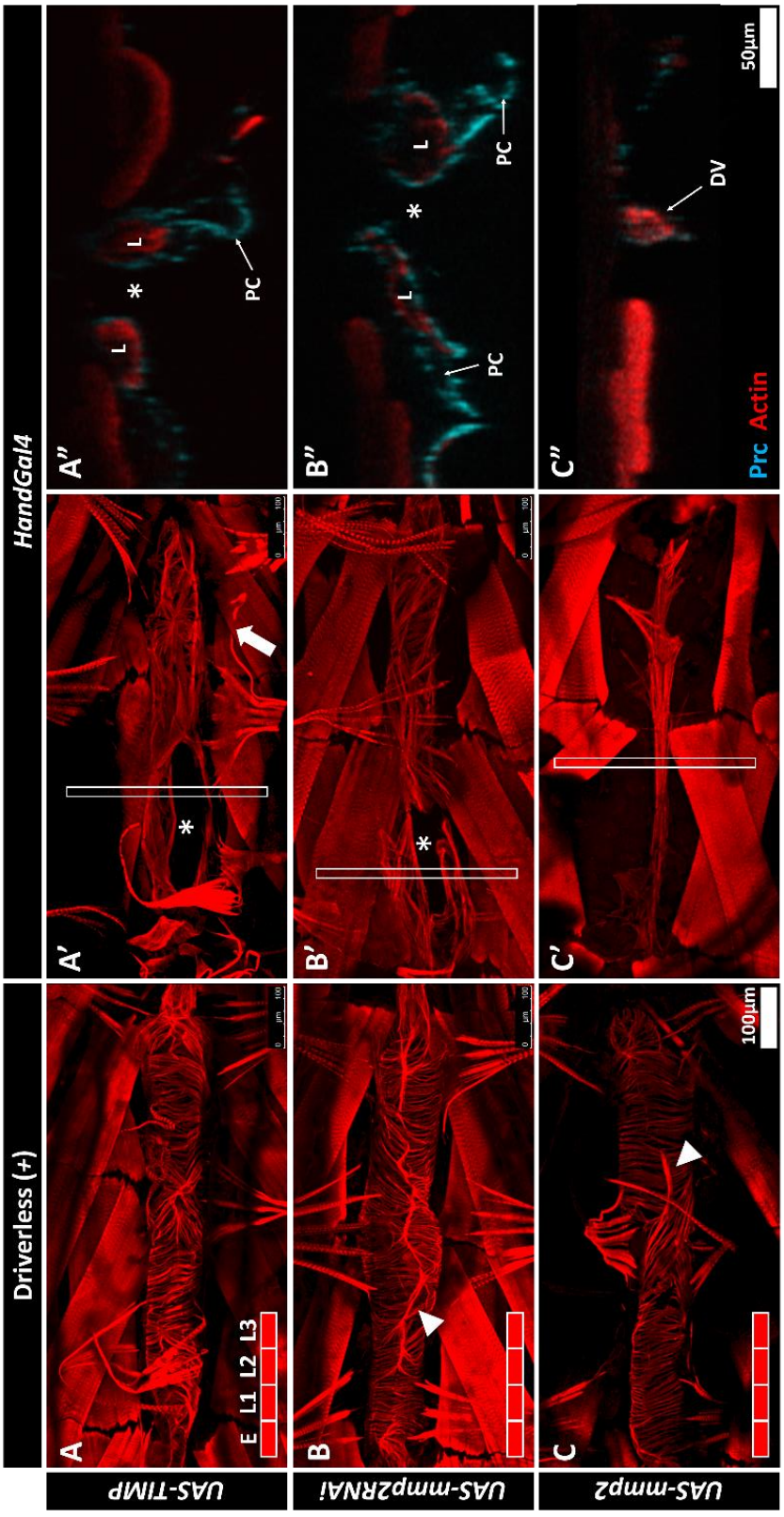
Driverless (+)
HandGal4
UAS-TIMP
UAS-mmp2RNAi
UAS-mmp2
A
A'
A''
B
B'
B''
C
C'
C''
E L1 L2 L3
100µm
50µm
PC
DV
L
Prc Actin

Figure 3.12: Altered expression of *Mmp2* within cardiac cells results in aberrant dorsal vessel morphology in late third instar larvae. DV segments A6 and A7 **(A,B,C)** Late third instar driverless controls reared at 29°C show no indication of cardia bifida. Myofibrils are circumferentially arrayed in parallel along the length of the vessel, though some longitudinal bundling is observed at the midline (arrowheads). **(A'-A")** Over-expression of *Timp* in cardiac cells with *HandGal4* is sufficient to cause cardia bifida (asterisks show gap between vessels). Alary muscle fibres extend longitudinally along the perimeter of the vessel, and are nearly continuous between primary attachment sites (arrow in A'). **(B'-B")** Localised inhibition of *Mmp2* with dsRNA in cardiac cells results in a phenotype similar to *Timp* over-expression. **(C'-C")** Larvae over-expressing *Mmp2* in cardiac cells have a reduced dorsal vessel and lack alary muscles. Myofibrils are arranged longitudinally along the vessel, and the lumenal cavity is reduced or non-existent. White rectangles on the coronal projections designate the regions shown in cross-section. DV: dorsal vessel; L: lumen; PC: pericardial cell.

Late third instar larvae exhibited cardia bifida at a rate of 3% (1/35) when TIMP was over-expressed in cardiac cells throughout embryonic and larval development, and at a rate of 33% (3/9) when over-expression occurs only during embryogenesis. Examination of the hearts of those specimens over-expressing TIMP that survive eclosion did not reveal the presence of pronounced morphological defects such as cardia bifida (Fig. S4). Cardia bifida was not observed when TIMP is over-expressed post-embryonically.

TIMP is a secreted protein and was therefore expected to act on surrounding tissues. Over-expression of TIMP in ectodermal stripes using *pairedGal4* was previously shown by Raza (2015) to disrupt cardiac lumenogenesis. However, ectopic expression of TIMP within the fat body using the *R4Gal4* driver did not appear to cause conspicuous cardiac defects upon examination of late third instar larvae; a majority of samples (15/16) revealed no myofibrillar disorganisation, whereas a minority (1/16) showed some disorganisation in the form of small gaps and longitudinal arrangement of myofibrils (Fig. S5).

3.2.3 Over-expression of MMP2 results in a novel cardiac phenotype

Over-expression of MMP2 protein, which localises to the leading edge of migrating cardioblasts during cardiogenesis (Raza *et al.* 2017) was predicted to promote the expansion of the junctional domain at the expense of the pre-lumenal domain in a manner similar to, if more extreme than, the loss of MMP1 function. Raza *et al*. (2017) observed disorganised cardioblast migration and the formation of multiple ectopic pocket lumens in embryos expressing *UAS-mmp* under the control of the muscle cell driver *mef2Gal4*.

Embryos ubiquitously over-expressing MMP2 were not viable, and temperature-shifted organisms with the *daGal80* driver experienced mortality within hours of being transferred to the non-permissive temperature (29°C). As such, the *HandGal4* driver was used exclusively.

Localised over-expression within cardiac cells resulted in the development of catastrophic cardiac defects but not immediate lethality. The dorsal vessel appeared truncated upon MMP2 over-expression throughout embryonic and larval development, leaving only the posterior-most segments (Fig. 3.12C). The anterior aorta was either entirely absent or formed a thin thread of Actin fibres. Lumenogenesis was compromised, such that either no lumen formed, or a reduced lumen emerged over a limited span of the vessel length. Myofibrils were arranged longitudinally along the vessel. Alary muscles were absent, with the exception of vestigial spurs at the posterior end of the vessel. Pericardial cells were likewise absent, with the exception of a minority of specimens that retained at most one or two such cells, which appeared degraded and were reduced in size. The loss of pericardial cells and alary muscles has been demonstrated to occur upon reduction of Lan, Vkg, or Prc function (Wolfstetter and Holz 2012; Drechsler *et al.* 2013; Hollfelder *et al.* 2014). However, explicit evidence of detachment was not observed. The gross morphology and myofibrillar arrangement of the dorsal vessel at third instar closely resembled that described by Drechsler *et al*. in both *loh* and *prc* trans-heterozygous deficiency mutants (Drechsler *et al.* 2013). This suggests that increased expression of

MMP2 during development may compromise cell polarisation and act to destabilise cell-matrix adhesions.

Temporal regulation of *Mmp2* expression was performed using *HandGal4* without the temperature-sensitive *Gal80^{TS}* allele. The full effect of MMP2 cardiac over-expression was partially mitigated (dampened) by rearing organisms at 18°C, though some *Gal4* activity persisted (personal observations). Individuals reared at the low temperature throughout embryogenesis successfully formed a posterior lumen, and possessed alary muscles and pericardial cells. However, pericardial cells were reduced in number and often flanked by smaller as-yet unidentified cells that were possibly hemocytes. It was not uncommon for alary muscles and nearby pericardial cells to appear under strain, and these were observed to pull away from the vessel (Fig. S6). The contractile heart chamber (A5 to A8) revealed some myofibrillar disorganisation in the form of gaps and longitudinal arrangement of fibrils but did enclose a lumen. Dampened over-expression of MMP2 appeared to more severely affect the anterior aorta, as this was reduced to a vestigial thread of Actin, and along this stretch pericardial cells were disorganised or entirely absent. The aorta was often observed to be anteriorly detached, possibly due to adhesion defects stemming from increased MMP2 activity at the lymph glands. Early and late third instar larvae transferred to 29°C at second instar resembled those reared entirely at 18°C. The increased expression of MMP2 during larval development with *HandGal4* was thus insufficient to induce the detachment of pericardial cells and alary muscles from the dorsal vessel. Localised over-expression of MMP2 limited to embryogenesis and first instar

revealed a similar phenotype to constitutive expression when larvae were examined at third instar, suggesting that no significant repair occurs between second instar and pupal remodelling.

3.2.4 Summary of cardiac structure

Organism-wide and heart-specific reduction of MMP2 function during embryogenesis was correlated with cardia bifida in larvae. Post-embryonic reduction of MMP2 was correlated with incomplete lumens. Reduced MMP1 function was correlated with disorganised cytoskeletal features but not compromised lumens. Organism-wide and heart-specific reduction over-expression of TIMP did not cause a cardiac phenotype obviously different from reduced MMP2 function. Over-expression of MMP2 was correlated with a truncated heart lacking an aorta, pericardial cells, and alary muscles.

3.3 Characterisation of Collagen-IV localisation and protein levels upon altered MMP expression

This section examines Collagen-IV protein levels and spatial localisation using a GFP gene trap construct (referred to here-on as Vkg-GFP). Protein levels were assumed to be proportional to the measured fluorescence signal, based on the protocols established by Acker (2016) and Cevik (2016). Quantitative data were generated by measuring the mean fluorescence signal within a consistent region of interest (ROI) comprising dorsal vessel segment A7 (see Methods). It is necessary to note that fluorescence signal does not directly correlate to protein expression; rather, it is a measure of protein levels within a specific region and so is affected by altered or aberrant patterns of localisation.

3.3.1 Characterisation of Collagen-IV protein levels and localisation in third instar larvae

In wildtype organisms, Collagen-IV was distributed along the lumenal and ablumenal domains of the cardiomyocytes, encompassing the pericardial cells. Although a majority of wildtype organisms revealed a uniform distribution of Collagen-IV, dense aggregates (plaques) were occasionally observed along portions of the lumenal or ablumenal surface (Fig. 3.13). Here plaques are defined as non-free-floating aggregates that either a) coat the ablumenal DV or PC surface, or b) coat the lumenal surface of the DV and obstruct no more than 50% of the lumenal space when viewed in cross-section. In severe cases, plaques expanded and coalesced to obstruct a majority or the entirety of the

lumenal space. However, such plaques have not been observed in cross-sectional electron micrographs of wildtype larvae without the Vkg-GFP trap construct (data not shown).

Collagen-IV protein levels are known to increase with age in *Drosophila* throughout both larval development and adult aging (Acker 2016; Vaughan *et al.* 2017). I verified these larval findings in dorsal vessel segment A7 through the quantification of mean Vkg-GFP signal (i.e. Collagen-IV density) to correct for differences in vessel size (Fig. 3.14). To determine whether temperature impacts Collagen-IV expression, I reared control larvae expressing Vkg-GFP at 18°C and 29°C. Neither early nor late third instar larvae reared at 29°C showed an obvious difference in mean protein density from their same-age counterparts reared at 18°C. Plaques were apparent in more individuals reared at 29°C (2/18) than 18°C (0/12), but exclusion of these individuals did not significantly alter the observed trend.

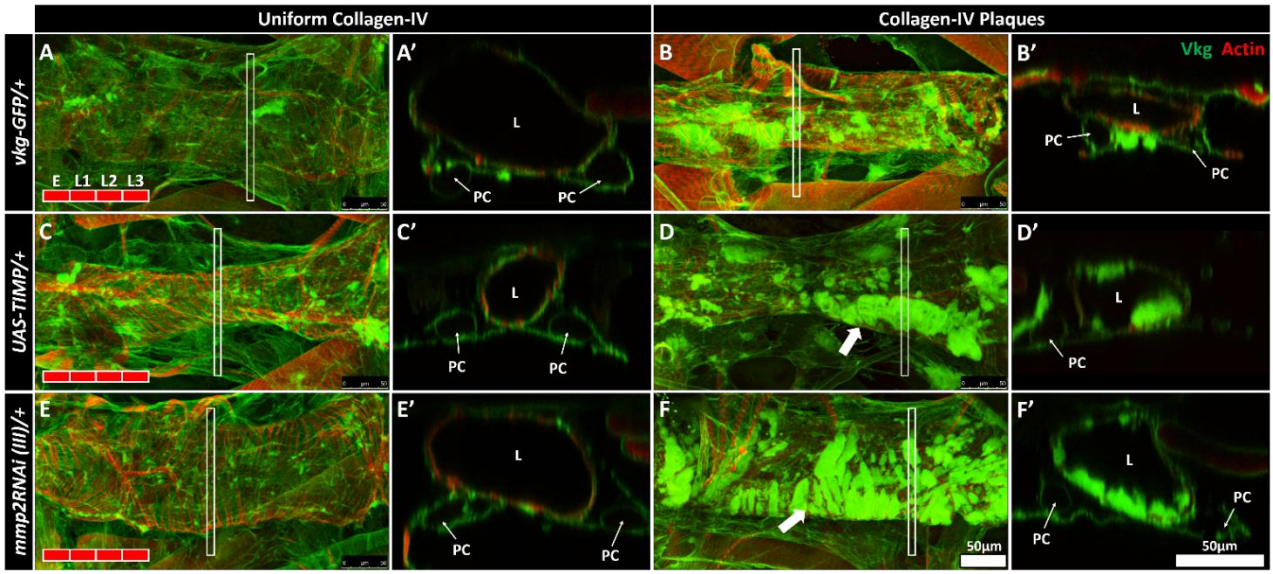

Figure 3.13: Collagen-IV is variably expressed in third instar larvae. Coronal projections and cross-sections of DV segments A6 and A7. Conjugated Phalloidin (**red**) labels Actin myofibrils. Endogenously expressed Vkg-GFP (GFP trap construct; **green**) labels Collagen-IV. **(A-B)** *vkg-GFP* controls raised at 29°C. **(A-A')** Collagen-IV is uniformly distributed along the DV. **(B-B')** Small aggregates (plaques) of Collagen-IV are associated with the ablumenal surface of the DV and PCs. **(C-D)** *UAS-TIMP* controls raised at 29°C. **(C-C')** Collagen-IV is uniformly distributed along the DV with the exception of small, discrete aggregates. **(D-D')** Dense Collagen-IV plaques are associated with the lumenal surface of the DV and the extracellular space surrounding the PCs. Plaques are nested between Actin myofilaments (arrow). Collagen-IV remains associated with the ablumenal DV surface and does not fill the lumenal cavity. **(E-F)** *mmp2RNAi(III)* controls raised at 29°C. **(E-E')** Vkg is uniformly distributed along the DV. **(F-F')** Vkg plaques are associated with the lumenal surface of the DV, but do not fill the lumenal cavity. White rectangles on the coronal projections designate the regions shown in cross-section. L: lumen; PC: pericardial cell.

3.3.2 Characterisation of Collagen-IV levels and localisation in *mmp* mutant larvae

mmp2 and *mmp1,mmp2* double mutants were notable for the aggregation of lumenal Collagen-IV, which manifested as large, dense clumps located principally within or adjacent to the site(s) of bifurcation (Fig. 3.15, Fig. 3.16). These aggregates completely obstructed the lumen along a portion of the vessel's length and were considered distinct from plaques. A majority of third instar homozygous *mmp2* and *mmp1,mmp2* double mutants (59-68% and 65%, respectively) exhibited lumenal obstruction by Collagen-IV aggregates, whereas this phenotype was not observed in the wildtype, and very rarely amongst heterozygous *mmp2* mutants and homozygous *mmp1* mutants (Fig. 3.17). Such lumenal aggregates were observed in late second instar homozygous *mmp2* mutant larvae (Fig. 3.16), suggesting that this phenotype emerges relatively early during larval development.

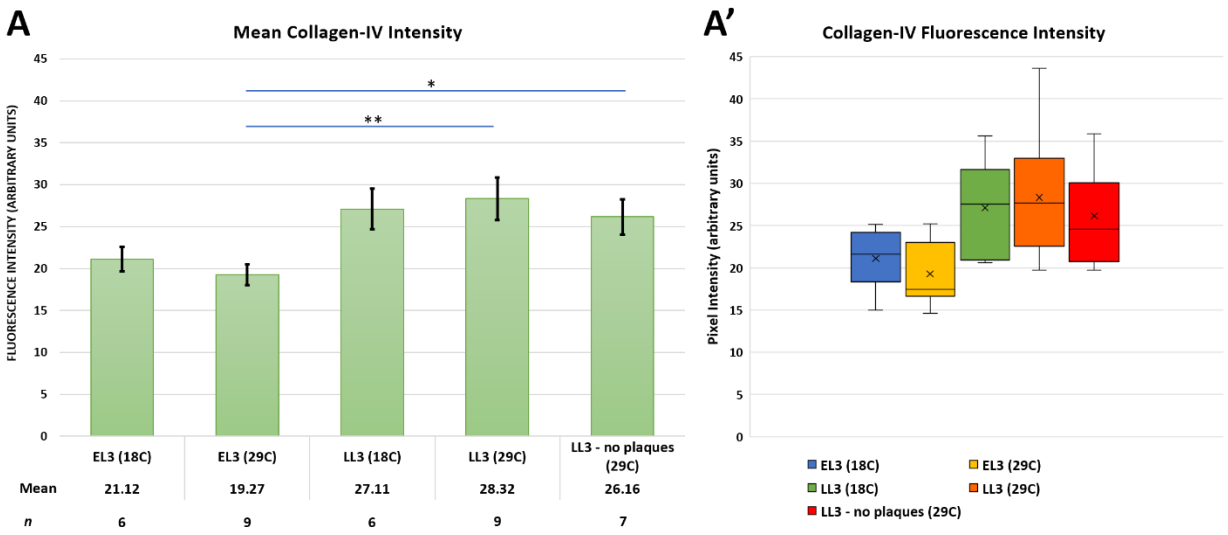

Figure 3.14: Collagen-IV protein level is increased in older larvae but is not affected by temperature. Quantification of endogenous Vkg-GFP signal at DV segment A7 in late third instar larvae. **(A-A')** Late third instar larvae show increased mean Vkg-GFP signal when compared to early third instar larvae, but this difference is only significant in larvae reared at 29°C. Same-age larvae do not show any difference in mean Vkg-GFP signal when reared at 18°C or 29°C. Exclusion of specimens exhibiting Collagen-IV plaques does not alter this trend. Two-tailed Welch's t-test test for parametric data. Error bars are SEM. * p≤0.05 ** p≤0.01 *** p≤0.005. **(A')** X is the mean. Horizontal bar is the median. Box is the first to third quartile. Whiskers show minimum and maximum values before the fence (1.5 x IQR). Genotype is *yw;vkg-GFP/+*. EL3: Early third instar larva; LL3: late third instar larva.

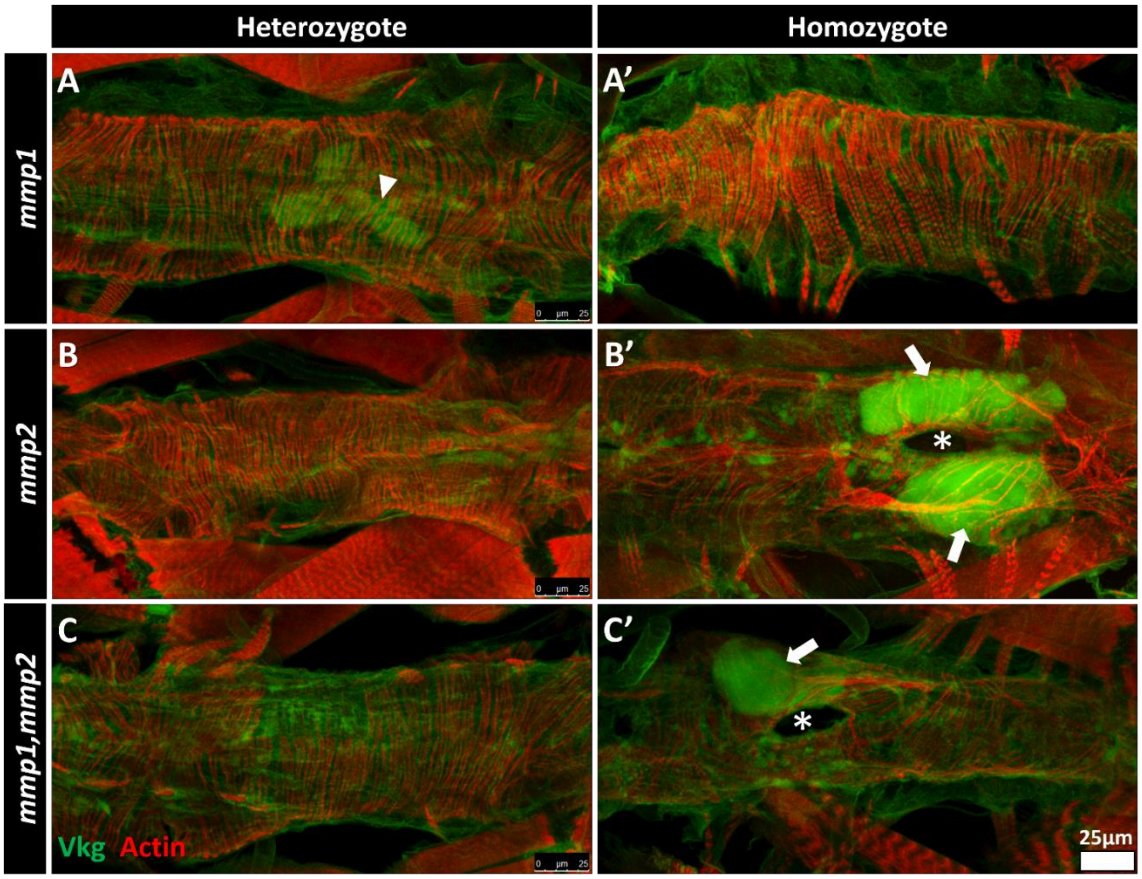

Figure 3.15: Collagen-IV localisation in hetero- and homozygous *mmp* mutant early third instar larvae. DV segment A7. **(A-A')** Collagen-IV is evenly distributed along the length of the cardiac vessel in hetero- and homozygous *mmp1* mutants, with the exception of some small ablumenal plaques (arrowhead in A). **(B)** Collagen-IV is evenly distributed along the length of the cardiac vessel in heterozygous *mmp2* mutants. **(B')** Conspicuous lumenal Collagen-IV aggregates (arrows) are apparent in homozygous *mmp2* mutants, particularly in close proximity to regions exhibiting bifurcation (asterisk shows gap between vessels). **(C-C')** *mmp1,mmp2* double mutants phenotypically resemble *mmp2* mutants.

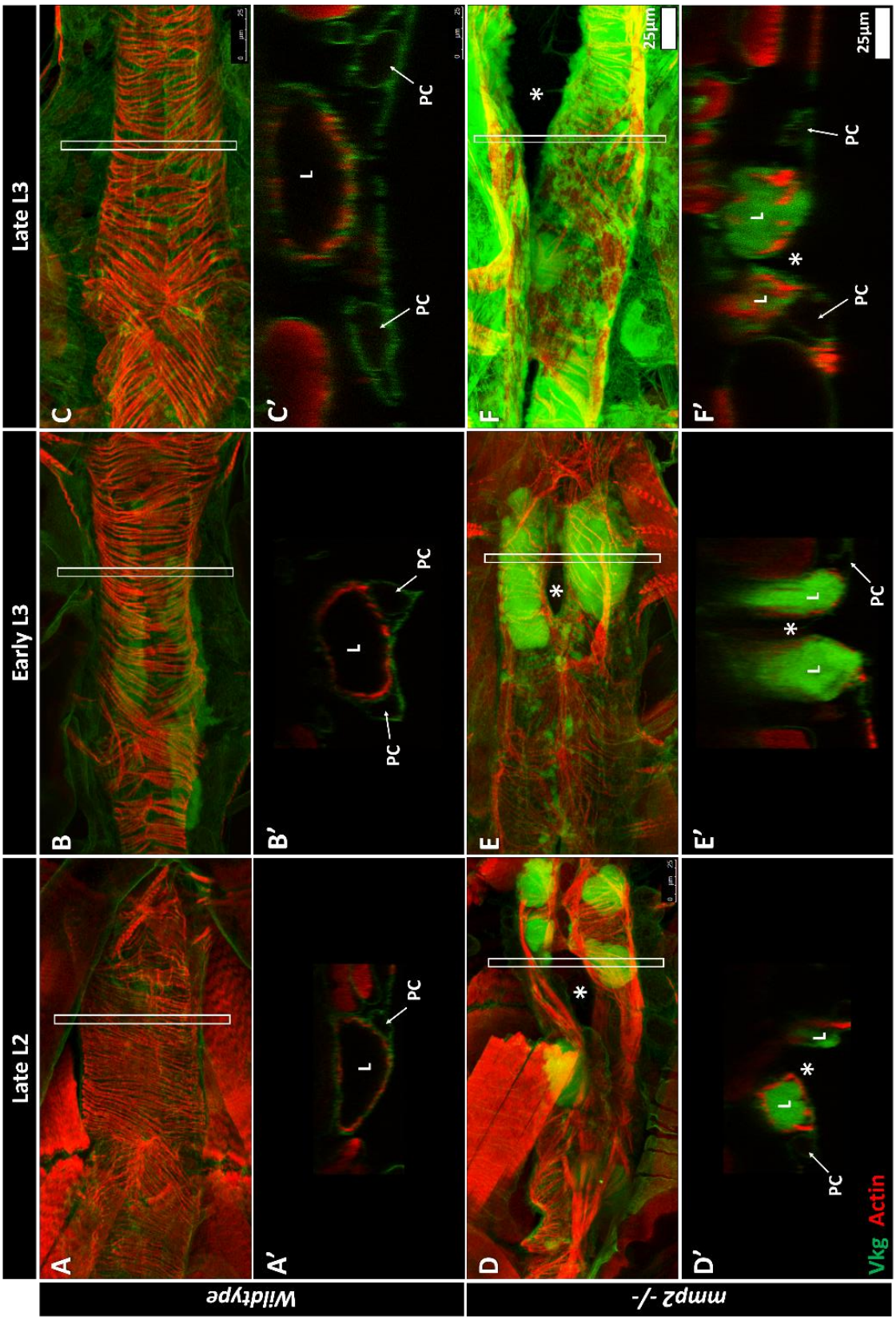
Late L2
Early L3
Late L3
Wildtype
mmp2 -/-
A
B
C
A'
B'
C'
D
E
F
D'
E'
F'
PC
L
*
25µm
Vkg Actin

Figure 3.16: Homozygous *mmp2* mutants exhibit cardia bifida and lumenal aggregation of Collagen-IV during second and third instar. DV segments A6 and A7. **(A-C)** Wildtype organisms display entire dorsal vessel lumens at late second instar **(A-A')**, early third instar **(B-B')**, and late third instar **(C-C')**. Coronal view shows uniform distribution of Collagen-IV along the cardiac vessel. Collagen-IV extends towards and envelops the PCs. **(A'-C')** Cross-sectional view showing uniform lumenal and ablumenal Collagen-IV distribution without significant aggregation within the lumenal space. **(D-F)** Homozygous *mmp2* organisms display cardia bifida (asterisks show gaps between vessels) at late second instar **(D-D')**, early third instar **(E-E')**, and late third instar **(F-F')**. Coronal view shows discrete accumulations of densely packed Collagen-IV along the cardiac vessel. Collagen-IV appears uniform outside of these aggregates, and extends towards and envelops the PCs. **(D'-F')** Cross-sectional view showing lumenal accumulation of Collagen-IV within a bifurcated region of the heart. Collagen-IV aggregates fill the entire lumenal space. *yw;vkg-GFP/+* is the wildtype. White rectangles on the coronal projections designate the regions shown in cross-section. L: lumen; PC: pericardial cell.

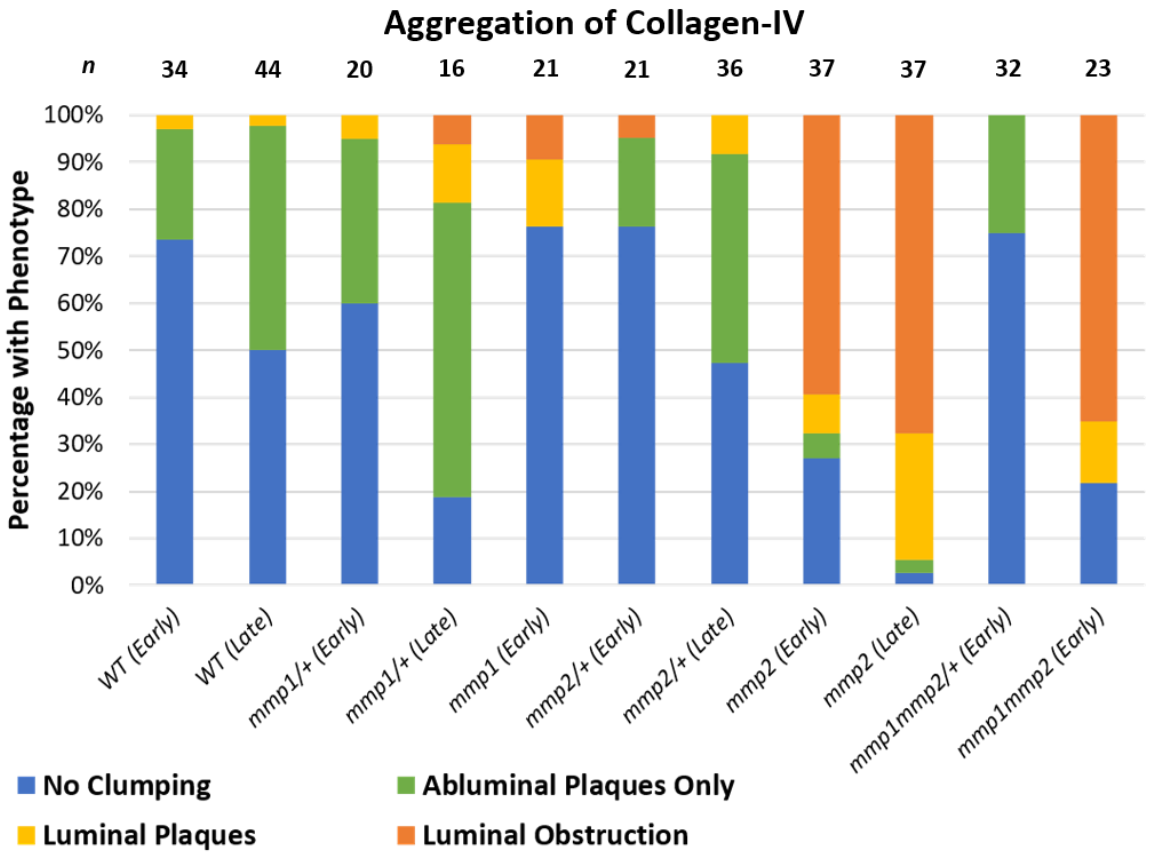

Figure 3.17: Third instar larvae mutant for *mmp2* reveal a high incidence of lumenal Collagen-IV aggregation. Endogenously expressed Vkg-GFP (GFP trap construct) labels Collagen-IV. No clumping (**blue**) indicates an even distribution of lumenal and ablumenal Collagen-IV along the length of the DV. Ablumenal plaques (**green**) indicates the presence of ablumenal but not lumenal plaques. Lumenal plaques (**yellow**) indicates the presence of lumenal plaques, with or without ablumenal plaques. Lumenal obstruction (**orange**) indicates complete coverage of the lumenal space by Collagen-IV at any point along the posterior DV, with or without lumenal or ablumenal plaques. Here lumenal plaques refer to Collagen-IV aggregates closely associated with the lumenal surface of the DV that cover not more than one half of the cross-sectional area. Wildtype organisms do not reveal lumenal Vkg-GFP aggregates at the posterior DV (segments A6-A7) beyond a low incidence of plaques (3% and 2% in early and late L3 larvae, respectively). Ablumenal plaques are present at a rate of 24% amongst early L3s (*n*=34) and 48% amongst late L3s (*n*=44). Complete lumenal obstruction by Vkg-GFP is observed in homozygous *mmp2* mutants at a rate of 10% amongst early L3 (*n*=21), in homozygous *mmp2* mutants at a rate of 59% amongst early L3 (*n*=37) and 68% amongst late L3 (*n*=37), and in homozygous *mmp1,mmp2* mutants at a rate of 65% amongst early L3s (*n*=32). *yw;vkg-GFP/+* is the wildtype.

Collagen-IV protein levels in and around the heart, as determined by fluorescence intensity, were elevated in homozygous but not heterozygous late third instar *mmp2* mutants when compared to the wildtype (Fig. 3.18). These findings were in line with those of Raza *et al.* (2017), who noted elevated Collagen-IV protein levels (lumenal and ablumenal) in stage 17 *mmp2* mutant embryos. Homozygous mutants showed a nearly two-fold increase in fluorescence signal along the DV compared to controls upon inclusion of samples with conspicuous Collagen-IV aggregates. Conspicuous Collagen-IV aggregates (including plaques) were observed in 48% (10/21) of the sampled homozygous mutants and 10% (2/20) of the sampled heterozygous mutants. Amongst homozygous mutants these comprised, on average, 25% of the measured area in samples within which aggregates were present, and exhibited a 6.8-fold increase in fluorescence signal per unit area over regions devoid of aggregates. Homozygous mutants lacking conspicuous aggregates still showed increased Collagen-IV protein levels at segment A7 when compared to the wildtype.

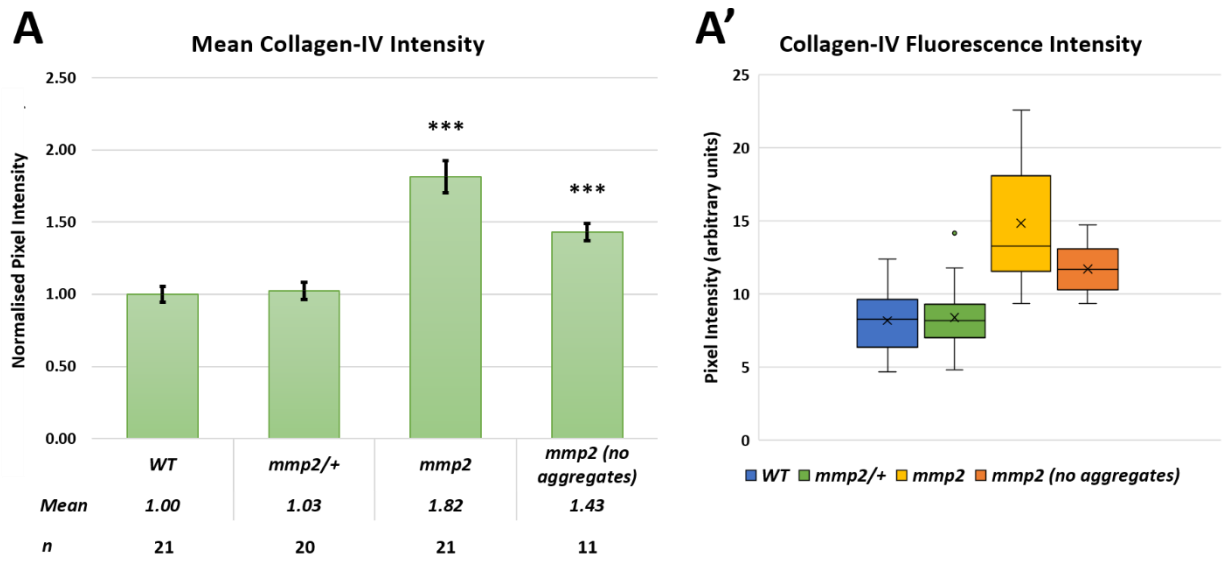

Figure 3.18: Collagen-IV protein level is increased in larval *mmp2* mutants in comparison to wildtype. Quantification of endogenous Vkg-GFP signal at DV segment A7 in late third instar larvae. **(A-A')** Homozygous but not heterozygous *mmp2* mutants show a significant increase in mean fluorescence signal compared to the wildtype. Removal of specimens with conspicuous lumenal Collagen-IV aggregates does not significantly alter this trend. **(A)** Mean fluorescence intensity is normalised to 1.00 with respect to wildtype levels. Kruskal-Wallis test for non-parametric data. Error bars are SEM. * p≤0.05 ** p≤0.01 *** p≤0.005. **(A')** X is the mean. Horizontal bar is the median. Box is the first to third quartile. Whiskers show minimum and maximum values before the fence (1.5 x IQR). Isolated data points are outliers or suspected outliers. Wildtype is *yw;vkg-GFP/+*.

3.3.3 Characterisation of Collagen-IV protein levels and localisation in third instar larvae over-expressing TIMP

Lumenal Collagen-IV aggregates were observed in early and late third instar larvae upon inhibition of MMP2 by ectopically expressed TIMP using the ubiquitous *daGal80* driver (Fig. 3.19) and the cardiac-specific *HandGal80* driver (Fig. 3.20). Aggregates were found principally near regions of the dorsal vessel exhibiting cardia bifida or otherwise disrupted lumens. Plaques were observed in all late third instar driverless *UAS-TIMP* control specimens reared at 29°C (7/7, with 1/7 showing very large, densely organised plaques), but in a minority of early third instars (3/19).

Collagen-IV protein levels in and around the heart, as determined by fluorescence intensity, were elevated in early and late third instar larvae over-expressing TIMP ubiquitously or in cardiac cells only throughout embryonic and larval development (Fig. 3.21). Early third instar larvae over-expressing TIMP from second instar onward did not show significantly altered Collagen-IV levels relative to controls. However, late third instar larvae did show a significant increase ($p<0.05$) in signal compared to the internal *daGal80* control reared at 18°C. This suggests that the reduction of MMPs and other TIMP targets during larval development impedes turnover, causing Collagen-IV to accumulate. Note that the measured fluorescence signal was inclusive of plaques and larger aggregates.

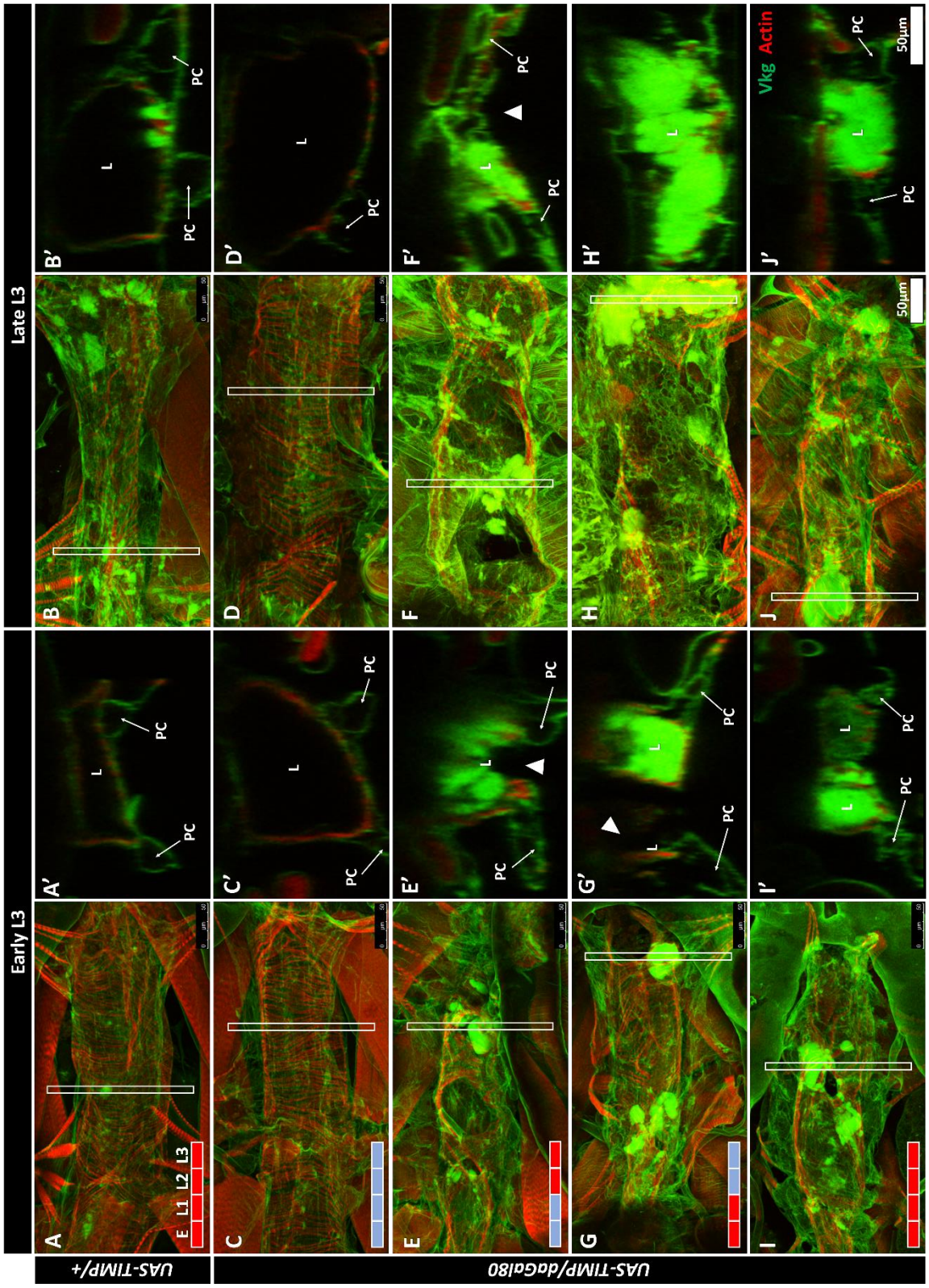
UAS-TIMP/+
UAS-TIMP/daGal80
Early L3
Late L3
A
A'
B
B'
C
C'
D
D'
E
E'
F
F'
G
G'
H
H'
I
I'
J
J'
L1 L2 L3
L
PC
Vkg Actin
50µm

Figure 3.19: Collagen-IV forms dense aggregates in early and late third instar larvae ubiquitously over-expressing *Timp*. DV segments A6 and A7. **(A-B)** *UAS-TIMP* driverless controls raised at 29°C. Collagen-IV is uniformly distributed along the DV with the exception of small plaques of Collagen-IV along the lumenal and ablumenal surface. **(C-J)** Over-expression of *Timp* under the regulation of a temperature-sensitive ubiquitous driver (*daGal80^{TS}*). **(C-D)** Organisms raised at the permissive temperature (18°C) throughout embryonic and larval development reveal a uniform distribution of Collagen-IV along the DV in early **(C)** and late **(D)** third instar larvae. **(C',D')** Cross-sections reveal a close association of Collagen-IV to the lumenal and ablumenal surface of the DV. **(E-F)** Organisms shifted from the permissive to non-permissive temperature (18 to 29°C) at second instar show dense Collagen-IV aggregates near regions with incomplete lumens. **(E',F')** Cross-sections reveal lumenal accumulation of Collagen-IV; aggregates fill a majority of the lumenal space in regions where the lumen is incomplete (arrowheads). **(G-H)** Organisms shifted from the non-permissive to permissive temperature (29 to 18°C) at second instar show similar Collagen-IV localisation to those shifted from 18 to 29°C. Incomplete lumens are evident and do not show accumulation of Collagen-IV (arrowhead in G'). **(I-J)** Organisms reared entirely at the non-permissive temperature (29°C) instar show a similar distribution of Collagen-IV when compared to temperature-shifted individuals. White rectangles on the coronal projection designate the region in cross-section. L: lumen; PC: pericardial cell.

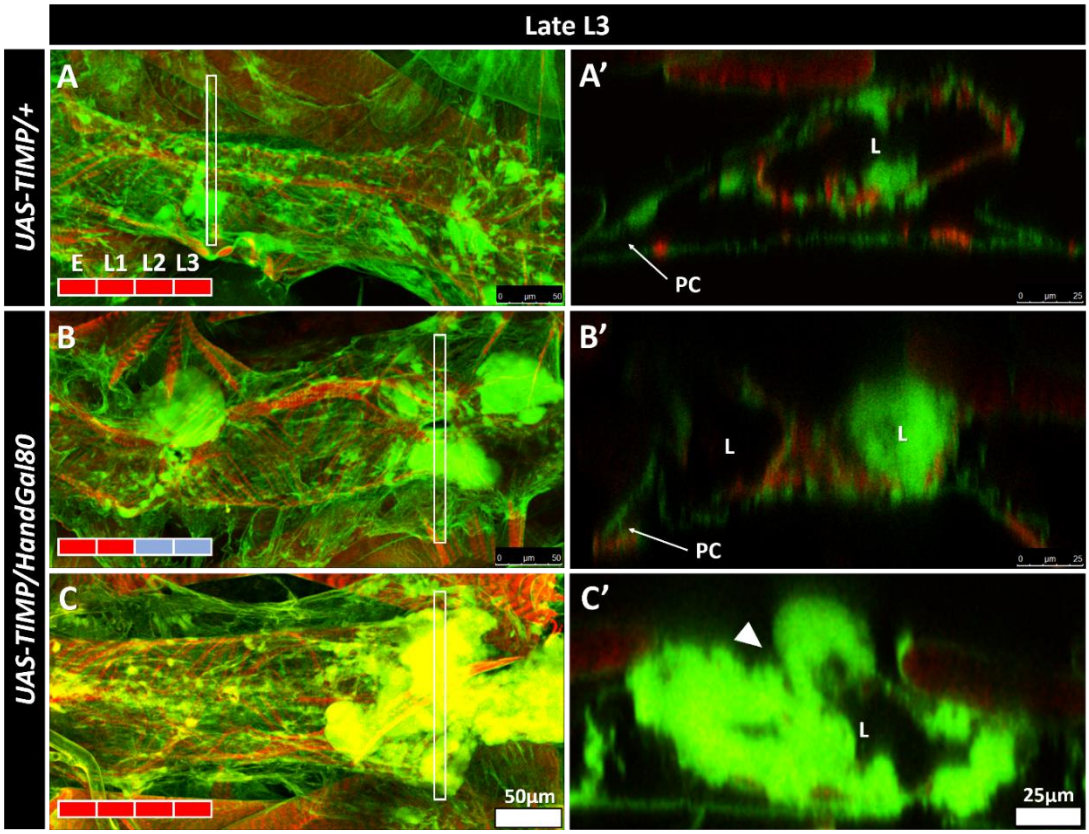

Figure 3.20: Collagen-IV forms dense aggregates in late third instar larvae over-expressing *Timp* in cardiac cells. DV segment A7. **(A-A')** *UAS-TIMP* driverless controls raised at 29°C. Collagen-IV is distributed along the DV and forms lumenal and ablumenal plaques. **(B-C)** Over-expression of *Timp* under the regulation of a temperature-sensitive cardiac cell driver (*HandGal80^{TS}*). **(B-B')** Dense lumenal aggregates are visible in larvae over-expressing *Timp* during embryogenesis and first instar (29 to 18°C shift), particularly at sites of bifurcation. **(C-C')** Organisms reared entirely at the non-permissive temperature (29°C) instar show a similar distribution of Collagen-IV to temperature-shifted individuals. **(C')** Cross-section of the posterior heart at a region exhibiting an incomplete lumen (no dorsal connection; arrowhead). White rectangles on the coronal projection designate the region in cross-section.

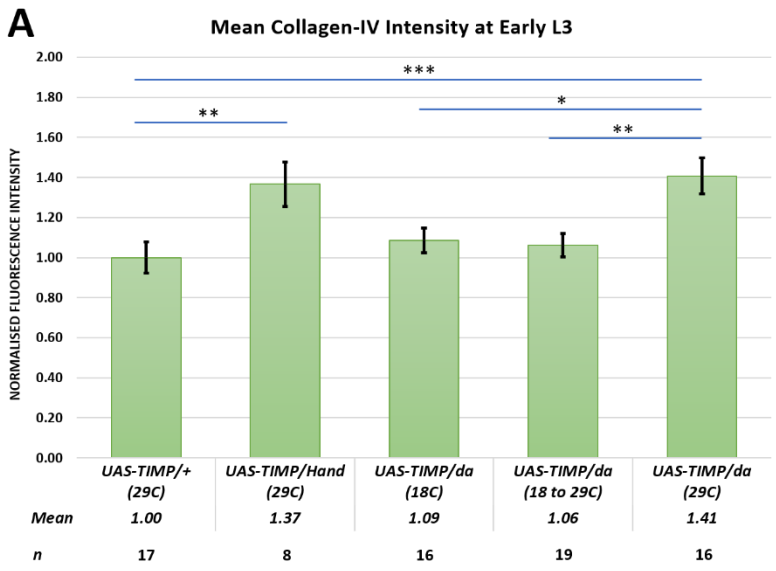
A
Mean Collagen-IV Intensity at Early L3
NORMALISED FLUORESCENCE INTENSITY
2.00
1.80
1.60
1.40
1.20
1.00
0.80
0.60
0.40
0.20
0.00
***
**
*
**
UAS-TIMP/+ (29C)
UAS-TIMP/Hand (29C)
UAS-TIMP/da (18C)
UAS-TIMP/da (18 to 29C)
UAS-TIMP/da (29C)
Mean 1.00 1.37 1.09 1.06 1.41
n 17 8 16 19 16

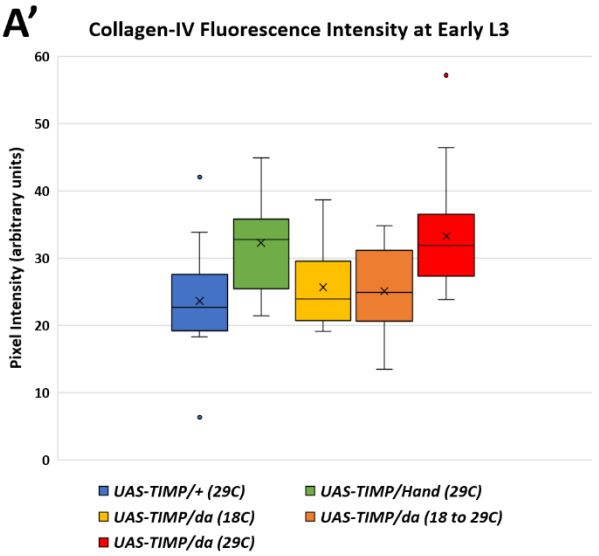
A'
Collagen-IV Fluorescence Intensity at Early L3
Pixel Intensity (arbitrary units)
60
50
40
30
20
10
0
UAS-TIMP/+ (29C)
UAS-TIMP/Hand (29C)
UAS-TIMP/da (18C)
UAS-TIMP/da (18 to 29C)
UAS-TIMP/da (29C)

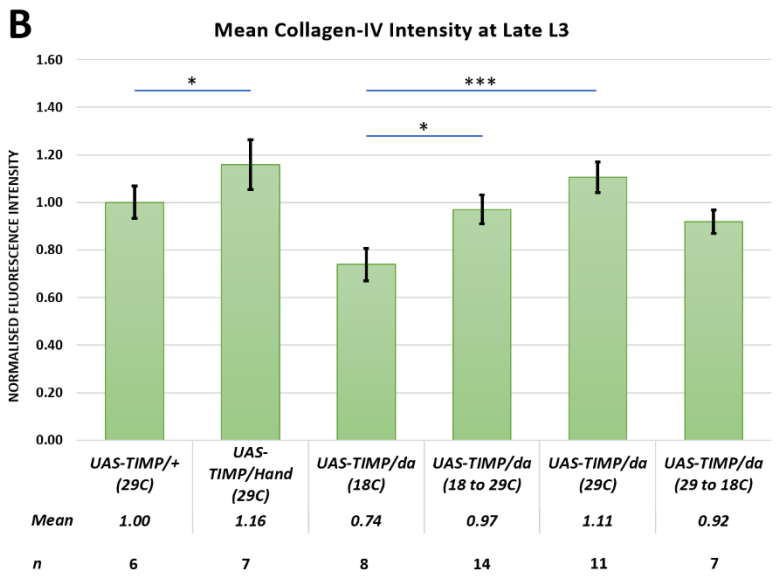
B
Mean Collagen-IV Intensity at Late L3
NORMALISED FLUORESCENCE INTENSITY
1.60
1.40
1.20
1.00
0.80
0.60
0.40
0.20
0.00
*
***
*
UAS-TIMP/+ (29C)
UAS-TIMP/Hand (29C)
UAS-TIMP/da (18C)
UAS-TIMP/da (18 to 29C)
UAS-TIMP/da (29C)
UAS-TIMP/da (29 to 18C)
Mean 1.00 1.16 0.74 0.97 1.11 0.92
n 6 7 8 14 11 7

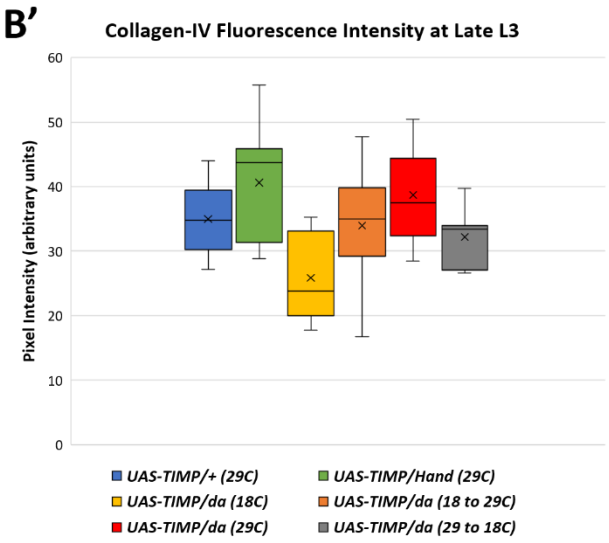
B'
Collagen-IV Fluorescence Intensity at Late L3
Pixel Intensity (arbitrary units)
60
50
40
30
20
10
0
UAS-TIMP/+ (29C)
UAS-TIMP/Hand (29C)
UAS-TIMP/da (18C)
UAS-TIMP/da (18 to 29C)
UAS-TIMP/da (29C)
UAS-TIMP/da (29 to 18C)

Figure 3.21: Collagen-IV protein level is increased in early third instar larvae over-expressing *Timp*. Quantification of endogenous Vkg-GFP signal at DV segment A7 in early and late third instar larvae. **(A-A')** Early third instar larvae. Vkg-GFP signal is significantly increased in samples locally over-expressing *Timp* within cardiac cells with *HandGal4* relative to the driverless *Timp* control. Vkg-GFP signal is significantly increased in samples ubiquitously over-expressing *Timp* within cardiac cells throughout embryonic and larval development with $daGal80^{TS}$ (29°C) relative to both control groups (*UAS-TIMP/+* at 29°C and *UAS-TIMP/da* at 18°C). **(B-B')** Late third instar larvae. Vkg-GFP signal is significantly altered in samples locally over-expressing *Timp* within cardiac cells with *HandGal4* relative to the driverless *Timp* control. Vkg-GFP signal is increased upon ubiquitous over-expression of *Timp* throughout embryonic and larval development with $daGal80^{TS}$ (29°C) relative to both control groups (*UAS-TIMP/+* at 29°C and *UAS-TIMP/da* at 18°C), but this difference is not significant in relation to the driverless *Timp* control. Vkg-GFP signal is significantly increased upon post-embryonic over-expression of TIMP (18 to 29°C) relative to the internal *daGal80* control (18°C) **(A,B)** Mean fluorescence intensity is normalised to 1.00 with respect to control levels. Kruskal-Wallis test for non-parametric data. Error bars are SEM. * $p \leq 0.05$ ** $p \leq 0.01$ *** $p \leq 0.005$. **(A',B')** X is the mean. Horizontal bar is the median. Box is the first to third quartile. Whiskers show minimum and maximum values before the fence (1.5 x IQR). Isolated data points are outliers or suspected outliers.

3.3.4 Characterisation of Collagen-IV protein localisation in third instar larvae expressing *Mmp2* dsRNA

vkg-GFP could not easily be recombined with the *UAS-mmp2RNAi* transposon insert capable of inducing cardia bifida (TRiP line 61309 on chromosome II) due to the proximity of both inserts. Therefore, the alternative *UAS-mmp2RNAi* (TRiP line 31371 on chromosome III) was used for analysis. Lumenal defects were not apparent upon ubiquitous or cardiac-specific expression of the *Mmp2* dsRNA. However, lumenal Collagen-IV plaques and complete lumenal obstruction by Collagen-IV aggregates was observed at a low incidence amongst the experimental genotypes and driverless controls (data not shown). Collagen-IV protein levels in and around the heart were not affected by the ubiquitous or cardiac cell-specific expression of *Mmp2* dsRNA upon examination of early and late third instar larvae. (Fig. 3.22).

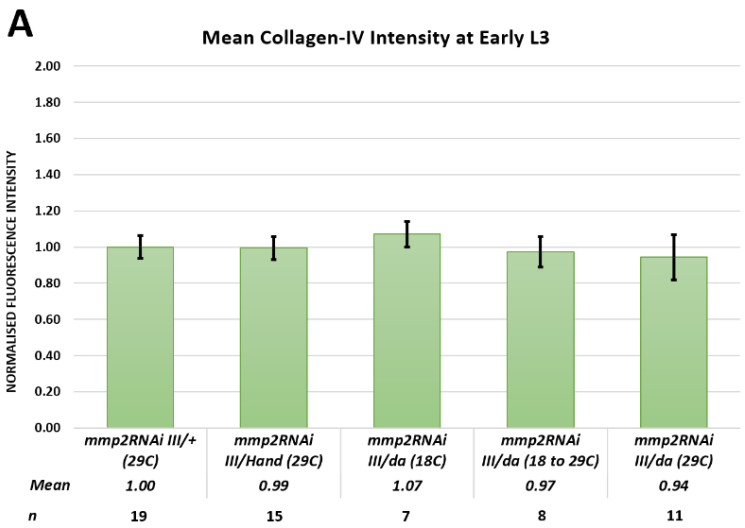
A
Mean Collagen-IV Intensity at Early L3
NORMALISED FLUORESCENCE INTENSITY
2.00
1.80
1.60
1.40
1.20
1.00
0.80
0.60
0.40
0.20
0.00
mmp2RNAi III/+ (29C)
mmp2RNAi III/Hand (29C)
mmp2RNAi III/da (18C)
mmp2RNAi III/da (18 to 29C)
mmp2RNAi III/da (29C)
Mean 1.00 0.99 1.07 0.97 0.94
n 19 15 7 8 11

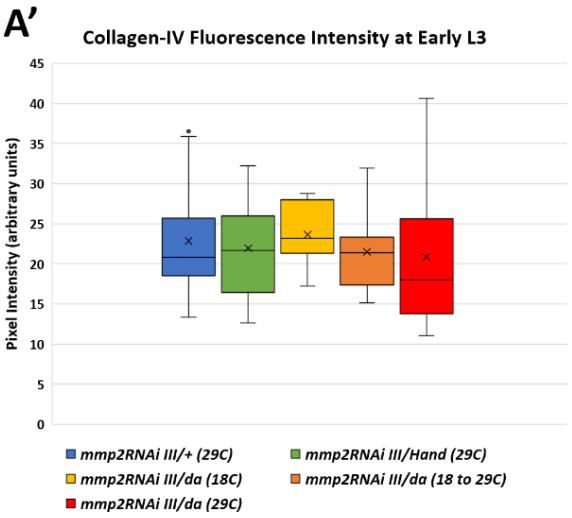
A'
Collagen-IV Fluorescence Intensity at Early L3
Pixel Intensity (arbitrary units)
45
40
35
30
25
20
15
10
5
0
mmp2RNAi III/+ (29C)
mmp2RNAi III/Hand (29C)
mmp2RNAi III/da (18C)
mmp2RNAi III/da (18 to 29C)
mmp2RNAi III/da (29C)

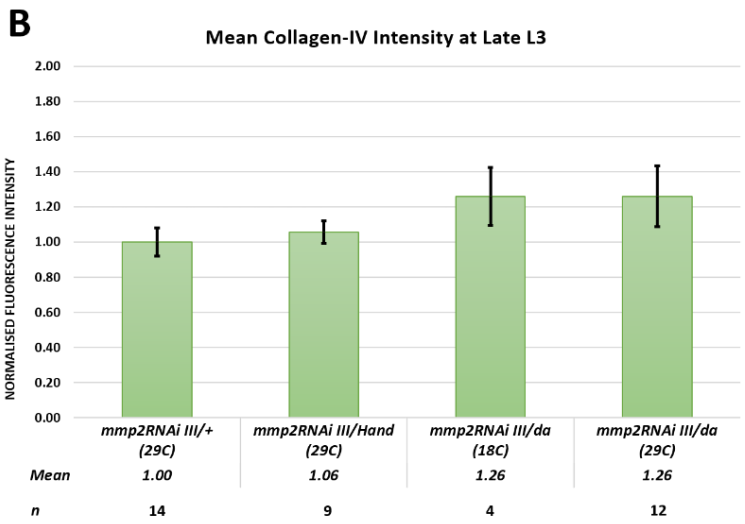
B
Mean Collagen-IV Intensity at Late L3
NORMALISED FLUORESCENCE INTENSITY
2.00
1.80
1.60
1.40
1.20
1.00
0.80
0.60
0.40
0.20
0.00
mmp2RNAi III/+ (29C)
mmp2RNAi III/Hand (29C)
mmp2RNAi III/da (18C)
mmp2RNAi III/da (29C)
Mean 1.00 1.06 1.26 1.26
n 14 9 4 12

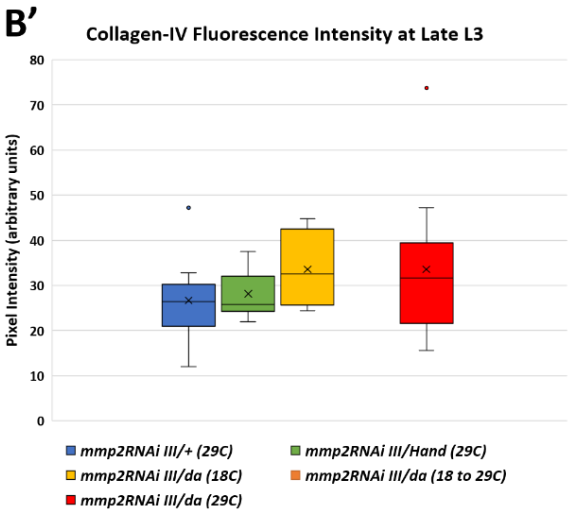
B'
Collagen-IV Fluorescence Intensity at Late L3
Pixel Intensity (arbitrary units)
80
70
60
50
40
30
20
10
0
mmp2RNAi III/+ (29C)
mmp2RNAi III/Hand (29C)
mmp2RNAi III/da (18C)
mmp2RNAi III/da (18 to 29C)
mmp2RNAi III/da (29C)

Figure 3.22: Collagen-IV protein level in third instar larvae with reduced *Mmp2* expression. Quantification of endogenous Vkg-GFP signal at DV segment A7 in early and late third instar larvae. **(A-A')** Early third instar larvae. Vkg-GFP signal is not significantly different from controls when *Mmp2* dsRNA is expressed ubiquitously (*daGal80^{TS}*) or locally within cardiac cells (*HandGal4*). **(B-B')** Late third instar larvae. Vkg-GFP signal is not significantly different from the driverless dsRNA control upon localised expression of *Mmp2* dsRNA with *HandGal4*. Vkg-GFP signal is elevated upon ubiquitous expression of *Mmp2* dsRNA throughout embryonic and larval development with *daGal80^{TS}* (29°C) relative to the driverless dsRNA control, but not the *daGal80^{TS}* internal control (18°C). This difference is not significant. **(A,B)** Mean fluorescence intensity is normalised to 1.00 with respect to control levels. Kruskal-Wallis test for non-parametric data. Error bars are SEM. * p≤0.05 ** p≤0.01 *** p≤0.005. **(A',B')** X is the mean. Horizontal bar is the median. Box is the first to third quartile. Whiskers show minimum and maximum values before the fence (1.5 x IQR). Isolated data points are outliers or suspected outliers.

3.3.5 Characterisation of Collagen-IV protein levels and localisation in third instar larvae over-expressing MMP2

Constitutive heart-specific up-regulation of *Mmp2* resulted in a greatly reduced dorsal vessel with severe structural defects. Collagen-IV was minimally present along the surface of the vessel vestige, with reduced expression beyond the immediate vessel periphery due to the lack of pericardial cells (Fig. 3.23G-H). Collagen-IV was present between the longitudinally arrayed Actin fibrils in specimens lacking a lumen (Fig. 3.23H'). When *UAS-mmp2* activity was dampened throughout embryogenesis (18°C) Collagen-IV was localised along the posterior vessel in a fashion similar to the wildtype (Fig. 3.23C-F). However, small plaques were common. Collagen-IV was localised to a lesser extent along the aortal remnant; fluorescence signal appeared reduced and is in some cases absent. In a minority of specimens, Collagen-IV appeared to form thick bundles at the vessel periphery, and exhibited an identical distribution to Prc (Fig. 3.24). It may be that these represent portions of the Collagen-IV network rendered inaccessible to MMP2 by surrounding proteins.

Vkg-GFP signal was significantly reduced ($p<0.005$) along the dorsal vessel when MMP2 was over-expressed constitutively from embryogenesis, even when considering the smaller surface area of the vessel (Fig. 3.25). No difference in signal was observed between controls and larvae over-expressing MMP2 from second instar onwards. This suggests that increasing MMP2 levels in the heart during larval development has little effect on local Collagen-IV levels.

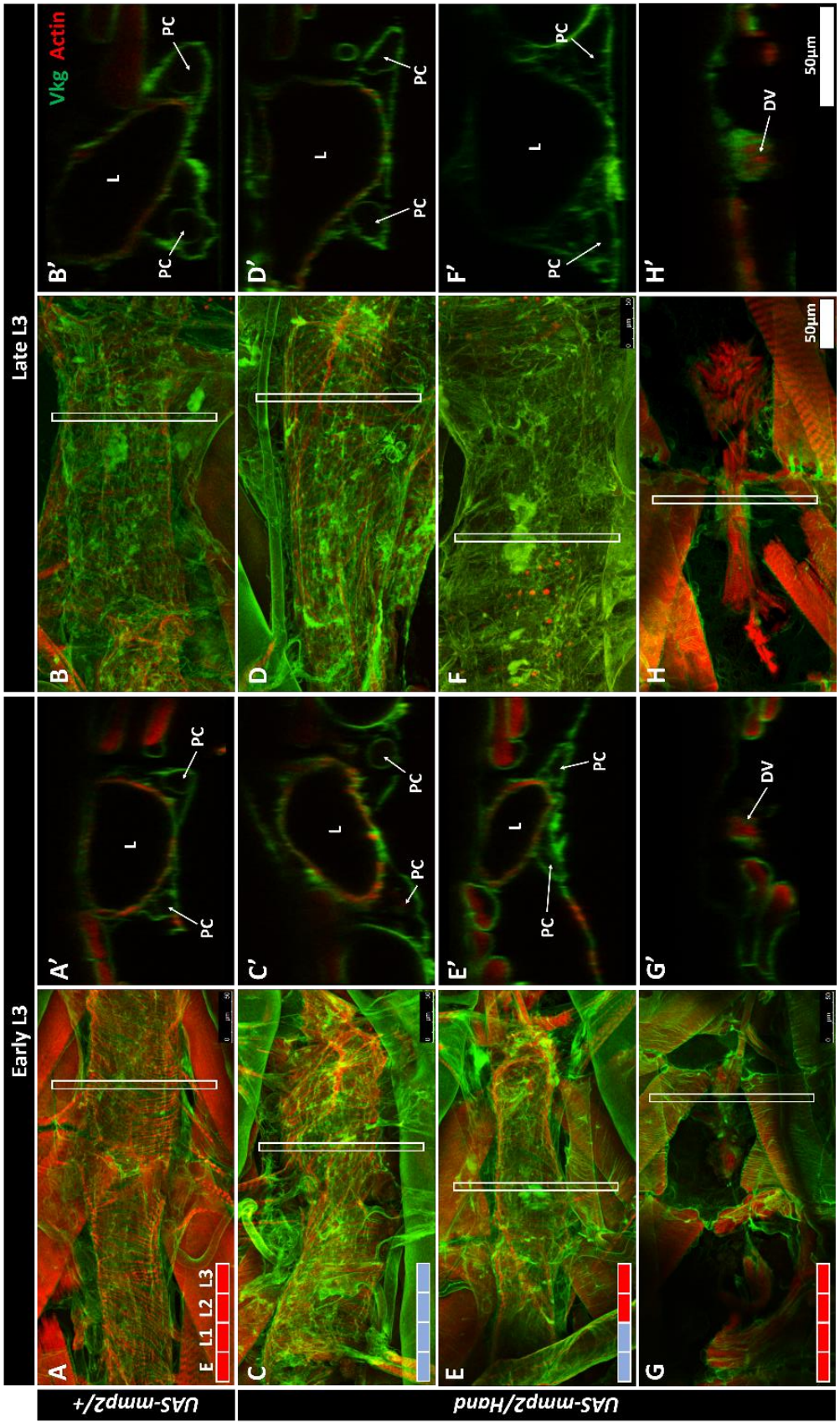
UAS-mmp2/+
UAS-mmp2/Hand
Early L3
Late L3
A
A'
B
B'
C
C'
D
D'
E
E'
F
F'
G
G'
H
H'
E L1 L2 L3
Vkg Actin
L
PC
DV
50µm

Figure 3.23: Collagen-IV localisation upon over-expression of *Mmp2* within the heart. DV segments A6 and A7. **(A-B)** Early and late third instar control larvae (*UAS-mmp2/+*) reared at 29°C reveal a uniform distribution of Collagen-IV with minimal clumping. Several small ablumenal plaques are apparent. **(C-H)** Early and late third instar larvae exhibiting cardiac-specific up-regulation of *Mmp2* with the *HandGal4* driver. **(C-D)** Organisms reared at 18°C show a similar distribution of Collagen-IV to the driverless control. **(E-F)** Collagen-IV shows a similar distribution to controls in organisms shifted from 18 to 29°C at second instar. Small ablumenal plaques are visible but these do not deviate from those observed in the wildtype. **(G-H)** In samples raised at 29°C, Collagen-IV appears more diffuse around the dorsal vessel. Expression along the vessel appears weaker, with pockets of high density. Collagen-IV envelops the exterior surface of the vestigial DV and is also present between the longitudinal Actin bundles comprising the structure. DV: dorsal vessel; L: lumen; PC: pericardial cell.

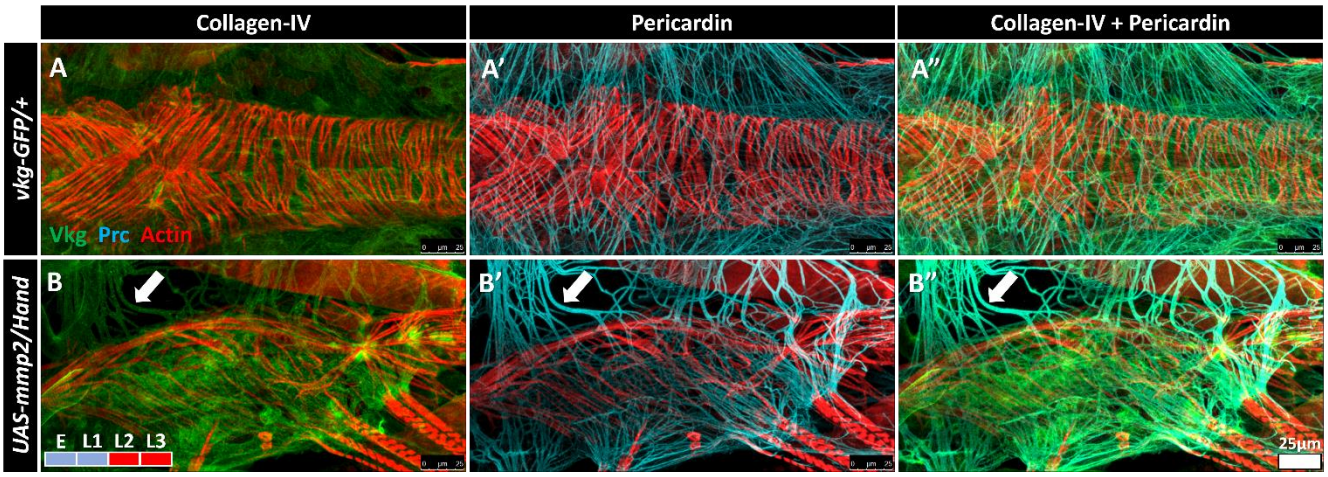

Figure 3.24. Collagen-IV and Pericardin co-localise upon over-expression of *Mmp2* within the heart. DV segment A7. Endogenously expressed Vkg-GFP (GFP trap construct; **green**) labels Collagen-IV. Vkg-GFP intensity is manipulated to ease viewing. Monoclonal Prc antibody (**cyan**) labels the Prc network. Conjugated Phalloidin (**red**) is used to visualise the dorsal vessel muscle fibres. **(A-A")** Late third instar wildtype control with Vkg-GFP insert. **(A)** Collagen-IV forms a uniform, sheet-like network along the DV. **(A')** Prc forms a uniform network of discrete bundles along the DV. **(A")** Overlay reveals different patterns of Collagen-IV and Prc localisation. **(B-B")** Over-expression of MMP2 is dampened from embryogenesis to second instar. **(B)** Vkg is aberrantly arrayed as a network of thick bundles along the periphery of the vessel. **(B')** Prc forms unusually thick bundles along the periphery of the vessel. **(B")** Overlay of Collagen-IV and Prc reveals the co-localisation of thick bundles (arrows).

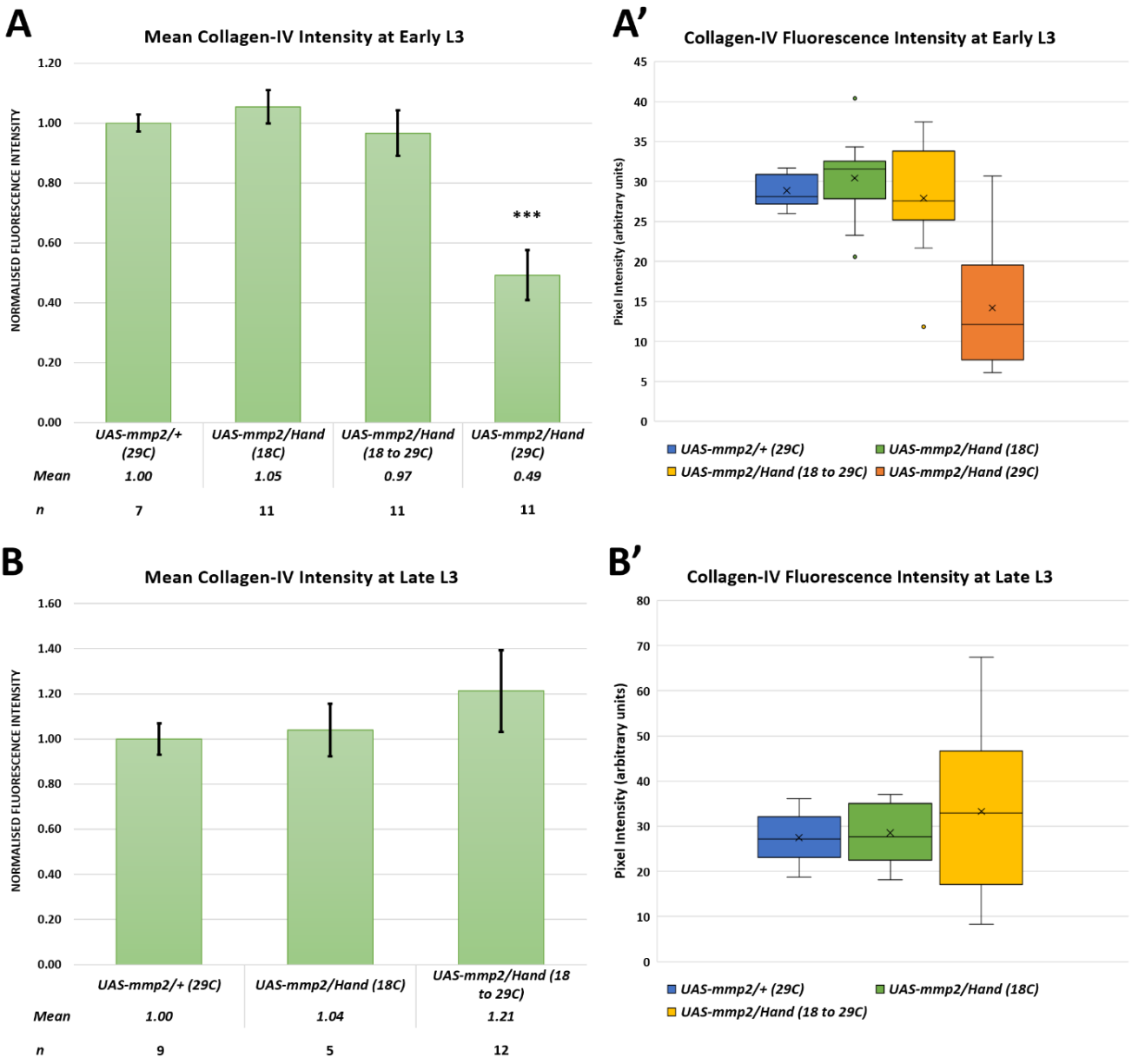
A
Mean Collagen-IV Intensity at Early L3
NORMALISED FLUORESCENCE INTENSITY
1.20
1.00
0.80
0.60
0.40
0.20
0.00
***
UAS-mmp2/+ (29C)
UAS-mmp2/Hand (18C)
UAS-mmp2/Hand (18 to 29C)
UAS-mmp2/Hand (29C)
Mean
1.00
1.05
0.97
0.49
n
7
11
11
11
A'
Collagen-IV Fluorescence Intensity at Early L3
Pixel Intensity (arbitrary units)
45
40
35
30
25
20
15
10
5
0
UAS-mmp2/+ (29C)
UAS-mmp2/Hand (18C)
UAS-mmp2/Hand (18 to 29C)
UAS-mmp2/Hand (29C)
B
Mean Collagen-IV Intensity at Late L3
NORMALISED FLUORESCENCE INTENSITY
1.60
1.40
1.20
1.00
0.80
0.60
0.40
0.20
0.00
UAS-mmp2/+ (29C)
UAS-mmp2/Hand (18C)
UAS-mmp2/Hand (18 to 29C)
Mean
1.00
1.04
1.21
n
9
5
12
B'
Collagen-IV Fluorescence Intensity at Late L3
Pixel Intensity (arbitrary units)
80
70
60
50
40
30
20
10
0
UAS-mmp2/+ (29C)
UAS-mmp2/Hand (18C)
UAS-mmp2/Hand (18 to 29C)

Figure 3.25: Collagen-IV protein level in third instar larvae over-expressing *Mmp2* in the heart. Quantification of endogenous Vkg-GFP signal at DV segment A7 in early and late third instar larvae. **(A-A')** Early third instar larvae. Vkg-GFP signal is not significantly different from the driverless *UAS-mmp2* control or the *daGal80^{TS}* internal control (18°C) when *Mmp2* is over-expressed within cardiac cells (*HandGal4*) after second instar. Constitutive over-expression from embryogenesis onwards is correlated with a significant reduction in signal when compared to controls. **(B-B')** Late third instar larvae. Vkg-GFP signal is not significantly different from controls upon localised over-expression of *Mmp2* dsRNA. Vkg-GFP signal shows a slight increase compared to both groups, likely due to the presence of plaques. Late third instar larvae showing constitutive over-expression are excluded due to low sample size. **(A,B)** Mean fluorescence intensity is normalised to 1.00 with respect to control levels. Kruskal-Wallis test for non-parametric data. Error bars are SEM. * $p \leq 0.05$ ** $p \leq 0.01$ *** $p \leq 0.005$. **(A',B')** X is the mean. Horizontal bar is the median. Box is the first to third quartile. Whiskers show minimum and maximum values before the fence (1.5 x IQR). Isolated data points are outliers or suspected outliers.

3.3.6 Summary of Collagen-IV protein levels and localisation

Collagen-IV density increased with age in larval hearts. Ubiquitous reduction of MMP2 function was correlated with increased Collagen-IV density along the dorsal vessel at segment A7, as well as Collagen-IV aggregates at sites of bifurcation. Over-expression of TIMP both ubiquitously and within cardiac cells resulted in a similar phenotype. Embryonic but not post-embryonic over-expression of MMP2 within cardiac cells was correlated with decreased Collagen-IV density.

3.4 Characterisation of Pericardin localisation and protein levels upon altered MMP expression

To determine the effect on the Pericardin (Prc) network of a loss of MMP-mediated turnover, I examined the spatial localisation and protein levels of fluorescently-labelled Prc in early and late third instar larvae. Protein levels were assumed to be proportional to the measured fluorescence signal, based on the protocols established by Acker (2016) and Cevik (2016). Quantitative data were generated by measuring the mean fluorescence signal within a consistent region of interest (ROI) located within segment A7 (see Methods). This ROI was extended as far as possible beyond the dorsal vessel midline to capture ectopic Prc bundles.

3.4.1 Characterisation of Pericardin protein levels and localisation

In wildtype organisms, Prc formed a uniform web-like superstructure that was distributed along the length of the dorsal vessel, and remained in close proximity to the cardiomyocytes. Prc was also localised along the larval fat body, from which it is secreted (Drechsler *et al.* 2013). Isolated Prc bundles were occasionally observed beyond the immediate periphery of the dorsal vessel. These bundles were not necessarily connected to the larger network. It is possible these filaments were in the process of recruitment to the heart, or were due to dissection-induced disruption of the Prc network. Prc fluorescence signal was highly variable between samples; even within genotypes there was a lack of consistency in signal intensity. This complicated quantitative analysis of protein levels.

3.4.2 Characterisation of Pericardin protein levels and localisation in *mmp* mutant larvae

Qualitative analysis of confocal projections revealed no obvious difference between the arrangement of the Prc network in heterozygous *mmp* mutants and the wildtype (Fig. 3.26). This held also for heterozygous *mmp1,mmp2* mutants lacking one functional copy of each *Mmp*. Homozygous *mmp1* mutants were likewise not conspicuously different from controls. Homozygous *mmp2* mutants exhibited some disorganisation of the Prc network; Prc bundles appeared more densely packed and longitudinally oriented along the separate vessels of bifurcated hearts (Fig. 3.27). Prc fibres fully enveloped the ablumenal domains of bifurcated vessels but were absent from the lumenal surface (Fig. 3.27C',D'). This is possibly a persistence of the ectopic medial Prc localised between non-adhering contralateral cardioblasts in *mmp2* mutant embryos, noted by Raza *et al*. (2017) Though the Prc network was largely absent from the intervening spaces, individual Prc bundles or small clusters of Prc bundles sometimes projected between the vessels. A fraction of these bundles appeared discontinuous across the intervening space, suggesting either breakage from mounting strain, or conversely the reparation or expansion of the network.

Contrary to predictions, mean Prc signal was not different between hetero- and homozygous *mmp2* mutants and the control at early third instar (Fig. 3.28). Prc signal was variable between specimens, although the highest signal was observed amongst homozygous *mmp2* mutants.

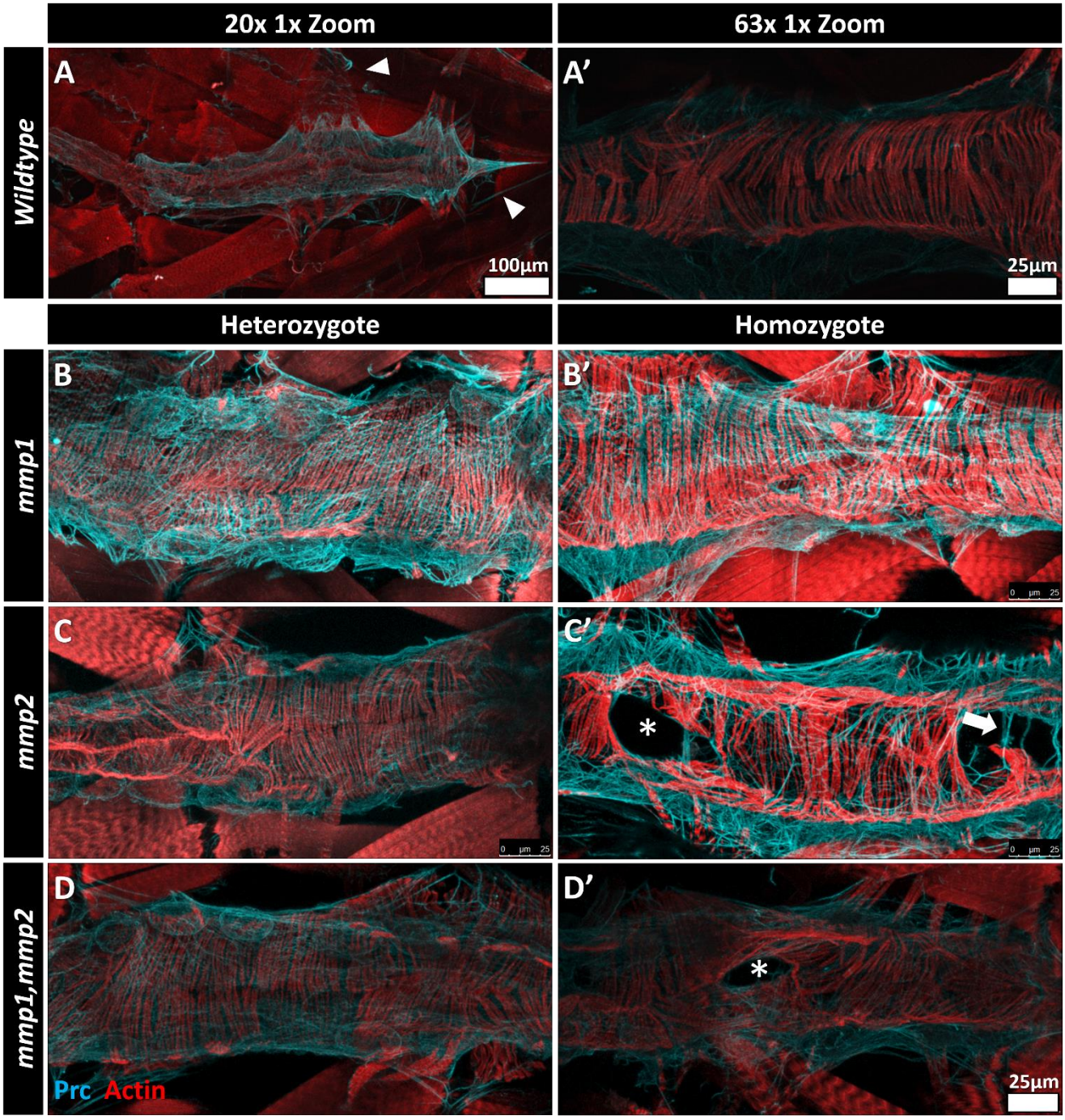
20x 1x Zoom
63x 1x Zoom
Wildtype
A
A'
100µm
25µm
Heterozygote
Homozygote
mmp1
B
B'
mmp2
C
C'
mmp1,mmp2
D
D'
Prc Actin
25µm

Figure 3.26: Pericardin localisation in early third instar hetero- and homozygous *mmp* mutant larvae. Coronal projections of DV segments A6 and A7 (posterior right). Monoclonal Prc antibody (**cyan**) is used to visualise the Prc network. Conjugated Phalloidin (**red**) is used to visualise the dorsal vessel muscle fibres. **(A-A')** Prc forms an evenly distributed network along the length of the posterior DV in wildtype organisms. Some ectopic Prc fibres are apparent beyond the periphery of the DV and in association with the alary muscles (arrowheads). **(B-B')** Prc is distributed along the length of the cardiac vessel in hetero- and homozygous *mmp1* mutants and is not visibly different from the wildtype. **(C)** Prc is evenly distributed along the length of the cardiac vessel in heterozygous *mmp2* mutants. **(C')** Isolated Prc bundles extend between the branched vessels (arrow) in homozygous *mmp2* mutants exhibiting cardia bifida (asterisk). Bundles are non-uniformly arranged near the regions of bifurcation. **(D-D')** *mmp1,mmp2* double mutants phenotypically resemble *mmp2* mutants. Wildtype is *yw;vkg-GFP/+*.

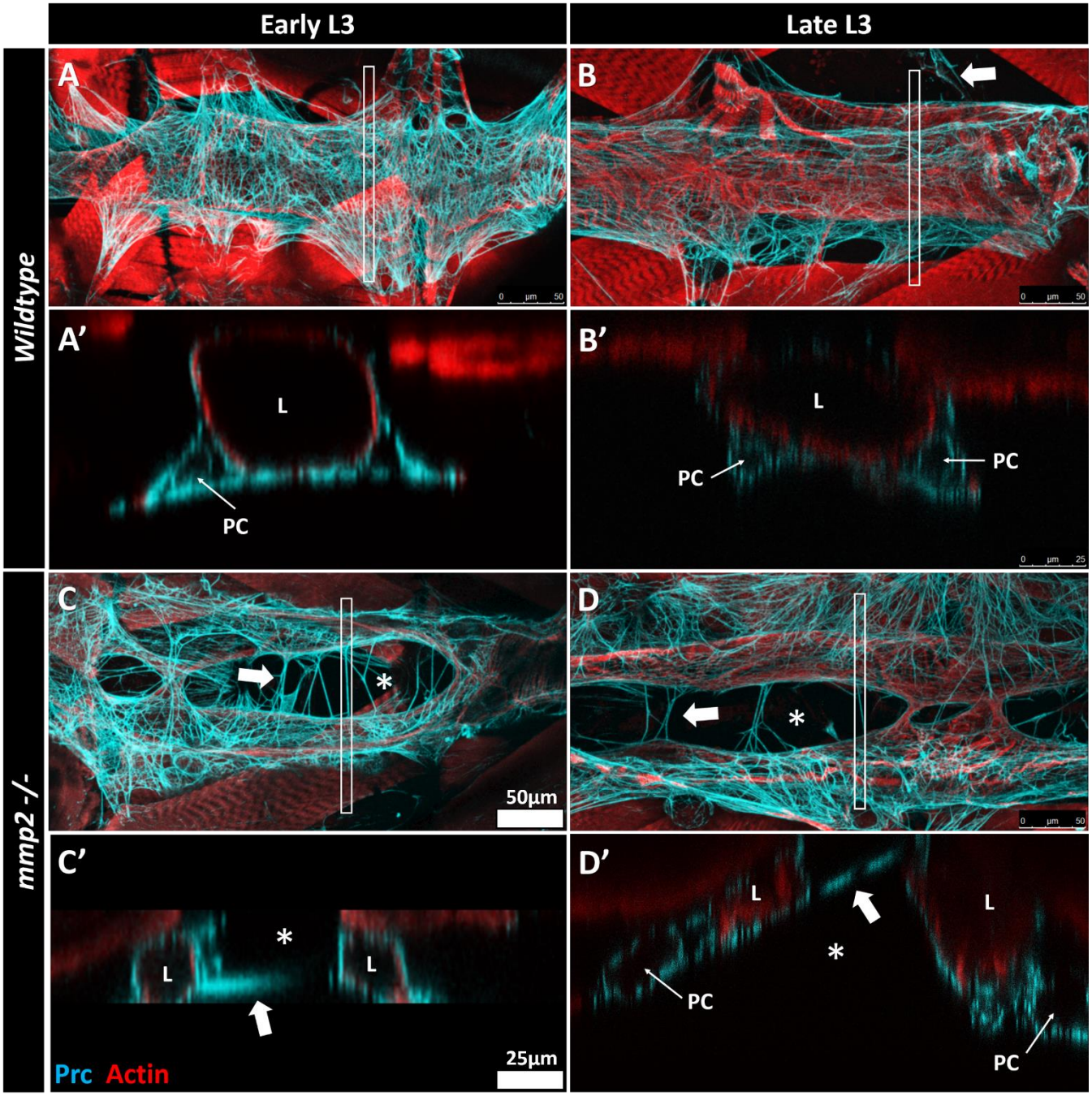
Early L3
Late L3
Wildtype
mmp2 -/-
A
B
A'
B'
C
D
C'
D'
L
PC
*
50µm
25µm
Prc Actin

Figure 3.27: Pericardin bundles are sparsely arrayed between bifurcated vessels of homozygous *mmp2* mutant larvae. DV segments A6 and A7. **(A-B)** Wildtype larvae at early **(A-A')** and late **(B-B')** third instar. Prc forms an evenly distributed network along the DV and PCs. Some ectopic Prc fibres are apparent (arrow in B). **(A',B')** Cross-sections reveal ablumenal but not lumenal distribution of Prc along the DV and PC surface. **(C-D)** Homozygous *mmp2* mutant larvae at early **(C-C')** and late **(D-D')** third instar. Prc forms a network along the DV and PCs, and is largely absent from the intervening space between bifurcated vessels (asterisks). Isolated Prc bundles traverse the region of bifurcation (arrows). **(C',D')** Cross-sections at the site of bifurcation reveal ablumenal but not lumenal distribution of Prc around both vessels. Prc bundles of varying thickness connect the bifurcated vessels. White rectangles on the coronal projections designate the regions shown in cross-section. L: lumen; PC: pericardial cell. Wildtype is *yw;vkg-GFP/+*.

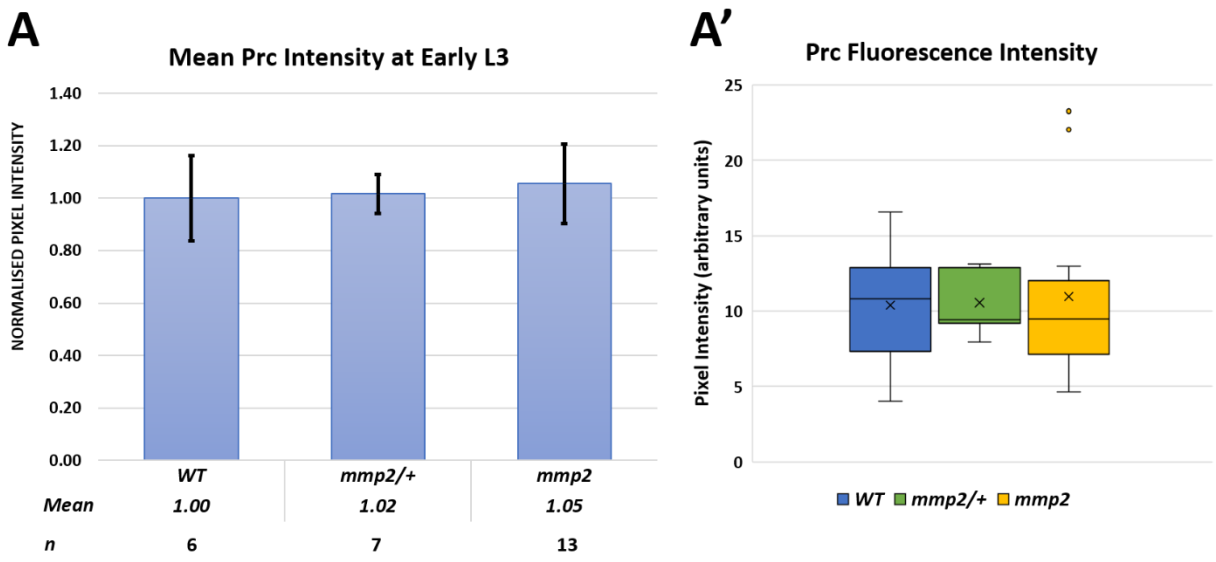

Figure 3.28: Pericardin protein levels in *mmp2* mutants. Quantification of immunolabelled Prc fluorescence signal in segment A7 in early third instar larvae. Samples were imaged at 63x and Prc beyond the PCs is not visualised. **(A)** Prc signal is not different between *mmp2* mutants and controls at early third instar. Note that the ROI includes bifurcated regions of the heart that are largely devoid of Prc. Mean fluorescence intensity is normalised to 1.00 with respect to control levels. Kruskal-Wallis test for non-parametric data. Error bars are SEM. **(A')** X is the mean. Horizontal bar is the median. Box is the first to third quartile. Whiskers show minimum and maximum values before the fence (1.5 x IQR). Isolated data points are outliers or suspected outliers. Wildtype is *yw;vkg-GFP/+*.

3.4.3 Characterisation of Pericardin protein levels and localisation in third instar larvae over-expressing TIMP

TIMP directly inhibits both *Drosophila* MMP proteins through the binding of the active site of the catalytic domain (Nagase *et al.* 2006; Brew and Nagase 2010). I therefore expected that its over-expression would reduce turnover in a manner similar to the loss of MMP function, resulting in an increase in the ECM protein Prc. In early and late third instar larvae over-expressing TIMP, Prc was localised beyond the periphery of the heart; loosely organised Prc bundles projected away from the dorsal vessel into the environs, partially enveloping the trachea and overlapping the fat body and non-cardiac muscle (Fig. 3.29). Though this phenotype emerged even amongst control specimens with inhibited *daGal80* activity, ectopic localisation of Prc appeared to be exacerbated when TIMP was ubiquitously over-expressed throughout embryogenesis. Specimens over-expressing TIMP either constitutively or throughout embryogenesis and first instar (but not later larval development) exhibited a lack of uniformity in the Prc network and a high concentration of isolated Prc bundles beyond the dorsal vessel (Fig. 3.29C-D). Localised over-expression of TIMP by cardiac cells with the *HandGal80* driver did not correlate with conspicuous ectopic Prc localisation (Fig. 3.30).

Relative Prc protein levels, as determined by fluorescence intensity, were not consistent between early and late third instar larvae over-expressing TIMP (Fig. 3.31). A non-significant increase in Prc protein level was observed in both early and late third instar larvae over-expressing TIMP in cardiac cells above those of the respective driverless

controls (Fig. 3.31A). Early third instar larvae that ubiquitously over-expressed TIMP throughout embryonic and larval development showed a significant increase over the internal *daGal80* control (reared at 18°C) as well as larvae over-expressing TIMP from second instar onwards, and a non-significant increase over the driverless control. The internal *daGal80* control and driverless control showed a similar level of mean Prc fluorescence. Late third instar larvae constitutively over-expressing TIMP showed a non-significant reduction in Prc when compared to the internal *daGal80* control and similar expression to the driverless control and larvae over-expressing TIMP from second instar onwards (Fig. 3.31B). It is notable that amongst late third instar larvae the internal *daGal80* control had a significantly ($p<0.05$) higher level of Prc than the driverless control.

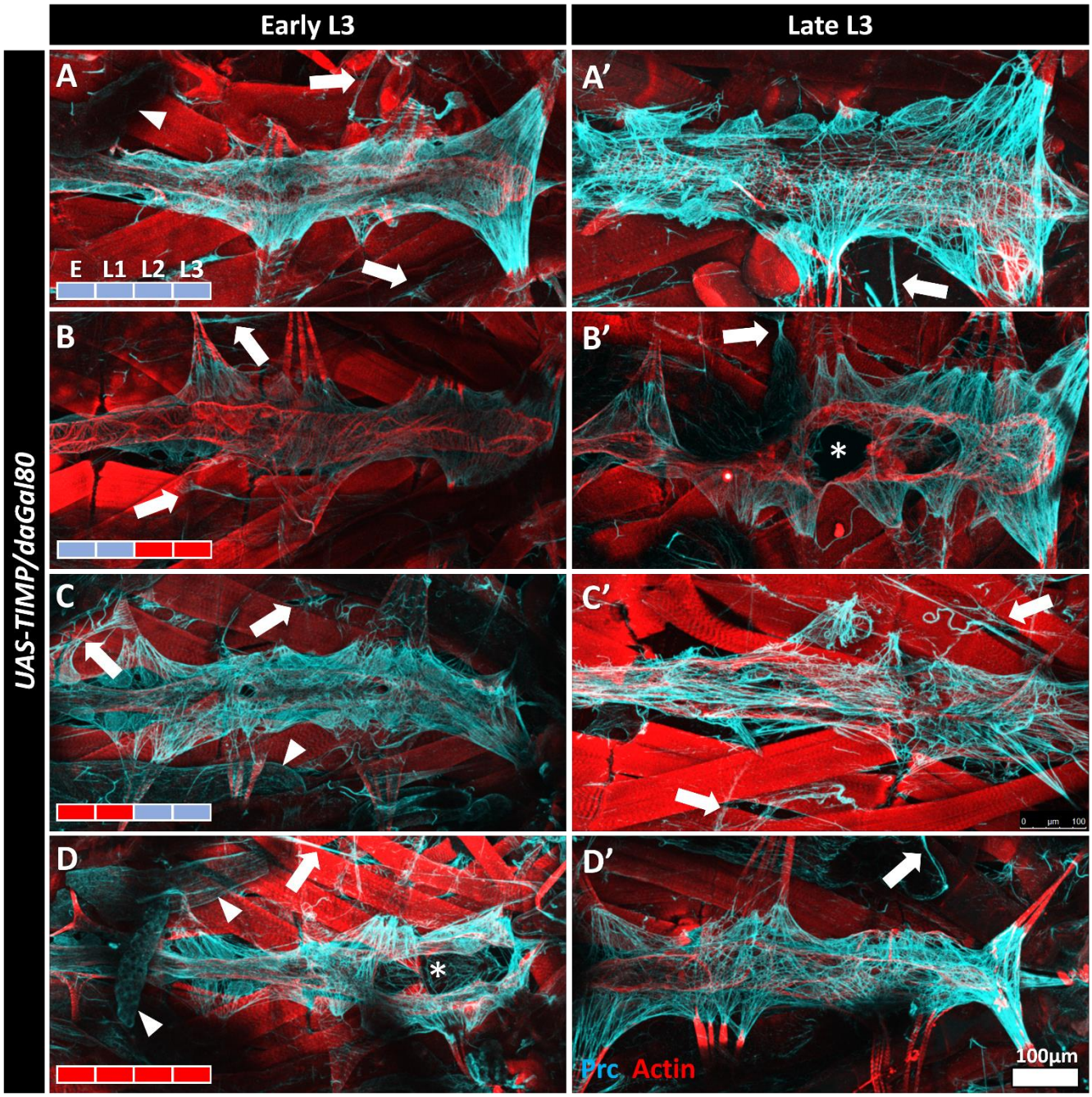
Early L3
Late L3
UAS-TIMP/daGal80
A
A'
E L1 L2 L3
B
B'
C
C'
D
D'
Prc Actin
100µm

Figure 3.29: Pericardin is ectopically localised in early and late third instar larvae ubiquitously over-expressing *Timp*. DV segments A6 and A7. Over-expression of TIMP under the regulation of a temperature-sensitive ubiquitous driver (*daGal80^{TS}*). Larvae were raised at 18°C throughout the grey timeline, and at 29°C throughout the red timeline. **(A-A')** Organisms raised at the permissive temperature (18°C) throughout embryonic and larval development reveal a uniform distribution of Prc in close proximity to the DV perimeter. Some ectopic Prc strands project beyond the immediate environs of the DV (arrows). Prc is localised along the fat body (arrowheads). **(B-B')** Organisms over-expressing *Timp* from second instar onwards (18 to 29°C shift) show a similar distribution of ectopic Prc to those reared at 18°C. **(B)** Prc bundles are absent from the intervening space between bifurcated regions of the DV (asterisks). **(C-C')** Organisms over-expressing *Timp* during embryogenesis and first instar (29 to 18°C) show ectopic Prc bundles beyond the immediate environs of the DV. **(C')** The Prc network is non-uniform, with inconsistent density and a high proportion of longitudinally-oriented bundles. **(D-D')** Organisms over-expressing *Timp* throughout embryonic and larval development (29°C) show a similar distribution of Prc to those of temperature shifted larvae. **(D)** Prc bundles span the intervening space between bifurcated regions of the DV.

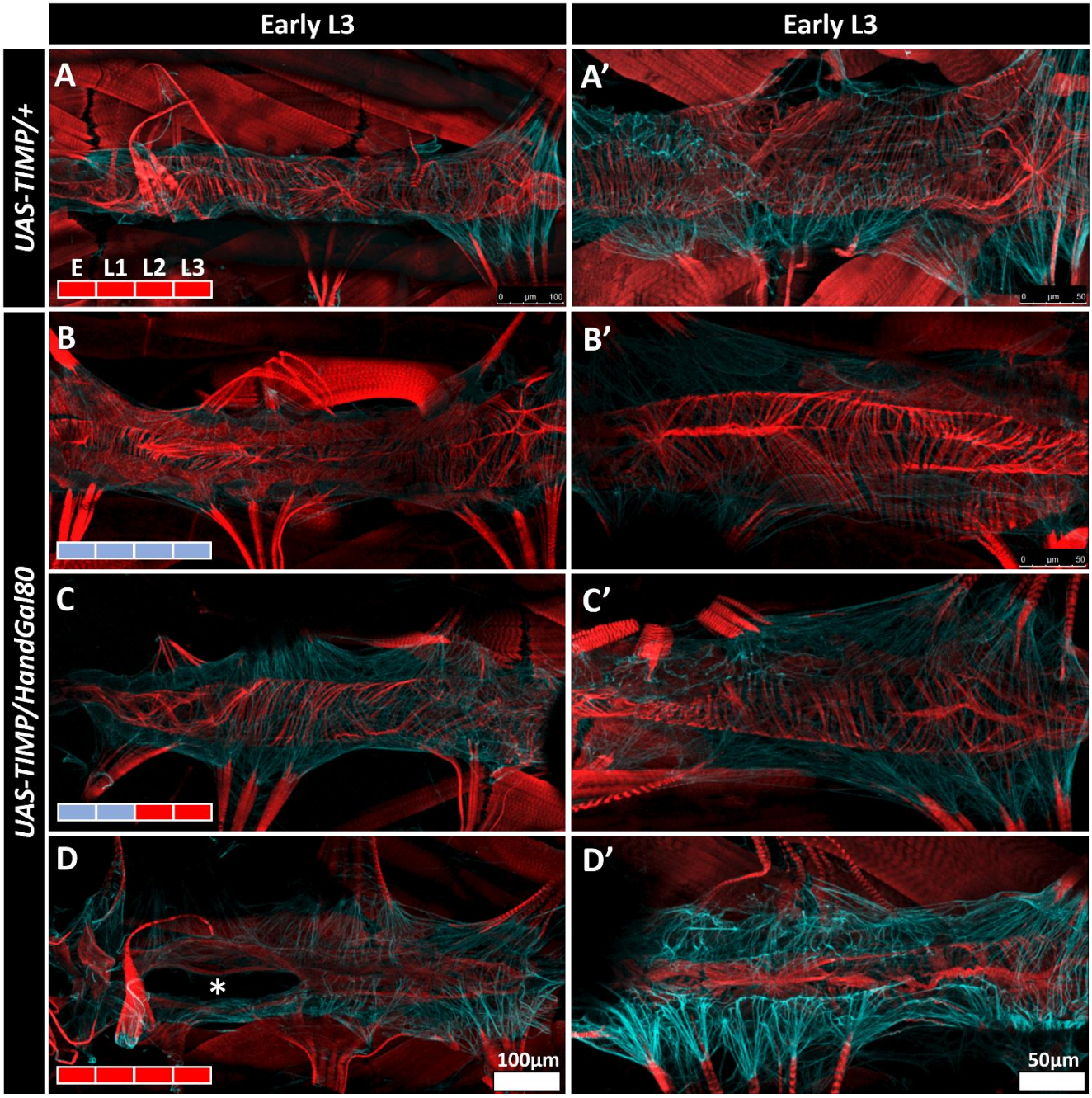
Early L3
Early L3
UAS-TIMP/+
UAS-TIMP/HandGal80
A
A'
B
B'
C
C'
D
D'
E L1 L2 L3
*
100µm
50µm

Figure 3.30: Pericardin localisation in early and late third instar larvae over-expressing *Timp* in cardiac cells. DV segments A6 and A7. **(A-A')** Driverless *UAS-TIMP* controls. Prc forms a uniform network in close proximity to the DV perimeter, enveloping the PCs and connecting the alary muscles. **(B-B')** Organisms raised at the permissive temperature (18°C) throughout embryonic and larval development reveal a uniform distribution of Prc in close proximity to the DV perimeter. **(C-C')** Organisms over-expressing *Timp* from second instar onwards (18 to 29°C shift) show a similar distribution of Prc to controls. **(D-D')** Organisms over-expressing *Timp* throughout embryonic and larval development (29°C) show a similar distribution of Prc to controls. **(D)** Prc is largely absent from the intervening space between bifurcated vessels (asterisk).

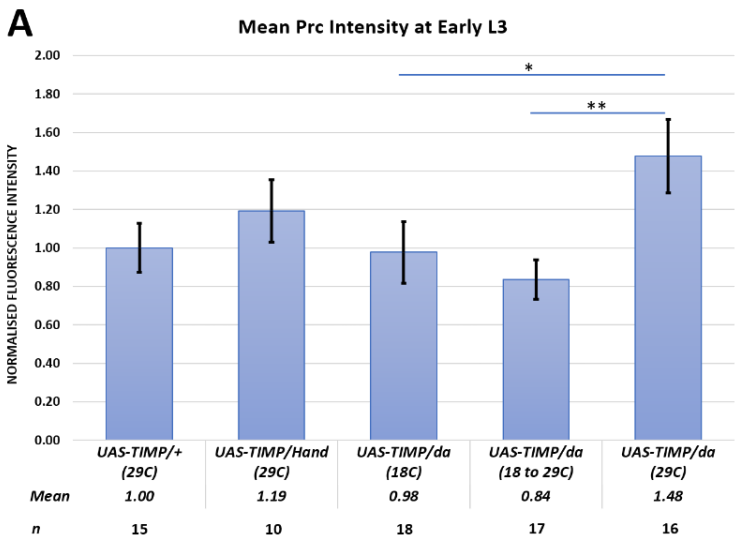
A
Mean Prc Intensity at Early L3
NORMALISED FLUORESCENCE INTENSITY
2.00
1.80
1.60
1.40
1.20
1.00
0.80
0.60
0.40
0.20
0.00
*
**
UAS-TIMP/+ (29C)
UAS-TIMP/Hand (29C)
UAS-TIMP/da (18C)
UAS-TIMP/da (18 to 29C)
UAS-TIMP/da (29C)
Mean 1.00 1.19 0.98 0.84 1.48
n 15 10 18 17 16

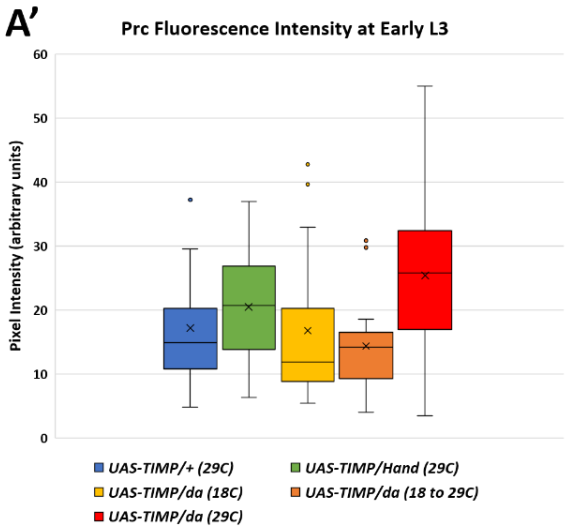
A'
Prc Fluorescence Intensity at Early L3
Pixel Intensity (arbitrary units)
60
50
40
30
20
10
0
UAS-TIMP/+ (29C)
UAS-TIMP/Hand (29C)
UAS-TIMP/da (18C)
UAS-TIMP/da (18 to 29C)
UAS-TIMP/da (29C)

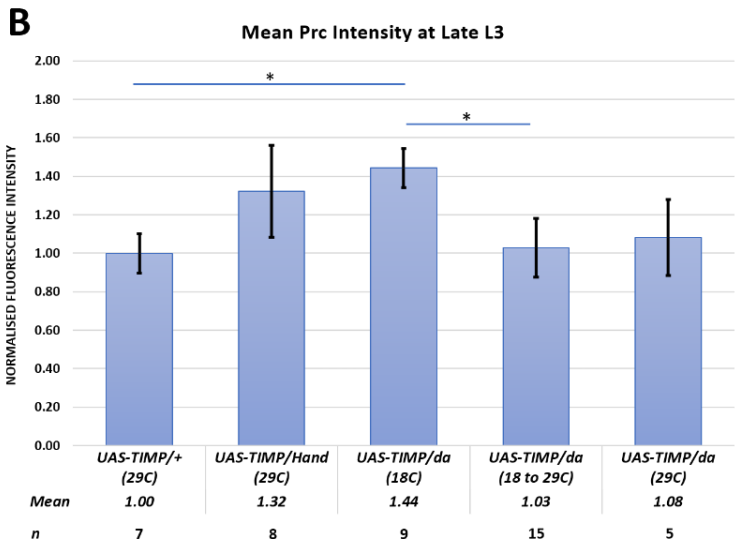
B
Mean Prc Intensity at Late L3
NORMALISED FLUORESCENCE INTENSITY
2.00
1.80
1.60
1.40
1.20
1.00
0.80
0.60
0.40
0.20
0.00
*
*
UAS-TIMP/+ (29C)
UAS-TIMP/Hand (29C)
UAS-TIMP/da (18C)
UAS-TIMP/da (18 to 29C)
UAS-TIMP/da (29C)
Mean 1.00 1.32 1.44 1.03 1.08
n 7 8 9 15 5

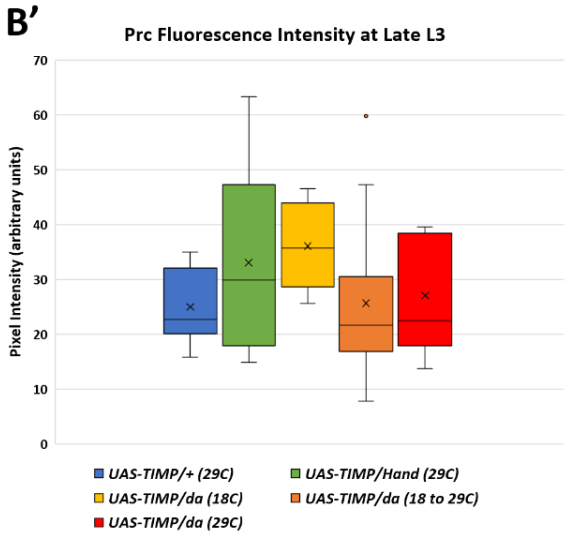
B'
Prc Fluorescence Intensity at Late L3
Pixel Intensity (arbitrary units)
70
60
50
40
30
20
10
0
UAS-TIMP/+ (29C)
UAS-TIMP/Hand (29C)
UAS-TIMP/da (18C)
UAS-TIMP/da (18 to 29C)
UAS-TIMP/da (29C)

Figure 3.31: Pericardin protein levels in third instar larvae over-expressing *Timp*. Quantification of immunolabelled Prc fluorescence signal in segment A7 in early and late third instar larvae. **(A-A')** Early third instar larvae. Prc signal is increased upon local over-expression *Timp* within cardiac cells with *HandGal4* relative to the driverless *Timp* control, but this difference is not significant. Prc signal is increased upon ubiquitous over-expression of *Timp* throughout embryonic and larval development with $daGal80^{TS}$ (29°C) relative to both control groups (*UAS-TIMP/+* at 29°C and *UAS-TIMP/da* at 18°C), but this difference is not significant in relation to the driverless *Timp* control. **(B-B')** Late third instar larvae. Prc signal is increased upon local over-expression *Timp* within cardiac cells with *HandGal4* relative to the driverless *Timp* control, but this difference is not significant. Prc signal is increased upon ubiquitous over-expression of *Timp* throughout embryonic and larval development with $daGal80^{TS}$ (29°C) relative to the driverless *Timp* control, and is reduced relative to the $daGal80^{TS}$ internal control (18°C), but this difference is not significant in either case. **(A,B)** Mean fluorescence intensity is normalised to 1.00 with respect to control levels. Kruskal-Wallis test for non-parametric data. Error bars are SEM. * $p \leq 0.05$ ** $p \leq 0.01$ *** $p \leq 0.005$. **(A',B')** X is the mean. Horizontal bar is the median. Box is the first to third quartile. Whiskers show minimum and maximum values before the fence (1.5 x IQR). Isolated data points are outliers or suspected outliers.

3.4.4 Characterisation of Pericardin protein levels and localisation in third instar larvae expressing Mmp2 dsRNA

Specific reduction of MMP2 function revealed a similar Prc phenotype to that described by TIMP over-expression, suggesting a prominent role for MMP2 in the distribution of this protein. Prc localisation and protein levels were preferentially examined using *Mmp2* dsRNA encoded on chromosome II (TRiP line 61309) as this insert was capable of producing a pronounced cardiac phenotype.

Qualitative analysis suggests that the Prc network is localised more broadly beyond the periphery of the heart in early and late third instar larvae when *Mmp2* expression is knocked down throughout development. However, this may also be explained by tension on the network caused by strained alary muscles pulling away from the vessel. Ectopic Prc bundles were present in all specimens, including controls. This phenotype appeared to be exacerbated when *Mmp2* dsRNA was expressed ubiquitously (Fig. 3.32) or locally within cardiac cells (Fig. 3.33) throughout embryonic and larval development.

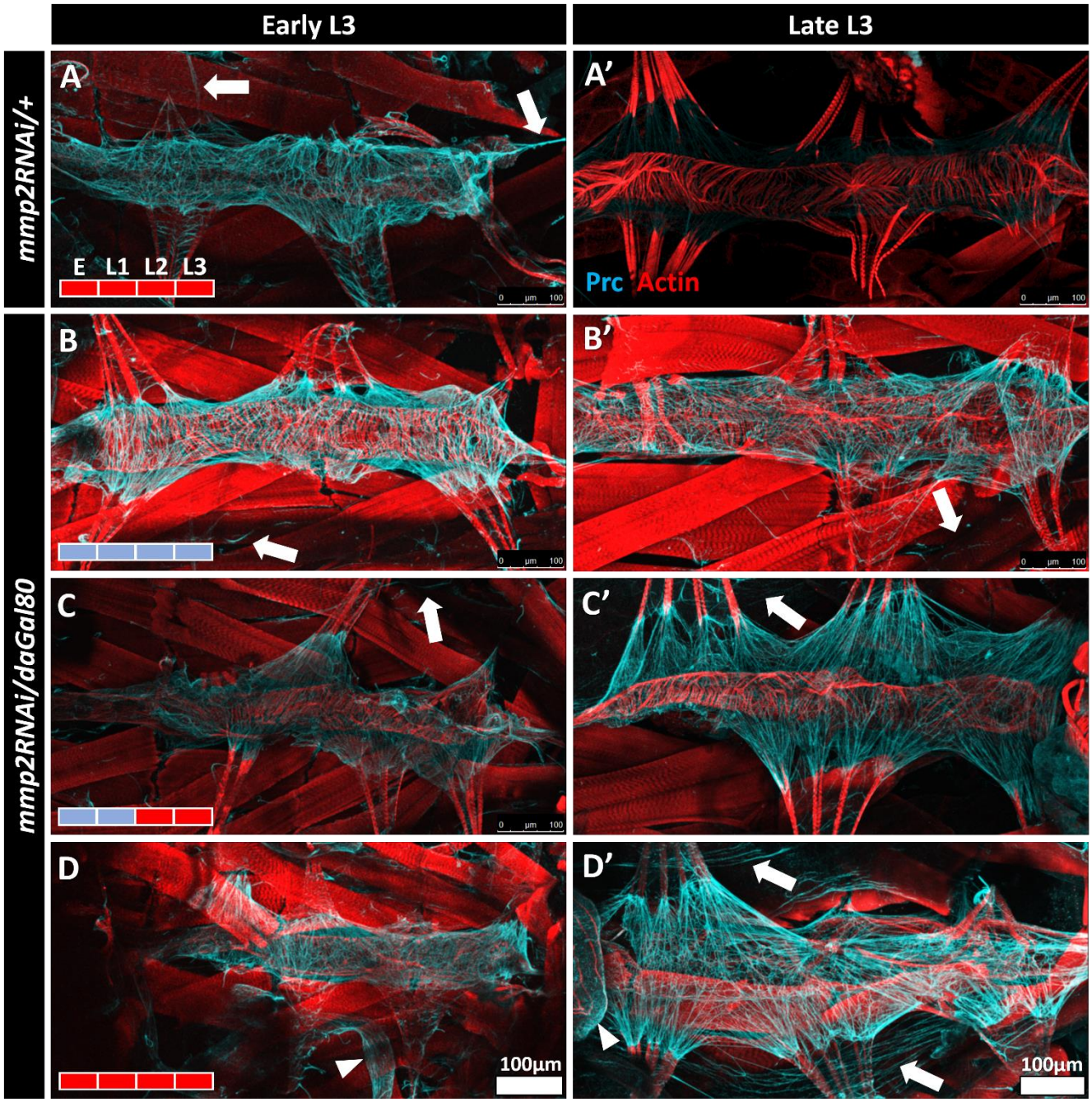
Early L3
Late L3
mmp2RNAi/+
mmp2RNAi/daGal80
A
A'
B
B'
C
C'
D
D'
E L1 L2 L3
Prc Actin
100µm
100µm

Figure 3.32: Pericardin is ectopically localised in late third instar larvae when Mmp2 expression is reduced ubiquitously at different developmental stages. DV segments A6 and A7. **(A-A')** Driverless *mmp2RNAi* controls at early **(A)** and late **(A')** third instar. Prc forms a network in close proximity to the DV perimeter, enveloping the PCs and connecting the alary muscles. Isolated ectopic strands of Prc extend beyond the DV (arrows). **(B-D)** Individuals expressing *Mmp2* dsRNA under the control of *daGal80^{TS}*. **(B-B')** Individuals reared at the permissive temperature (18°C) throughout embryonic and larval development are not obviously different from the wildtype. Some ectopic Prc bundles are visible. **(C-C')** Larvae expressing of *Mmp2* dsRNA from second instar onwards (18 to 29°C) reveal broadly expressed Prc localisation around the perimeter of the DV and the presence of isolated ectopic strands beyond the DV. **(D-D')** Expression of *Mmp2* dsRNA throughout embryonic and larval development (29°C) reveals the presence of ectopic strands beyond the DV. Prc is localised along the fat body (arrowhead).

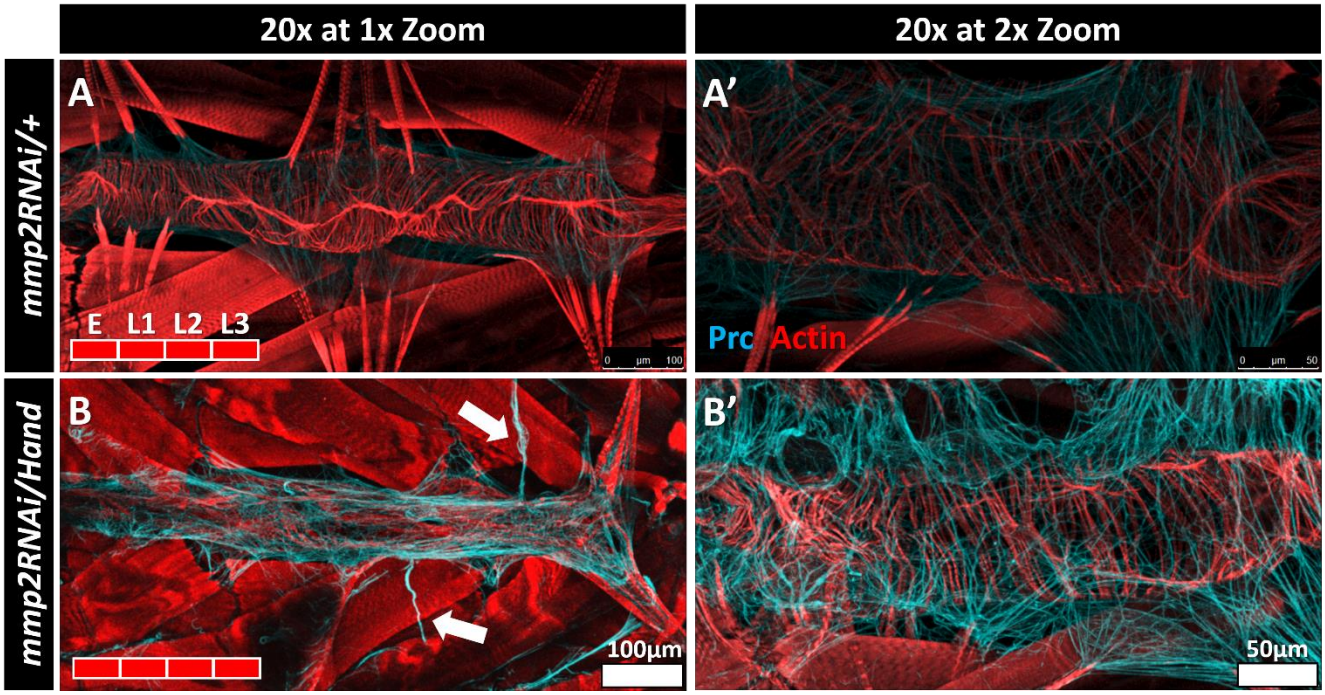

Figure 3.33: Pericardin is ectopically localised in late third instar larvae with reduced *Mmp2* expression in cardiac cells. DV segment A7. **(A-A')** Controls (*UAS-mmp2RNAi/+*) reared at 29°C do not exhibit any defects or abnormalities in Prc expression or localisation. **(B-B')** Ectopic Prc strands project beyond the immediate environs of the DV (arrows) upon cardiac-specific reduction of *Mmp2* from embryogenesis onwards with the *HandGal4* driver.

Prc protein levels were significantly ($p<0.05$) elevated in late third instar larvae expressing cardiac-specific *Mmp2* dsRNA (Fig. 3.34). The internal *daGal80* control and those larvae ubiquitously expressing dsRNA showed a significant increase in Prc relative to the driverless control, but were not significantly different from each-other. Larvae ubiquitously expressing dsRNA constitutively, or throughout larval development only, showed an increase in mean Prc fluorescence intensity when compared to *dagal80* control, but this difference was not significant. Interestingly, mean fluorescence signal was similar in larvae expressing *Mmp2* dsRNA constitutively and larvae expressing the dsRNA only after second instar.

Qualitative analysis performed using *Mmp2* dsRNA encoded on chromosome III (TRiP line 31371) did not reveal a non-wildtype phenotype when expressed ubiquitously or locally within cardiac cells (data not shown). This, along with similar findings for Collagen-IV, and relatively high survival to eclosion, suggests weak activity of the RNAi. Early third instar larvae expressing *Mmp2* dsRNA were similar to same-aged larvae over-expressing TIMP with respect to Prc levels (Fig. 3.35A). Late third instar larvae expressing cardiac-specific *Mmp2* dsRNA showed a non-significant reduction in protein signal compared to the driverless control, whereas larvae with ubiquitous expression of *Mmp2* dsRNA showed a non-significant reduction in protein signal compared to the internal *daGal80* control (Fig. 3.35B). As with late third instar larvae over-expressing TIMP, the internal *daGal80* control had significantly higher Prc signal than the driverless control.

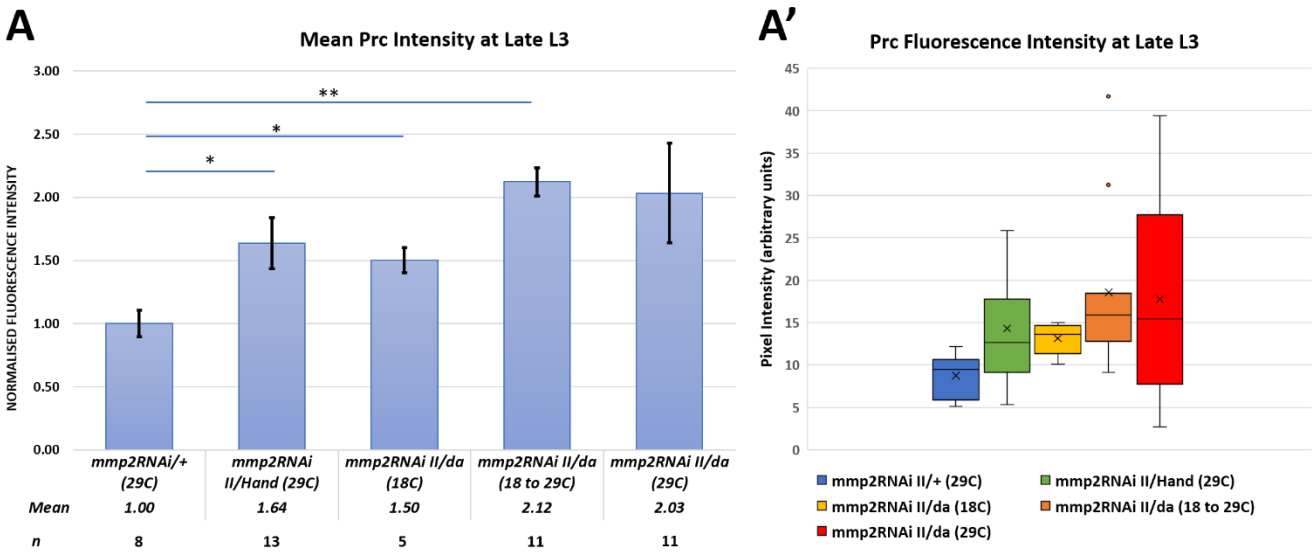

Figure 3.34: Pericardin protein levels are increased in late third instar larvae with reduced *Mmp2* expression. Quantification of immunolabelled Prc fluorescence signal in segment A7 in late third instar larvae. Prc signal is significantly increased upon localised expressing mmp2 dsRNA within cardiac cells with *HandGal4* relative to the driverless dsRNA control. Prc signal is elevated upon ubiquitous expression of dsRNA throughout embryonic and larval development with *daGal80^{TS}* (29°C) relative to both control groups (*mmp2RNAi/+* at 29°C and *mmp2RNAi/da* at 18°C), but this difference is not significant in either case. Prc signal is elevated upon ubiquitous expression of dsRNA from second instar onwards (18 to 29°C) relative to both control groups (*mmp2RNAi/+* at 29°C and *mmp2RNAi/da* at 18°C), but this difference is not significant in the case of the latter. **(A)** Mean fluorescence intensity is normalised to 1.00 with respect to control levels. Kruskal-Wallis test for non-parametric data. Error bars are SEM. * p≤0.05 ** p≤0.01 *** p≤0.005. **(A')** X is the mean. Horizontal bar is the median. Whiskers show minimum and maximum values before the fence (1.5 x IQR). Isolated data points are outliers or suspected outliers.

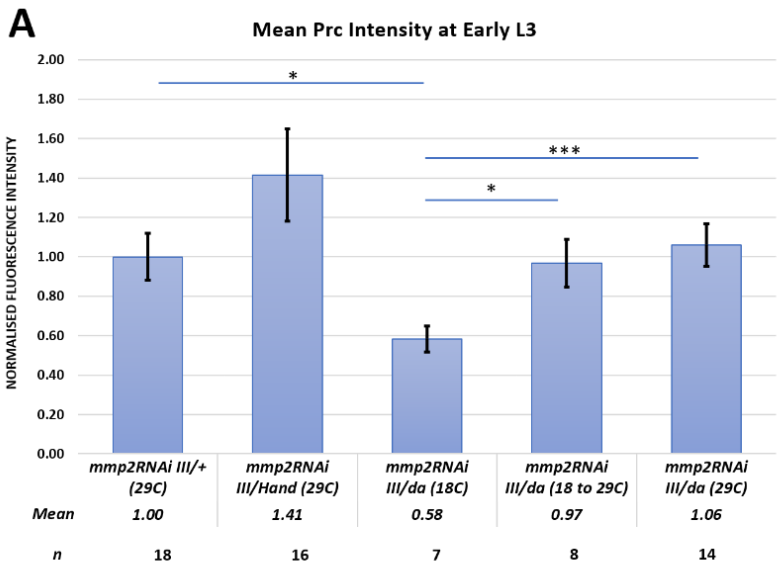
A
Mean Prc Intensity at Early L3
NORMALISED FLUORESCENCE INTENSITY
2.00
1.80
1.60
1.40
1.20
1.00
0.80
0.60
0.40
0.20
0.00
*
***
*
mmp2RNAi III/+ (29C)
mmp2RNAi III/Hand (29C)
mmp2RNAi III/da (18C)
mmp2RNAi III/da (18 to 29C)
mmp2RNAi III/da (29C)
Mean 1.00 1.41 0.58 0.97 1.06
n 18 16 7 8 14

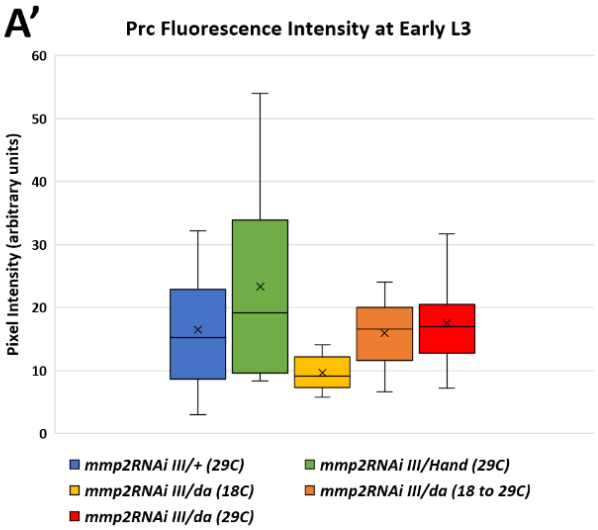
A'
Prc Fluorescence Intensity at Early L3
Pixel Intensity (arbitrary units)
60
50
40
30
20
10
0
mmp2RNAi III/+ (29C)
mmp2RNAi III/Hand (29C)
mmp2RNAi III/da (18C)
mmp2RNAi III/da (18 to 29C)
mmp2RNAi III/da (29C)

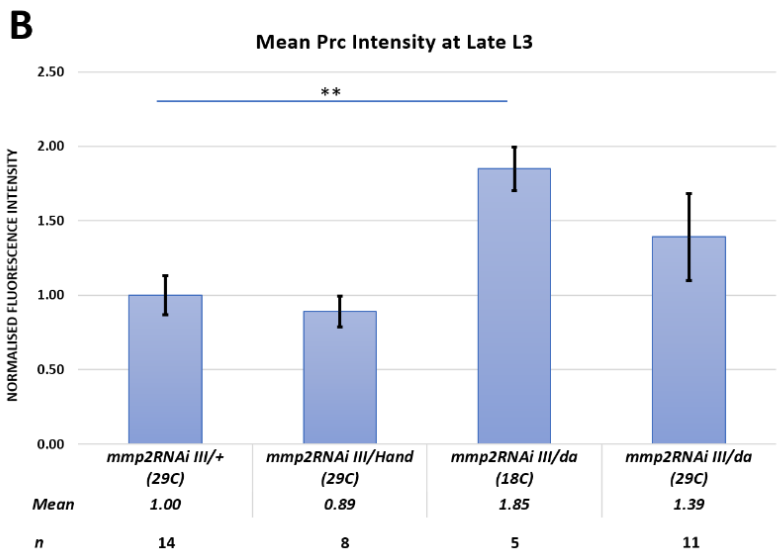
B
Mean Prc Intensity at Late L3
NORMALISED FLUORESCENCE INTENSITY
2.50
2.00
1.50
1.00
0.50
0.00
**
mmp2RNAi III/+ (29C)
mmp2RNAi III/Hand (29C)
mmp2RNAi III/da (18C)
mmp2RNAi III/da (29C)
Mean 1.00 0.89 1.85 1.39
n 14 8 5 11

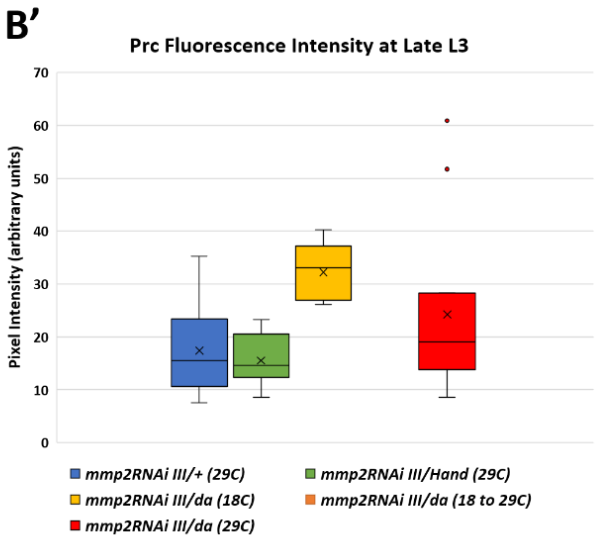
B'
Prc Fluorescence Intensity at Late L3
Pixel Intensity (arbitrary units)
70
60
50
40
30
20
10
0
mmp2RNAi III/+ (29C)
mmp2RNAi III/Hand (29C)
mmp2RNAi III/da (18C)
mmp2RNAi III/da (18 to 29C)
mmp2RNAi III/da (29C)

Figure 3.35: Pericardin protein levels in third instar larvae with reduced *Mmp2* expression. Quantification of immunolabelled Prc fluorescence expression in segment A7 in early and late third instar larvae. **(A-A')** Early third instar larvae. Prc signal is increased upon local expression of *Mmp2* dsRNA within cardiac cells with *HandGal4* relative to the driverless *dsRNA* control, but this difference is not significant. Prc signal is increased upon ubiquitous over-expression of *Timp* throughout embryonic and larval development with $daGal80^{TS}$ (29°C) relative to the $daGal80^{TS}$ internal control (18°C) but not the driverless dsRNA control. **(B-B')** Late third instar larvae. Prc signal shows a non-significant decrease upon localised expression of *Mmp2* dsRNA with *HandGal4*, with respect to the driverless dsRNA control. Prc signal is increased upon ubiquitous expression of *Mmp2* dsRNA throughout embryonic and larval development with $daGal80^{TS}$ (29°C) relative to the driverless dsRNA control, and is reduced relative to the $daGal80^{TS}$ internal control (18°C), but this difference is not significant in either case. **(A,B)** Mean fluorescence intensity is normalised to 1.00 with respect to control levels. Kruskal-Wallis test for non-parametric data. Error bars are SEM. * $p \leq 0.05$ ** $p \leq 0.01$ *** $p \leq 0.005$. **(A',B')** X is the mean. Horizontal bar is the median. Box is the first to third quartile. Whiskers show minimum and maximum values before the fence (1.5 x IQR). Isolated data points are outliers or suspected outliers.

3.4.3 Characterisation of Pericardin protein levels and localisation in third instar larvae over-expressing MMP2

Cardiac-specific up-regulation of *Mmp2* resulted in the ectopic localisation of Prc bundles. Prc was expressed beyond the immediate periphery of the heart when MMP2 was over-expressed during embryogenesis and first instar; individual bundles projected from the vessel or were entirely disconnected from the Prc network surrounding the vessel (Fig. 3.36D). Prc was not arrayed as a uniform network of fibres, instead forming an uneven condensate along the vessel.

Aberrant localisation also manifested when mis-expression of *Mmp2* was induced post-embryonically at second instar. In such organisms, Prc was not uniformly distributed; regions of the ablumenal cardiac surface displayed either high or low fibre density due to the presence of large gaps between bundles (Fig. 3.36B',C). Prc localised to the vestigial aorta, even when Collagen-IV was only weakly present at the site, suggesting that aortal Prc may be more resilient to increased MMP2 activity than is Collagen-IV. A minority of specimens with dampened over-expression of MMP2 throughout embryogenesis and first instar showed thicker-than-normal Prc bundles along the heart periphery. These thicker bundles overlapped with Collagen-IV bundles (Fig. 3.24).

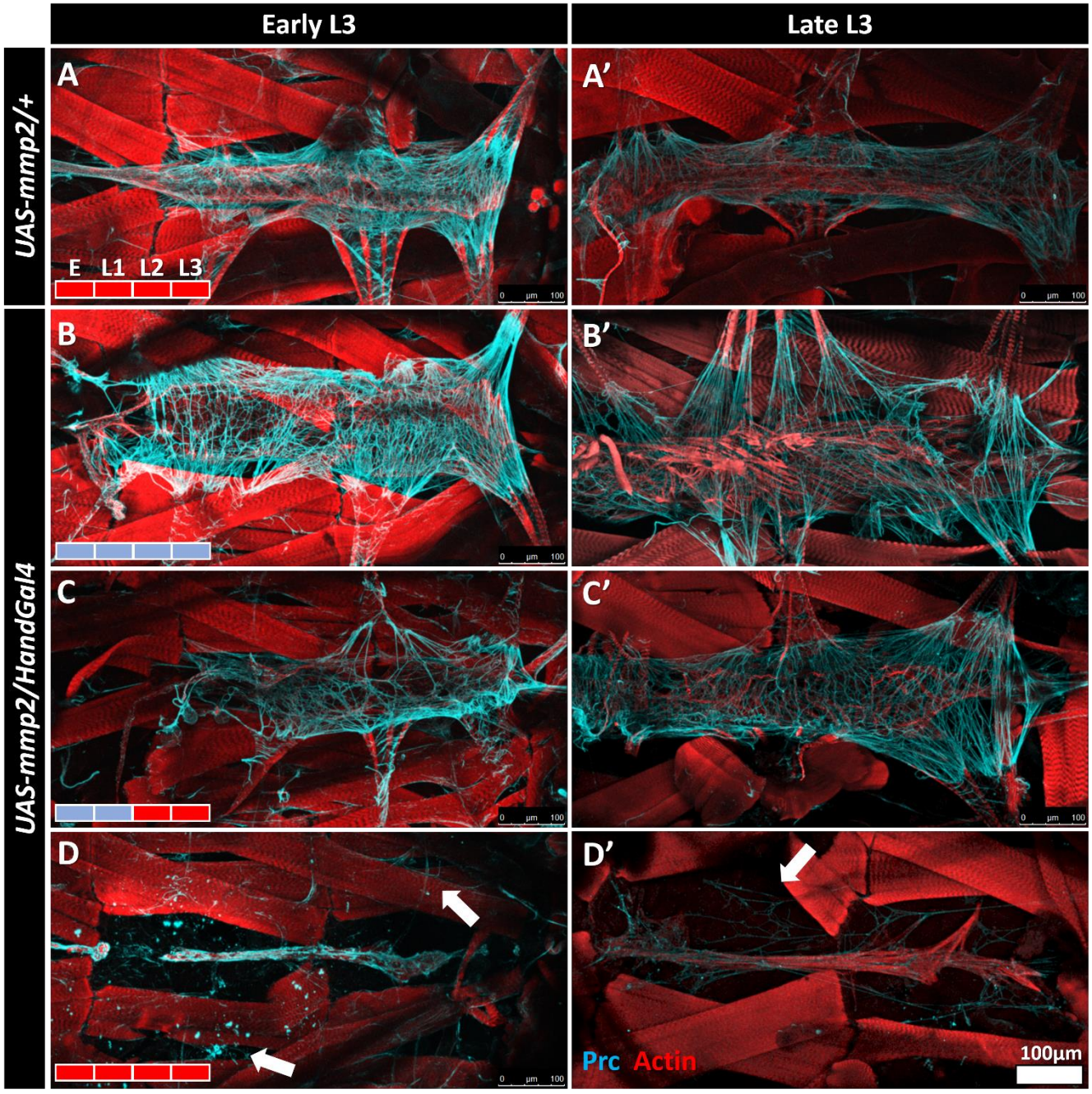
Early L3
Late L3
UAS-mmp2/+
UAS-mmp2/HandGal4
A
A'
B
B'
C
C'
D
D'
E L1 L2 L3
0 µm 100
Prc Actin
100µm

Figure 3.36: Pericardin exhibits aberrant localisation upon over-expression of *Mmp2* within the heart. DV segments A7 and A7. **(A-A')** Early and late third instar control larvae (*UAS-mmp2/+*) reared at 29°C or temperature-shifted reveal a uniform distribution of Prc bundles. **(B-D)** Early and late third instar larvae exhibiting cardiac-specific up-regulation of *mmp2* with *HandGal4*. Note that *HandGal4* does not contain a temperature sensitive $Gal80^{TS}$ and may show basal activity even at low temperatures. **(B-B')** Prc bundles appear disorganised and sparsely distributed along the dorsal vessel in organisms reared at 18°C. Prc is present in association with the vestigial aorta. **(C-C')** The Prc network is sparse in regions. Prc bundles are broadly expressed along the margins of the dorsal vessel in temperature-shifted organisms. **(D-D')** The normal web-like arrangement of Prc bundles is disrupted when *Mmp2* is over-expressed throughout embryonic and larval development (29°C). Prc bundles appear discontinuous and form fewer attachments, resulting in a less dense arrangement of fibres. Prc fibres are present beyond the immediate environs of the DV (arrows).

Mean Prc fluorescence intensity at segment A7 was quantified to determine whether protein levels were locally affected by MMP2 over-expression within the heart. Early third instar larvae over-expressing MMP2 with *HandGal4* throughout embryonic and larval development at 29°C showed a significant decrease in Prc protein levels when compared to same-age larvae with dampened over-expression at 18°C throughout the same period, but not when compared to the driverless control (Fig. 3.37). Early third instar larvae with dampened over-expression of MMP2 throughout embryogenesis and first instar but full over-expression from second instar onwards showed a non-significant decrease compared to controls.

3.4.4 Summary of Pericardin protein levels and localisation

Prc bundles were ectopically localised beyond the dorsal vessel and the Prc network was disorganised upon reduction of MMP2 function or over-expression of TIMP throughout embryogenesis and first instar (i.e. during cardiogenesis). Prc levels across segment A7 were increased upon reduction of protease activity throughout embryogenesis and first instar in some samples. Constitutive over-expression of MMP2 within the dorsal vessel compromised the Prc network and was correlated with reduced Prc levels across segment A7.

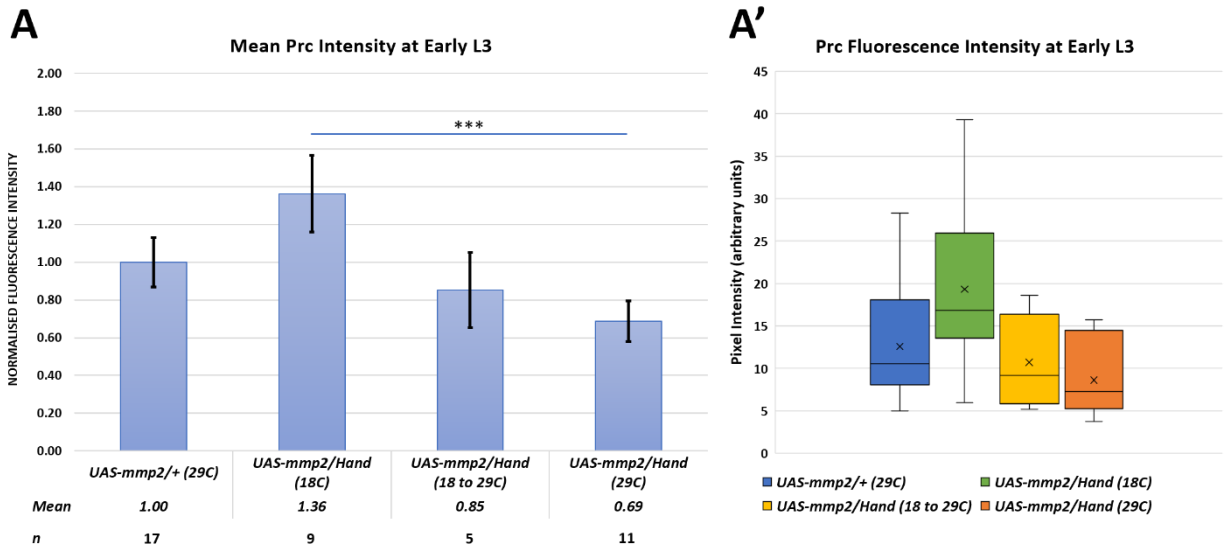

Figure 3.37: Pericardin protein levels in third instar larvae with increased *Mmp2* expression. Quantification of immunolabelled Prc fluorescence signal in segment A7 in early third instar larvae. Prc signal is reduced upon cardiac-specific over-expression of *Mmp2* throughout embryonic and larval development with *HandGal4* (29°C) relative to controls, but this difference is not significant in relation to the driverless *UAS-mmp2* control. **(A)** Mean fluorescence intensity is normalised to 1.00 with respect to control levels. Kruskal-Wallis test for non-parametric data. Error bars are SEM. * p≤0.05 ** p≤0.01 *** p≤0.005. **(A')** X is the mean. Horizontal bar is the median. Box is the first to third quartile. Whiskers show minimum and maximum values before the fence (1.5 x IQR). Isolated data points are outliers or suspected outliers.

3.5 Heart function in larvae with altered MMP expression

Accumulation and increased cross-linking of ECM components are associated with normal aging as well as cardiac disease states amongst vertebrates and *Drosophila* (Sessions and Engler 2016). Interstitial fibrosis has been linked to cardiac dilation in vertebrates (Brooks *et al.* 2003). Basement membrane thickening and stiffening are correlated with impaired contractility in *Drosophila*, whereas reduced expression of basement membrane proteins such as LanA, Vkg, and Prc mitigates age-related loss in cardiac compliance (e.g. reduced fractional shortening) (Sessions *et al.* 2017). Loss of MMP2 function and the resultant accumulation of ECM components was therefore predicted to impair normal fractional shortening and to alter diastolic diameter, as is the case with individuals suffering from age-related fibrosis and cardiomyopathy (Eghbali *et al.* 1988; Nishimura *et al.* 2014). *Drosophila* adults, like vertebrates, show an age-related decline in heart rate concomitant with Collagen build-up (Vaughan *et al.* 2017). Heart rate was therefore predicted to decline in individuals with reduced MMP2 function.

3.5.1 Contractile function in *mmp2* mutants

In this section I examine the dilation and contractility of late third instar larval hearts using non-invasive optical coherence tomography (OCT) to determine whether cardiac function is compromised in *mmp2* mutants. Early third instars were not included in this analysis because preliminary tests failed to adequately resolve the smaller lumenal space due to the low of resolution of the OCT imager. As such, homozygous *mmp1* and *mmp1,mmp2* mutants could not be examined, as a majority of these larvae expired before

reaching late third instar. *mmp2* heterozygotes were excluded from this analysis due to small sample size (*n*=4).

Dorsal vessels exhibiting cardia bifida maintained contractile competency even at the site of bifurcation. Live imaging revealed that both vessels within the bifurcated segments of *mmp2* mutant hearts underwent cycles of contraction and expansion, and that these cycles occurred synchronously (Fig. 3.38).

I compared measures of dilation and contraction in wildtype late third instar larvae to those in *mmp2* mutants that did not display bifurcation within segments A6 or A7. Non-bifurcated hearts were selected to ensure the imaged slices were comparable. Heart dilation (lumenal area at maximal expansion; diastole) was not different between *mmp2* mutants and the wildtype (Fig. 3.39A). The lumenal area at maximal contraction (systole) was likewise not significantly different in mutant larvae (Fig. 3.39B). The degree of contraction, as measured by the ratio of diastole to systole, was not significantly different between *mmp2* mutants and the wildtype (Fig. 3.39C). Consideration of the median degree of contraction revealed a non-significant increase amongst *mmp2* mutants, but this trend was reversed for mean values due to the presence of outliers; a single *mmp2* mutant showed an increase in lumenal area at both diastole and systole that was reminiscent of dilated cardiomyopathy.

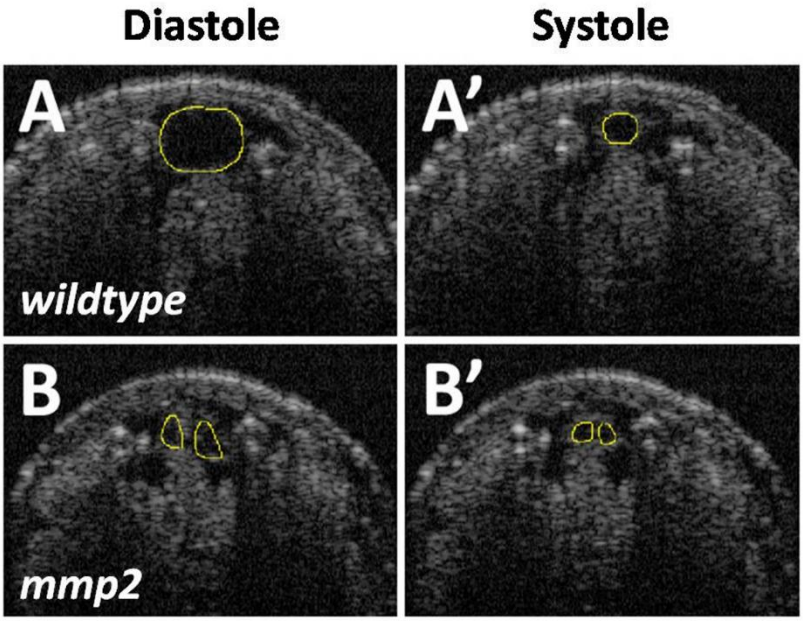

Figure 3.38: Bifurcated vessels of *mmp2* mutants contract synchronously. Examination of cardiac function using OCT live-imaging on anaesthetised larvae. **(A-B)** Cross-sectional view of wildtype and homozygous *mmp2* mutant hearts during diastole and systole. Lumenal spaces are traced in yellow for ease of identification. **(B-B')** An *mmp2* mutant heart is displayed at a site of bifurcation. The two vessels are contractile and show synchronicity; both are maximally dilated and contracted within the same frame. *yw* is the wildtype control.

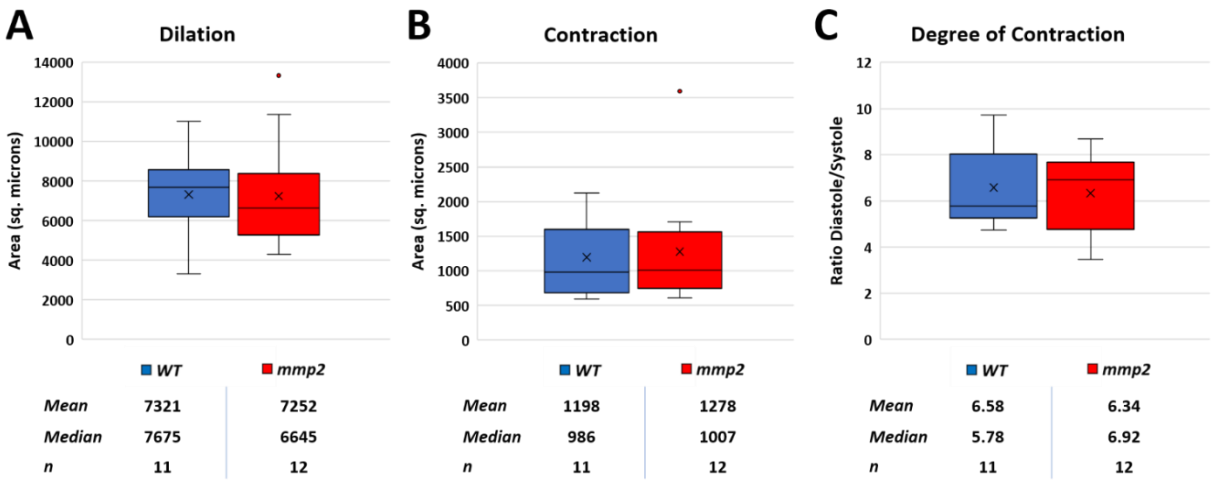

Figure 3.39: Loss of *Mmp2* does not significantly alter contractile capacity or expansion in late third instar larvae. Examination of cardiac function using OCT live-imaging on anaesthetised larvae. **(A-A')** Lumenal area at diastole (maximal expansion) is not significantly different between homozygous *mmp2* mutants and the wildtype. **(B-B')** Lumenal area at systole (maximal contraction) is not significantly different between homozygous *mmp2* mutants and the wildtype. **(C-C')** Heart chamber contractility (diastole/systole) is not statistically different between homozygous *mmp2* mutants and the wildtype. Kruskal-Wallis test for non-parametric data. X is the mean. Horizontal bar is the median. Box is the first to third quartile. Whiskers show minimum and maximum values before the fence (1.5 x IQR). Isolated data points are outliers or suspected outliers. *yw* is the wildtype control.

3.5.2 Heart rate of *mmp2* mutants

I examined the heart rate of *mmp* mutant larvae via light microscopy. Due to high levels of mortality throughout third instar, homozygous *mmp1* and *mmp1,mmp2* mutants could be examined only as early third instar larvae. Live-imaging revealed a high incidence of arrhythmia or complete cardiac arrest amongst *mmp1* mutants (65% of those observed, *n*=20), as well as *mmp1,mmp2* double mutants (55% of those observed, *n*=31), with hearts frequently arresting for periods of several seconds, or beating erratically. Reliable measures of heart rate could not be ascertained due to the low number of individuals exhibiting consistent contractions over the timeframe required for video image capture. *mmp1* and *mmp1,mmp2* mutants were therefore excluded from the analysis.

Heart rate of wildtype larvae and *mmp2* mutants was shown to decrease approaching pupariation; the heart rates of early third instar larvae were higher than those of late third instars of the same genotype. This difference was significant for all genotypes at p=0.05.

When compared to wildtype controls, homozygous *mmp2* mutants exhibited a significantly reduced basal heart rate at both early and late third instar (Fig. 3.40). Heterozygous mutants exhibited a significantly reduced basal heart rate compared to the wildtype only as early third instar larvae. Heart rate was not significantly different between hetero- and homozygous *mmp2* mutants at the early third instar stage. A significant difference was observed at the late third instar stage, whereupon homozygous mutants revealed a lower basal rate.

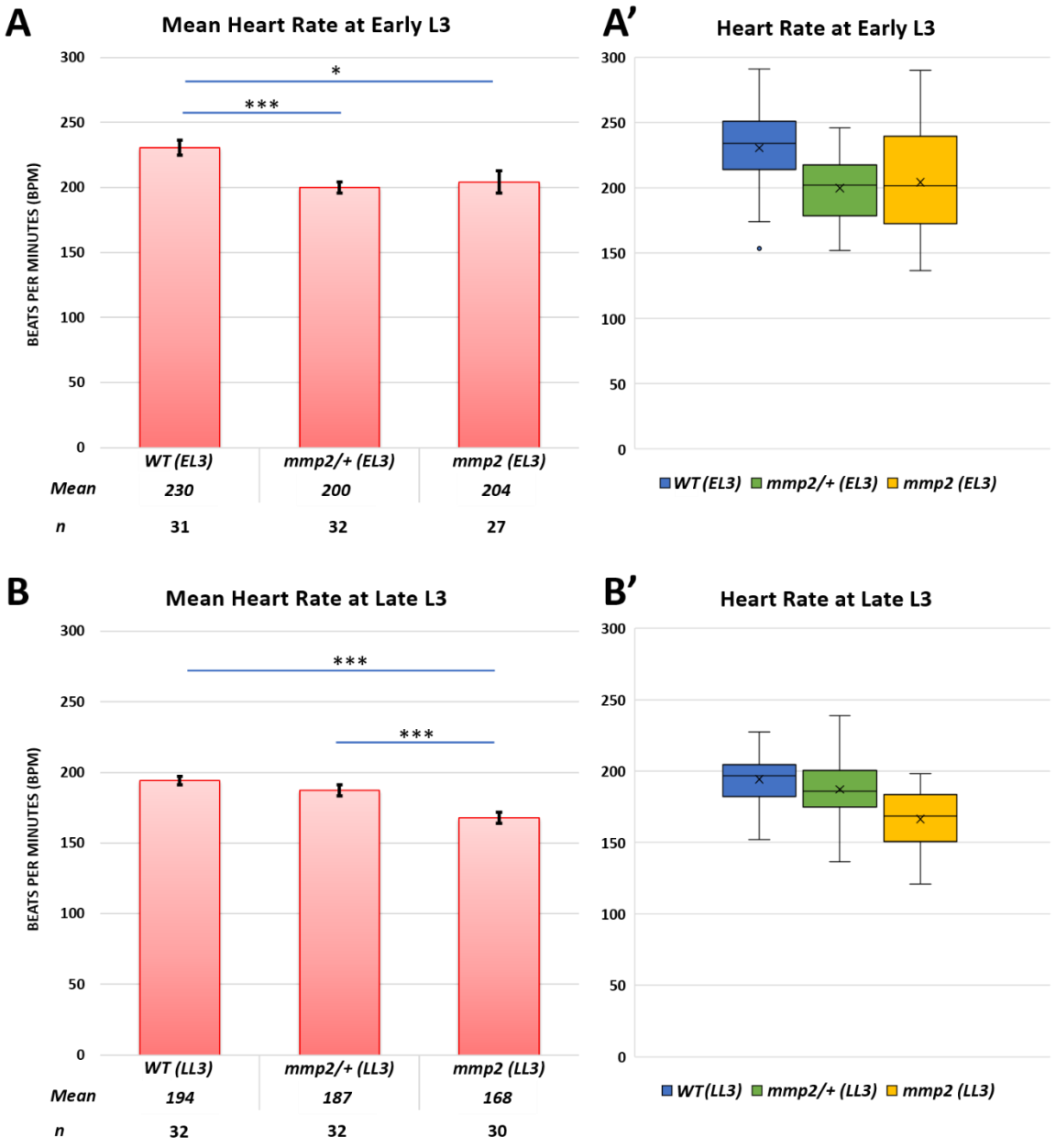
A
Mean Heart Rate at Early L3
BEATS PER MINUTES (BPM)
300
250
200
150
100
50
0
*
***
WT (EL3)
mmp2/+ (EL3)
mmp2 (EL3)
Mean
230
200
204
n
31
32
27
A'
Heart Rate at Early L3
WT (EL3)
mmp2/+ (EL3)
mmp2 (EL3)
B
Mean Heart Rate at Late L3
***
***
WT (LL3)
mmp2/+ (LL3)
mmp2 (LL3)
Mean
194
187
168
n
32
32
30
B'
Heart Rate at Late L3
WT(LL3)
mmp2/+ (LL3)
mmp2 (LL3)

Figure 3.40: Loss of *Mmp2* is correlated with lowered heart rate in third instar larvae. Examination of heart period using light microscope-based live-imaging of third instar larvae. **(A, B)** Mean heart rate of early **(A)** and late **(B)** third instar larvae. Heart rate is significantly different between control and homozygous mutant organisms at both early and late larval stages. **(A-A')** At early third instar, control organisms have a median heart rate of 234 BPM compared to 202 BPM for heterozygous *mmp2* mutants and 201 BPM for homozygous *mmp2* mutants. Heart rate of *mmp2* mutants is significantly different from wildtype, but is not significantly different between hetero- and homozygotes. **(B-B')** At late third instar, control organisms have a median heart rate of 197 BPM compared to 186 BPM for heterozygous *mmp2* mutants and 169 BPM for homozygous *mmp2* mutants. Heart rate of homozygous *mmp2* mutants is significantly different from wildtype and heterozygous mutants. Heterozygous mutants are not significantly different from wildtype. Heart rate is calculated as beats per minute (BPM). **(A,B)** Mean heart rate. Two-tailed t-test. Error bars are SEM. * $p \leq 0.05$ ** $p \leq 0.01$ *** $p \leq 0.005$. **(A',B')** X is the mean. Horizontal bar is the median. Box is the first to third quartile. Whiskers show minimum and maximum values before the fence (1.5 x IQR). *yw* is the wildtype control.

3.5.3 Summary of cardiac function

Heart rate decreased as larvae approached pupariation. The heart rate of homozygous *mmp2* mutants was significantly less than that of the wildtype at both early and late third instar. The area of the lumenal cavity at diastole and systole was not different between *mmp2* mutants and the wildtype at late third instar when considering non-bifurcated hearts, suggesting no difference in size or contractile ability.

4.0 Discussion and Future Directions:

The ECM is a dynamic structure that must accommodate considerable growth and re-arrangement throughout an organism's lifetime, and it is thought that matrix metalloproteinases (MMPs) and other proteases play a large role in modulating this turnover and remodelling (Frantz *et al.* 2010). Changes to the levels of structural proteins and proteases are observed in older and/or diseased vertebrate hearts (Bonnema *et al.* 2007; Raza 2015; Hughes and Jacobs 2017). Collagens are substrates for both *Drosophila* MMPs (Llano *et al.* 2000, 2002) and are of interest to studies of heart development and aging because these are noted to accumulate in aging and diseased adult *Drosophila* hearts (Na *et al.* 2013; Sessions *et al.* 2017; Vaughan *et al.* 2017). Similar accumulation and cross-linking is evident in vertebrates, coincident with changes in the levels of certain MMPs and TIMPs (Horn and Trafford 2016).

Despite the existence of a significant body of research on the expression of matrix metalloproteinases (MMPs) and their inhibitors (TIMPs) in the context of vertebrate cardiac dysfunction, little was known until recently about the role played by MMPs and TIMPs in *Drosophila* heart morphogenesis, growth, and maintenance. Studies performed by Raza *et al.* (2015, 2017) have revealed a critical role for MMP-mediated remodelling during cardiogenesis in *Drosophila* embryos. This thesis aimed to expand on this research by elucidating the role of MMPs in mediating post-embryonic heart development (heart growth) by answering three core questions; 1) does the loss of MMP function compromise larval heart morphology and growth?, 2) are MMPs required for the normal distribution

and expression of ECM structural proteins during larval development?, and 3) does MMP function determine heart size and cardiac function in third instar larvae?

This first question addressed how embryonic abnormalities manifest and change during larval development and cardiac growth when MMP function is altered constitutively versus throughout embryogenesis alone, as well as what defects arise when MMP function is altered post-embryonically after cardiogenesis is complete. I answered this by visualising the organisation of cardiomyocyte myofibrils in dissected third instar larvae via immunohistochemistry and microscopy. The second question aimed to describe the composition and distribution of the ECM, with explicit consideration of Collagen-IV and Prc, when MMP function is altered constitutively or at specific points during development. This allowed me to ascertain the specific requirement of MMPs for normal ECM distribution at various points in the organism's early life. The third question addressed the requirement of MMP2 for the preservation of cardiac function, and examined whether the loss of MMP2 can induce an old-age/diseased cardiac phenotype with respect to heart rate and contractile function.

With respect to all of these questions, I examined segment A7 of the dorsal vessel as this segment was the easiest to resolve without risk of anterior heart detachment and disruption of other tissues, and provided a good a means of examining ECM turnover during larval growth and the interplay between the ECM and contractile competency. As with a majority of the segments of the posterior heart chamber, A7 is lost during

metamorphosis and so is not a candidate for the study of adults (Sellin *et al.* 2006; Tao and Schulz 2007).

These questions were examined using loss-of-function mutants as well as induced genetic mosaics via Gal4-UAS-mediated over-expression or inhibition. The Gal4-UAS system provides both spatial and temporal control over protease activity with the addition of the temperature-sensitive $Gal80^{TS}$ allele. However, the efficacy of temperature shift-mediated changes to expression may be limited due to the unknown perdurance of MMP2 or TIMP proteins subsequent to the activation of the RNAi (18 to 29°C shift), and that of the *Mmp2* or *Timp* dsRNA subsequent to the activation of $Gal80^{TS}$ (29 to 18°C shift), as well as the rate at which the MMP2 and TIMP proteins are synthesised. A tagged protein or antibody may resolve this uncertainty; however, a reliable MMP2 antibody is not available at this time and the available *mmp2Gal4* and *mmp2-GFP* lines show weak/diffuse signal. Additionally, Gal4 controls were not examined due to time and resource limitations. It is noteworthy that the heterozygous expression of Gal4 in certain tissues has been shown to have phenotypic effects such as up-regulation of genes involved in apoptosis, particularly with heat shock stress (Duffy 2002; Kramer and Staveley 2003; Liu and Lehmann 2008).

Prior research conducted by Raza (2015) examined the embryonic roles of MMPs and associated signalling factors in mediating collective cell migration, cell polarity, and lumenogenesis. Raza noted disparate phenotypes in stage 17 embryos with reduced

MMP1 function versus MMP2 function, suggesting that these two proteases serve different functions in heart development and growth.

4.1 MMP2

Studies by Raza *et al.* (2015, 2017) demonstrated that homozygous but not heterozygous *mmp2* mutants exhibit non-uniform cardioblast migration and do not form a single uniform lumen. These embryos have increased Collagen-IV levels along the cardioblast surface and ectopically localised Prc at the cardioblast medial surface, suggesting a partial or complete loss of apical identity. Conversely, the over-expression of MMP2 in muscle tissues with the myocyte enhancer factor driver *mef2Gal4* compromises ECM-Integrin adhesions and disrupts the lumenal domain, resulting in the mis-alignment of cardioblasts and the formation of ectopic pocket lumens. In these larvae, Vkg-GFP signal is dramatically reduced.

Drosophila do not possess cardiac stem cells (Drechsler *et al.* 2013; Bogatan *et al.* 2015), so recovery from structural defects was not anticipated, leading me to predict the absence of a lumen amongst *mmp2* mutant larvae, as well as elevated Collagen-IV and Prc levels in larvae with reduced MMP2 function as a result of decreased turnover. Larvae over-expressing MMP2 were predicted to exhibit pocket lumens and reduced Collagen signal.

4.1.1 Organism-wide MMP2 function is not required for larval survivorship

A key measure of the importance of MMP-mediated regulation of the ECM is the effect of mis-regulation on survival. Partial or complete loss of MMP2 function does not impede embryogenesis or pupariation, corroborating the findings of Page-McCaw *et al.* (2003). Heterozygous *mmp2* mutants survive to adulthood without significant mortality during larval growth. Homozygous *mmp2* mutants and larvae ubiquitously expressing *Mmp2* dsRNA (*mmp2RNAi/daGal4*) successfully pupariate, but expire prior to eclosion. This indicates that the activity of MMP2 is dispensable for survival throughout embryonic and larval development but its function is required during metamorphosis. However, ubiquitous over-expression of MMP2 induces embryonic mortality, and larvae that undergo normal embryonic development experience mortality within hours of over-expressing MMP2, reinforcing the importance of maintaining precise regulation of ECM turnover throughout development.

Post-embryonic reduction of MMP2 function via ectopic expression of *Mmp2* dsRNA also causes pupal lethality, indicating that MMP2-mediated remodelling during metamorphosis is necessary for survival to adulthood. The converse (embryonic but not larval reduction) results in successful eclosion amongst a significant proportion of the population (Fig. S1), suggesting that 1) otherwise lethal defects arising during embryogenesis are repaired during larval development, 2) embryonic defects are not lethal in adults, or 3) those individuals that survive to eclosion are escapers or exhibit only mild defects.

4.1.2 Normal MMP2 function in the heart is dispensable for survival

Constitutive cardiac cell-specific reduction of MMP2 function does not result in significant mortality. This is as expected with respect to the larval growth stages, as a functioning heart is not required for larval survival (reviewed in Medioni *et al.* 2009). However, this would also suggest that MMP2 function in the heart is dispensable for survival throughout metamorphosis and early adulthood, though further studies on adults are needed to clarify whether MMP2 function in the heart is necessary for long-term survival. It should also be noted that *HandGal4* is activated later in embryogenesis (stage 12) (Kölsch and Paululat 2002) and is not as strongly or consistently expressed as the ubiquitous *daGal4* driver. It remains possible that non-cardiac cell-derived MMP2 localises to the heart, should *Mmp2* encode a secreted isoform as suggested by LaFever *et al.* (2017).

Cardiac cell-specific over-expression of MMP2 does not appear to have a negative effect on embryonic viability, as mortality is primarily observed in larvae. This larval lethality is unexpected, given that heart function is not essential throughout larval growth (Medioni *et al.* 2009), and so may result from increased MMP2 activity at the lymph gland, where *HandGal4* is also expressed (Kölsch and Paululat 2002). An alternative explanation might be that the excess MMP2 compromises other systems if certain isoforms are secreted.

4.1.3 Loss of MMP2 function results in lumenal defects, including cardia bifida

Lumenal defects are apparent in a large proportion of *mmp2* and *mmp1,mmp2* double mutants, principally in the form of cardia bifida. The cardia bifida phenotype is recapitulated with expression of *Mmp2* dsRNA, providing good evidence that loss of MMP2 function is indeed the cause. That cardia bifida is observed only in specimens with reduced MMP2 function throughout embryogenesis and first instar suggests that this phenotype originates during cardiogenesis as a result of failed cardioblast adhesion at the midline. Previous research by Raza *et al.* (2017) showed that the cardioblasts in *mmp2* mutant embryos do not correctly polarise; Integrin localises ectopically around the cell, whereas Slit and Robo accumulate at the lateral but not apical domains, and Dystroglycan is expressed in the plasma membrane. A majority of the bifurcated vessels observed in third instar larvae envelop a lumen along their entire length or portions thereof. This result is surprising because it suggests that lumenogenesis is not reliant upon the fusion of contralateral partners, as the current model of cardiogenesis predicts, and that a single row of cardioblasts is capable of co-ordinating to enclose a continuous cavity. The *Drosophila* dorsal vessel contains no stem cells (Drechsler *et al.* 2013; Bogatan *et al.* 2015), so it is not the case that additional cardioblasts proliferate at the site of bifurcation. The formation of ectopic lumens may arise in part from the lateral mis-localisation of lumenal determinants such as Slit and Robo; these formations are shown by Raza *et al.* (2017) to also contain Vkg and Integrin, which are characteristic of lumenal domains. Alternatively, non-paired cells may still able to polarise and recruit determinants of the dorsal and

ventral junctional domains, and thus envelop a lumenal domain via adhesion at an autocellular junction. This is not unprecedented; a superficially analogous phenomenon is observed in unicellular secondary tracheal branches (Samakovlis *et al.* 1996), though it is not known whether the mechanism might be similar.

The penetrance of cardia bifida is lower amongst mutant third instar larvae lacking functional *Mmp2* than is the penetrance of lumenal defects amongst embryos, of which upwards of 80% are found to have cardioblasts that fail to localise lumenal markers or fail to make contralateral contact, based on the observations of Raza *et al*. (2015, 2017). This is in spite of low mortality between these two stages. This disparity suggests some degree of recovery between embryogenesis/first instar and third instar that is not reliant upon cell proliferation.

Incomplete (torn) lumens are observed upon reduction of MMP2 either embryonically or post-embryonically. These take the form of large gaps in the vessel, most commonly along the ventral surface. This suggests that embryonic reduction in MMP2 compromises adhesion at the ventral (or dorsal) junctional domain, making the heart more susceptible to growth-related damage or strain. Hollfelder *et al.* (2014) posit that the ECM between the dorsal vessel cardiomyocytes and the flanking pericardial cells is a 'weak link' in the interplay of forces between the pulling by the alary muscles and the pumping action of the vessel, given that a reduction in ECM protein levels results in pericardial cell and alary muscle detachment. An increase in ECM protein levels arising from a reduction in MMP-mediated turnover, and a potential stiffening of the matrix,

might then place additional stress on cardiomyocytes, facilitating tearing at the compromised midline junction.

4.1.4 Over-expression of MMP2 compromises heart structure

Heart-specific over-expression of MMP2 throughout embryogenesis reveals a penetrant phenotype of failed lumenogenesis along a truncated dorsal vessel missing the anterior aorta. Larvae are also notable for a lack of alary muscle and pericardial cell attachment. The over-expression of MMP2, which localises to the leading edge of migrating cardioblasts during cardiogenesis (Raza *et al.* 2017), might disrupt cell polarity by promoting the expansion of the junctional domain at the expense of the pre-lumenal domain in a manner similar to, if more extreme than, the loss of MMP1 function, resulting in the observed lack of a lumen in the larval heart. The gross morphology and myofibrillar arrangement of the dorsal vessel at third instar very closely resembles that described by Drechsler *et al*. (2013) in *loh* and *prc* deficiency mutants, granting further confidence that mis-regulated MMP2 activity compromises ECM integrity. The loss of pericardial cells and alary muscles also bears similarity to the loss-of-function of the ECM proteins Lan, Vkg, or Prc, which are known substrates of MMP2, suggesting that normal MMP2 activity is necessary to stabilise cell-matrix adhesions that maintain the epidermal suspension of the vessel (Wolfstetter and Holz 2012; Drechsler *et al.* 2013; Hollfelder *et al.* 2014).

Surprisingly, cardiac phenotype is not conspicuously worsened upon heightened MMP2 over-expression at second instar when compared to larvae experiencing dampened MMP2 over-expression throughout development, and alary muscles and pericardial cells

remain associated with the vessel. While it may be that the more established larval ECM is more resilient to an increase in MMP2 activity, this unaltered phenotype may be the result of relatively weaker *HandGal4* expression throughout larval development; *Hand* transcription is elevated during embryogenic and pupal stages (Kölsch and Paululat 2002; Tögel *et al.* 2013), but protein levels appear lower in larvae based upon cursory observations of fluorescence (personal observations, data not shown). It is also unclear to what extent *HandGal4* activity is reduced at 18°C, and it is possible that a temperature shift to 29°C results in only a moderate increase in activity.

An unanticipated result of MMP2 over-expression is the greater severity of aortal defects, even with dampened Gal4 activity, whereby the aorta is reduced to a thread of longitudinal myofibrils or is entirely absent. A targeted study of aortal segments T2 through A4 at embryonic and larval stages will elucidate if this region of the vessel is indeed more susceptible to altered MMP2 levels, but this is beyond the purview of the thesis.

4.1.5 Collagen-IV

Collagens are important structural proteins of the ECM, and so act as indicators of ECM remodelling. Collagen-IV (formed of Vkg and Cg25C chains) is a core component of the basement membrane and interstitial matrix, where it plays a critical role in the stabilisation and reinforcement of the matrix as a whole; it is required to maintain adhesion between the dorsal vessel, pericardial cells, and alary muscles (Martinek *et al.* 2008; Hollfelder *et al.* 2014). It must be mentioned that although vertebrate collagenases

are known through substrate zymography to degrade multiple Collagens (Inanc *et al.* 2017), there is only indirect evidence that MMP2 degrades Collagen-IV (Guha *et al.* 2009; Raza *et al.* 2017). More direct measures (e.g. Collagen zymography) are necessary to verify MMP2 substrate affinity.

To visualise and quantify Collagen-IV at early and late third instar, I used a GFP protein trap construct labelling the Vkg α2-chain. Fluorescence signal was used as a proxy for protein level, as per the protocol followed by Acker (2016), Cevik (2016), and Raza *et al*. (2017).

Collagen-IV accumulates naturally in growing wildtype larval hearts, even when correcting for increased surface area, and a significant increase in Vkg density is noted between early and late third instar. These findings resemble those of Acker (2016) who posited that an increase in larval Collagen might be required accommodate subsequent growth. However, this may simply be a feature of older hearts, as non-growing adult *Drosophila* and vertebrate hearts also reveal an increased density of Collagens with age (Biernacka and Frangogiannis 2011; Na *et al.* 2013; Horn and Trafford 2016; Sessions *et al.* 2017; Vaughan *et al.* 2017).

The dense Collagen-IV plaques that sometimes form along the lumenal and ablumenal surfaces of the dorsal vessel may occur transiently during normal turnover, as these plaques appear across all genotypes so far examined using Confocal microscopy. However, cross-sectional electron micrographs of wildtype organisms lacking the Vkg-GFP trap construct fail to duplicate this phenotype. All lines used in this thesis were back-

crossed for multiple generations into the *yw* lab wildtype background, so it seems unlikely that these plaques arise due to specific background effects. However, all sampled organisms were heterozygous for the insert, and it is possible that these plaques/aggregates result from aberrant cross-linking between Collagen-IV heterotrimers with and without the terminal GFP tag on the α2 chain. Examination of larvae homozygous for the Vkg-GFP trap construct may shed light on this.

Collagen-IV forms conspicuous lumenal aggregates in *mmp2* mutant larvae, principally near regions of the heart that show cardia bifida. Although lumenal obstruction by Collagen-IV aggregates is not completely novel to larvae with reduced MMP2 function, this phenotype is much more penetrant amongst these specimens, suggesting that MMP2-mediated proteolysis throughout embryogenesis and/or larval growth plays a significant role in mitigating the accumulation of lumenal Collagen-IV. This would suggest that reduced MMP2 activity (i.e. reduced proteolysis) results in the accretion of Collagen-IV along the lumenal surface, possibly derivative of lumenal plaques or fibrotic deposits, and that this mass is then sloughed away by hemolymph as it is propelled through the heart chamber, accumulating where the vessel narrows. This phenotype resembles the fibrotic Collagen-IV aggregates that arise pericellularly or cytoplasmically in adipocytes when endocytosis or secretion is impaired in these cells (Pastor-Pareja and Xu 2011; Zang *et al.* 2015).

Mean Vkg-GFP signal suggests that there is increased Collagen-IV distribution at the dorsal vessel in third instar homozygous *mmp2* mutants compared to controls and

heterozygotes, in line with the results of Raza *et al.* (2017) for late-stage embryos. A single functional copy of *Mmp2* therefore appears sufficient to preserve normal Collagen-IV protein levels. The exclusion of specimens with conspicuous aggregates does not alter the observed trend, suggesting that it is not just re-distribution of Collagen-IV that causes this increase in signal. These findings cannot be corroborated with *Mmp2* dsRNA due to the weak cardiac phenotype exhibited by the alternative RNAi line expressing *vkg-GFP*.

As predicted, the constitutive over-expression of MMP2 has the opposite effect, and I observe a significant reduction in the Vkg-GFP signal along the heart, even when taking into account the reduced surface area. However, post-embryonic over-expression of MMP2 in the heart does not reduce Vkg-GFP signal along the posterior vessel. This is corroborated by visual inspection; embryonic over-expression of MMP2 correlates with the absence of Collagen-IV along the dorsal vessel surface, whereas post-embryonic over-expression does not appear to alter its distribution except along the aortal remnant, where its signal is weaker. Thus MMP2 plays a significant role in mediating Collagen-IV distribution throughout embryogenesis, but less so during larval growth.

4.1.6 Pericardin

Pericardin is a *Drosophila*-specific Collagen that forms a web-like network along the ablumenal surface of the dorsal vessel, where it serves preserve matrix stability via pericardial cell and alary muscle adhesion (Chartier *et al.* 2002; Drechsler *et al.* 2013). The use of immunohistochemistry to visualise and quantify Prc distribution at third instar, as per the protocol followed by Acker (2016), is problematic due to the susceptibility of the

Prc network to mechanical damage, as well as the variability of Prc fluorescence signal within and between sample groups. Though this variability may be a result of normal turnover during larval growth, the possibility cannot be dismissed that this is an artefact of the staining process.

Embryonic MMP2 activity at the dorsal vessel is required for the normal distribution of Prc in larvae, as both the ubiquitous and cardiac cell-specific reduction of MMP2 during embryogenesis correlate with the ectopic and non-uniform arrangement of Prc. However, these disruptions are not observed when MMP2 function is reduced from second instar onwards, which suggests that they arise primarily during embryonic development as a result of cardiogenic defects. These core findings are supported by quantitative fluorescence analysis, although this is confounded by some inconsistencies in the data. Larvae expressing MMP2 dsRNA do show significantly increased Prc signal when MMP2 function is reduced within cardiac cells, in line with predictions (an increase is also observed upon ubiquitous dsRNA expression, but this is below the threshold of significance). Similarly elevated levels of Prc fluorescence signal are found amongst larvae with post-embryonic reduction versus constitutive reduction of MMP2, implying that MMP2 activity during larval development may be involved in mediating Prc protein levels around the heart. This would suggest that accumulation of Prc does not necessarily correlate with ectopic distribution. Surprisingly, homozygous *mmp2* mutants at early third instar show no significant difference in Prc signal when compared to the wildtype and to heterozygous mutants, though it must be noted that peripheral Prc is not considered in

these samples due to imaging constraints. Of interest also is the larval distribution of the recruitment factor Loh, which is known to localise Prc to tissues within which it is embryonically expressed, and which is believed to associate with βPS-Integrin (Drechsler *et al.* 2013).

MMP2's developmental importance in regulating Prc is substantiated by over-expression, which results in a significant reduction in Prc signal at segment A7. Prc is still localised to the heart vestige upon embryonic over-expression of MMP2 but the network is not organised, and appears to collapse around the vessel in the absence of pericardial cells and alary muscles. Post-embryonic over-expression of MMP2 does not reveal an obviously worse Prc phenotype when compared to that of larvae reared entirely at 18°C; in both cases the network is often disorganised or damaged, possibly due to a weakening of the matrix from the basal *HandGal4* activity. Nor does this significantly reduce Prc signal, although the overall trend shows that the signal is less than that of the control. This would imply that MMP2 might not be a principal contributor to Prc levels during larval development. Given the variability experienced by both Acker (personal communication) and myself, more reliable quantitative tests are necessary to determine whether Prc protein levels around the heart are altered upon reduced MMP2 function. Plans are presently underway to perform Western Blotting using the entire hearts of *mmp2* mutants, as well as larvae expressing *Mmp2* dsRNA.

4.1.7 Effect of altered MMP2 levels on cardiac function

The levels of ECM proteins such as Lan, Vkg, and Prc are correlated with basement membrane thickness, though not necessarily matrix stiffness (Sessions *et al.* 2017). Accretion of ECM proteins such as Collagens and Integrins has been linked to fibrosis in adult organisms (rats and *Drosophila*), resulting in decreased elasticity, diastolic diameter, and fractional shortening (Eghbali *et al.* 1988; Nishimura *et al.* 2014). Though this evidence comes from adult hearts, it seems reasonable that a similar trend might be apparent in larvae. Counter to my prediction that contractility would decrease in third instar larvae with reduced MMP2 function, the loss of *Mmp2* function did not affect the capacity of the larval heart to contract. Even bifurcated vessels demonstrate the ability to contract in synchrony with the rest of the heart, suggesting that these hearts are functional and that myocardial pacemakers and proteins responsible for excitation-contraction coupling (Bodmer *et al.* 2005; Ocorr *et al.* 2007) are not severely compromised.

Homozygous *mmp2* mutants are no smaller than their wildtype counterparts, and their hearts are similarly sized in regions devoid of bifurcation, suggesting that the enlargement of cardiomyocytes is not compromised by the accumulation of ECM proteins in the absence of MMP2 function. However, bifurcated vessels are smaller in cross-sectional area both individually and in sum than their non-bifurcated counterparts. The maximum dilation (diastole) and contraction (systole) of non-bifurcated homozygous *mmp2* mutant hearts are not different from the wildtype. This would suggest that

decreased *Mmp2* expression in larvae does not fully replicate aged or diseased cardiac phenotypes such as restrictive or dilated cardiomyopathies. Whatever fibrotic accretion of ECM Collagens (and other proteins) is experienced by these hearts, it is insufficient to compromise their contractile function. It is possible that the growing larval heart is more resilient to increases in ECM protein levels, or that these proteins simply do not reach a threshold level within the larval growth phase when only MMP2 function is compromised. Given that previous studies showing the significant effects of altered ECM protein expression have focused on adult flies, an obvious next step would be the examination of adults deficient for *Mmp2*.

Heart rate is shown to decrease with age in wildtype adult *Drosophila* (Paternostro *et al.* 2001) following accumulation of Collagen-IV and Prc, and it has been demonstrated that this age-related decline can be mitigated by a reduction in SPARC-mediated Collagen deposition (Vaughan *et al.* 2017). My findings demonstrate that MMP2 function is necessary to maintain a normal larval heart rate; at both early and late third instar, heart rate is significantly lower in homozygous *mmp2* mutants than the wildtype. It might be that heart rate is more noticeably influenced by mild cross-linking and ECM stiffening than other measures of heart function, or this could be symptomatic of defects arising elsewhere in the organism due to the loss of MMP2 function. *mmp2* mutants do not show obvious signs of arrhythmia or arrest as is the case with *mmp1* mutants, suggesting that the hearts are not failing. There is an emerging difference between hetero- and

homozygous *mmp2* mutants between early and late third instar, suggesting that the system is more resilient to the partial loss of MMP2 function during later growth.

4.2 MMP1

Prior research by Raza *et al.* (2015, 2017) showed that homozygous but not heterozygous *mmp1* mutants exhibit retarded/disorganised cardioblast migration, eventually forming a single lumen of reduced diameter due to the expansion of the cardioblast adhesion domain. Given that MMP1 function is not restored subsequent to cardiogenesis, embryonic defects were anticipated to persist throughout subsequent growth, leading me to predict a reduced lumen size amongst *mmp1* mutant larvae.

4.2.1 Organism-wide MMP1 function is required for larval survival

My analysis of the survivorship of individuals with ubiquitously reduced MMP1 function corroborates that of Page-McCaw *et al.* (2003), who note that a single functional copy of *Mmp1* is sufficient to ensure survival to adulthood. Complete loss of MMP1 function does not impede embryogenesis, but homozygous *mmp1* and *mmp1,mmp2* double mutants, as well as *mmp1RNAi/daGal4* larvae, expire before pupariation, indicating that the activity of MMP1 is required for larval development.

4.2.2 Loss of MMP1 compromises larval growth

Homozygous *mmp1* and *mmp1,mmp2* double mutants appear smaller than their wildtype and heterozygous counterparts throughout larval growth. These findings match those of Page-McCaw *et al.* (2003), who note defects in tracheal growth, resulting in broken and necrotic trachea, and posit that these larvae may be oxygen-starved. It is presently not clear whether this stunted growth is a direct result of the loss of MMP1-mediated turnover or a side-effect of oxygen deficiency, or a combination of both. Unfortunately, the small early third instar heart cannot easily be resolved by OCT or light microscope live-imaging, so accurate measures of lumen size are not available.

4.2.3 Loss of MMP1 function results in mild disorganisation of the cardiac cytoskeleton

Larvae with reduced *mmp1* function do not exhibit conspicuous lumenal defects. Unfortunately, direct comparisons of lumen size between *mmp1* mutants and the control are confounded by disparities in larval size. However, the cardiomyocytes of *mmp1* mutant larvae do exhibit cytoskeletal defects in the form of non-uniform myofibrillar arrangements and uneven midline attachments, which may stem from the compromised collective cell migration described by Raza *et al.* (2015, 2017).

4.2.4 ECM protein distribution

An in-depth analysis of Collagen-IV and Prc protein distribution was not performed, as priority was given to the examination of MMP2 owing to the more prominent cardiac

phenotypes exhibited by larvae with reduced MMP2 function. However, qualitative analysis reveals no consistent defects in Collagen-IV localisation; lumenal aggregates appear rarely in both heterozygous and homozygous *mmp1* mutants, but the majority of third instar larvae are not distinct from wildtype. With respect to Prc, some increase in ectopic localisation as well as fluorescence signal is observed, which bears closer examination using confocal and Western Blotting techniques.

4.3 TIMP

4.3.1 Over-expression of TIMP reduces larval survivorship to an extent comparable to the loss of MMP1 function

TIMP is an inhibitor of multiple proteases such as ADAMs and ADAMTs, in addition to MMP1 and MMP2, and so may exhibit pleiotropy (Wei *et al.* 2003; Nagase *et al.* 2006). Constitutive organism-wide over-expression of TIMP is lethal during larval development, but does not result in worse survival than the loss of MMP1 function alone, at any stage. This implicates MMP1 as the protease critical for larval survival, though a closer examination of the other TIMP targets (ADAMS and ADAMTS) is necessary to confirm this.

Interestingly, temporally-controlled mis-expression of TIMP reveals a similar trend to the inhibition of MMP2. As previously illustrated through reduction of MMP2 function, growth and metamorphosis are critical phases for protease activity, and their inhibition throughout these stages is lethal. More revealing, however, is that the embryonic activity

of multiple proteases is dispensable for survival. This again suggests that embryonic defects might be repaired during larval development, though it cannot be discounted that those surviving individuals are escapers exhibiting only mild defects.

As with the inhibition of MMP2 function, mis-regulation of TIMP within cardiac cells does not result in significant mortality throughout larval development or metamorphosis. This is in line with evidence that suggests cardiac function is not necessary for larval survivorship (Medioni *et al.* 2009). It remains unclear whether protease activity in the heart might be dispensable for survival, or if a dysfunctional heart is not immediately lethal to adults. However, the previously-mentioned caveats regarding *HandGal4* cannot be discounted.

4.3.2 Over-expression of TIMP reproduces cardiac phenotypes observed upon loss of MMP2 function

The lumenal defects observed by Raza *et al.* (2015, 2017) in stage 17 embryos upon ectopic TIMP over-expression are apparent amongst third instar larvae in the form of cardia bifida and/or incomplete lumens, in common with larvae experiencing reduced MMP2 function. Curiously, cardia bifida is also apparent in larvae upon cardiac cell-specific over-expression, despite ostensibly normal lumenogesis (Raza *et al.* 2015, 2017). This may relate to the specific expression patterns of *mef2Gal4* versus *HandGal4*, though the former is activated in cardioblasts earlier in development (Han and Bodmer 2003). It seems more likely, however, that adhesion defects were not observed amongst embryos due to their relatively low penetrance.

A novel alary muscle defect noted by Mahan Ghodrati upon constitutive and ubiquitous over-expression of TIMP was not reproduced upon my examination of this genotype. His confocal projections reveal thick longitudinal fibres along the heart vessel, similar to the distribution observed in adults or along the larval aorta. It is unclear why this phenotype cannot be replicated. If this is a legitimate consequence of TIMP over-expression, its uniqueness from *mmp1* and *mmp2* mutant phenotypes suggests a role for ADAMs or ADAMTs. However, that my own work reveals a phenotype identical to that of reduced MMP2 function suggests that these other proteases play a minimal or overlapping role in cardiac morphogenesis and growth.

Timp is expressed embryonically in cardioblasts, though TIMP protein is reported as being secreted (Godenschwege *et al.* 2000; Dear *et al.* 2015). Prior research by Raza (2015) showed that ectopic over-expression of TIMP in the ectoderm but not in cardioblasts prevents the apical localisation of cardioblast lumenal markers, resulting in impaired cardiac lumenogenesis, manifesting either as a reduced lumen or no lumen (gaps between contralateral cardioblasts). However, unlike the ectopic ectodermal over-expression of TIMP, its over-expression within the mesodermally-derived fat body does not correlate with conspicuous structural defects except in a minority of cases, suggesting that inhibition of proteases in the fat body has little or no effect upon heart development or growth. This comes in spite of the tissue's close proximity to the dorsal vessel and its role as a source of Collagen-IV and Pericardin throughout larval devlopment (Pastor-Pareja and Xu 2011; Drechsler *et al.* 2013). It is possible that the activation of *R4Gal4* during late

embryogenesis (Lee and Park 2004) comes about too late to noticeably compromise cardiogenesis, or that *Timp* expression in the fat body is not sufficiently local to affect the heart.

4.3.3 Collagen-IV

TIMP-mediated loss of protease function, either ubiquitously or locally within the heart, correlates with increased Collagen-IV density (Vkg-GFP signal) as well as the presence of lumenal obstructions. That cardiac cell-specific over-expression of TIMP is sufficient to induce these obstructions in bifurcated but otherwise intact hearts suggests that excess Collagen-IV is not being carried from elsewhere in the organism via hemolymph travelling through the ostia into the heart lumen. The presence of Collagen-IV aggregates near regions of the dorsal vessel with disrupted (torn) lumens may correspond to an outflow of lumenal Collagen, or this may indicate a fibrotic response to damage, although this is more typical of interstitial Collagens (Pelouch *et al.* 1993; Biernacka and Frangogiannis 2011; Na *et al.* 2013).

Ubiquitous over-expression of TIMP from second instar onwards correlates with increased Collagen-IV density amongst late but not early third instar larvae. This implies that MMPs, or other proteases targeted by TIMP, are required during larval development to mediate turnover and mitigate excess Collagen-IV accumulation during later larval growth. That similarly timed over-expression of MMP2 in the heart does not reduce Collagen-IV levels along the posterior vessel implies that MMP2 might not be a principal mediator of cardiac Collagen-IV turnover during larval growth.

4.3.4 Pericardin

Inhibition of multiple proteases by TIMP over-expression does not result in a conspicuously different or worse Prc phenotype than the reduction of MMP2 on its own. This would suggest that MMP2 is an important mediator of Prc localisation amongst those proteases targeted by TIMP. Ectopic Prc bundles and disorganisation of the Prc network are frequently observed with embryonic TIMP mis-expression, and these features are not noticeably improved by the restoration of normal protease activity at second instar. The disorganisation of the Prc network is closely associated with cardiac morphological defects that arise throughout development. This suggests that Prc localisation is largely dependent on the embryonic environment and the changing topography of the larval heart vessel.

Quantitative analysis of Prc fluorescence signal at early and late third instar suggests a subtle increase in Prc protein levels following embryonic inhibition of protease activity, as is observed with reduced MMP2 function. However, these data are victim to the same variability described previously. There is a trend of increased Prc levels across segment A7 upon cardiac cell-specific over-expression of TIMP that is replicated with ubiquitous over-expression of TIMP in early but not late third instar larvae. However, that post-embryonic restoration of protease activity does not promote an increase in Prc protein levels in early third instar larvae runs counter to my findings upon MMP2 reduction. Analysis of protein expression with the Western Blot technique will resolve this uncertainty.

4.4 Conclusion

Based on my observations of the dorsal vessel following reduced or ectopic protease activity, it appears that heart morphology and the density and distribution of ECM proteins are predominantly determined by embryonic events. However, normal protease activity throughout larval development is critical for the maintenance of cardiac integrity; the loss of protease function during larval development compromises cardiomyocyte adhesion, resulting in the disruption of the lumen. Although the distribution of ECM proteins is not much altered upon mis-regulation of proteases in larvae, the resulting pupal mortality suggests that metamorphosis is impaired. Interestingly, protease activity at the heart is not necessary for survival to any life stage, which may speak to the dispensability of dorsal vessel.

4.5 Future Directions

4.5.1 Mechanism for lumenogenesis in non-adhering cardioblasts

The formation of lumens within bifurcated hearts was not predicted by the current model of cardiogenesis (as reviewed in Tao and Shulz 2007 and described by Raza *et al.* 2017), and instead suggests that lumenogenesis is not reliant upon the dorsal and ventral adhesion of contralateral partners. A closer examination of heart development from embryonic stage 17 through first instar, including the localisation of lumenal and

junctional domain markers, will provide insight into how lumen formation within a single cardioblast occurs.

4.5.2 Adult requirement of MMP activity for cardiac function

This thesis characterises MMP-mediated remodelling of the *Drosophila* dorsal vessel. However, my analysis of cardiac morphology, ECM protein levels and localisation, and cardiac function is limited to larval stages of development, specifically the third instar. Of particular interest is the effect on these metrics of altered MMP function in adult organisms. Considerable remodelling occurs during metamorphosis (Sellin *et al.* 2006; Tao and Schulz 2007), and this is a critical juncture for MMP activity, as illustrated by the high mortality of *mmp2* mutants at the pupal stage. Moreover, the adult heart is of interest in the study of aging and emergent cardiac pathologies (Ocorr *et al.* 2007; Nishimura *et al.* 2011; Sessions *et al.* 2017). Over-expression of TIMP and MMP2, or the expression of *Mmp1/2* dsRNA, can be induced during or after metamorphosis to examine the role of MMPs in heart remodelling and aging. It is already known that the reduction of MMP2 throughout embryogenesis (but not larval development or pupariation) permits successful eclosion. The examination of adult specimens would provide insight into the how persistent are those embryonic defects, and the extent to which they compromise adult heart function.

4.5.3 Effect of reduced TIMP function on ECM remodelling and protein distribution

This thesis examines the requirement of proteases for larval development with *Mmp* mutants and dsRNA- and TIMP-mediated inhibition, as well as the over-expression of MMP2. Of interest are the consequences for dorsal vessel morphology and cardiac ECM upon reduced TIMP expression, and the resultant release of multiple proteases from regulated inhibition. The research presently underway (performed by Samantha Turner) will answer this question using *Timp* mutants and dsRNA, with a similar focus on cardiac structure and the ECM components Collagen-IV and Prc.

4.5.4 Function and distribution of hemocytes at the dorsal vessel upon protease mis-regulation

Preliminary tests using a βPS1-Integrin antibody suggest the accumulation of hemocytes around sites of bifurcation in larvae with reduced MMP2 function, and surrounding pericardial cells in larvae mildly over-expressing MMP2 (Fig. S6). Their presence at the dorsal vessel would not be surprising, given that hemocytes are analogous to mammalian blood cells and are known to aggregate as an immune response to tissue damage and degradation of the basement membrane by MMP2 (Pastor-Pareja *et al.* 2008). An in-depth examination with a hemocyte marker (e.g. *HmldsRed*) will confirm the presence of hemocytes. In the context of MMP2 over-expression, hemocytes might indicate the degradation of pericardial cells, as per the observations of Acker (2016).

References

Acker M., 2016 Pericardial cells and extracellular matrix remodelling. MSc ThesisMcMaster Univ.: 1–87.

Albrecht S., Wang S., Holz A., Bergter A., Paululat A., 2006 The ADAM metalloprotease Kuzbanian is crucial for proper heart formation in Drosophila melanogaster. Mech. Dev. 123: 372–387.

Ali M. A. M., Fan X., Schulz R., 2011 Cardiac Sarcomeric Proteins: Novel Intracellular Targets of Matrix Metalloproteinase-2 in Heart Disease. Trends Cardiovasc. Med. 21: 112–118.

Arpino V., Brock M., Gill S. E., 2015 The role of TIMPs in regulation of extracellular matrix proteolysis. Matrix Biol. 44–46: 247–254.

Bataillé L., Frendo J. L., Vincent A., 2015 Hox control of Drosophila larval anatomy; The Alary and Thoracic Alary-Related Muscles. Mech. Dev. 138: 170–176.

Biernacka A., Frangogiannis N. G., 2011 Aging and Cardiac Fibrosis. Aging Dis. 2: 158–173.

Bodmer R., 1995 Heart Development and Its Relationship in Drosophila to Vertebrates. Trends Cardiovasc. Med. 5: 21–28.

Bodmer R., Venkatesh T. V., 1998 Heart development in Drosophila and vertebrates: Conservation of molecular mechanisms. Dev. Genet. 22: 181–186.

Bodmer R., Wessells R. J., Johnson E. C., Dowse H. B., 2005 Heart development and function. Compr. Mol. Insect Sci. 2: 199–250.

Bogatan S., Cevik D., Demidov V., Vanderploeg J., Panchbhaya A., *et al.*, 2015 Talin is required continuously for cardiomyocyte remodeling during heart growth in Drosophila. PLoS One 10: 1–16.

Bonnans C., Chou J., Werb Z., 2014 Remodelling the extracellular matrix in development and disease. Nat rev mol cell biol 15: 786–801.

Bonnema D. D., Webb C. S., Pennington W. R., Stroud R. E., Leonardi A. E., *et al.*, 2007 Effects of age on plasma matrix metalloproteinases (MMPs) and tissue inhibitor of metalloproteinases (TIMPs). J. Card. Fail. 13: 530–540.

Brew K., Nagase H., 2010 The tissue inhibitors of metalloproteinases (TIMPs): An ancient family with structural and functional diversity. Biochim. Biophys. Acta - Mol. Cell Res. 1803: 55–71.

Brooks A., Schinde V., Bateman A. C., Gallagher P. J., 2003 Interstitial fibrosis in the dilated

non-ischaemic myocardium. Heart 89: 1255–6.

Brown J. B., Boley N., Eisman R., May G. E., Stoiber M. H., *et al.*, 2014 Diversity and dynamics of the Drosophila transcriptome. Nature 512: 393–399.

Bryantsev A. L., Cripps R. M., 2009 Cardiac gene regulatory networks in Drosophila. Biochim. Biophys. Acta - Gene Regul. Mech. 1789: 343–353.

Bunt S., Hooley C., Hu N., Scahill C., Weavers H., *et al.*, 2010 Hemocyte-secreted type IV collagen enhances BMP signaling to guide renal tubule morphogenesis in Drosophila. Dev. Cell 19: 296–306.

Burgess M. L., McCrea J. C., Hedrick H. L., 2001 Age-associated changes in cardiac matrix and integrins. Mech. Ageing Dev. 122: 1739–1756.

Cevik D., 2016 Hemocyte-pericardial cell interaction. MSc Thesis, McMaster Univ.: 1–106.

Chartier A., Zaffran S., Astier M., Sémériva M., Gratecos D., 2002 Pericardin, a Drosophila type IV collagen-like protein is involved in the morphogenesis and maintenance of the heart epithelium during dorsal ectoderm closure. Development 129: 3241–3253.

Cieslik K. A., Taffet G. E., Carlson S., Hermosillo J., Trial J. T., *et al.*, 2012 Immune-inflammatory Dysregulation Modulates the Incidence of Progressive Fibrosis and Diastolic Stiffness in the Aging Heart. J. Mol. Cell. Cardiol. 50: 248–256.

Colognato H., Yurchenco P. D., 2000 Form and function: The laminin family of heterotrimers. Dev. Dyn. 218: 213–234.

Conrad C. H., Brooks W. W., Hayes J. A., Sen S., Robinson K. G., *et al.*, 1995 Myocardial Fibrosis and Stiffness With Hypertrophy and Heart Failure in the Spontaneously Hypertensive Rat. Circulation 91: 161–170.

Dear M. L., Dani N., Parkinson W., Zhou S., Broadie K., 2015 Two matrix metalloproteinase classes reciprocally regulate synaptogenesis. Development: 75–87.

Drechsler M., Schmidt A. C., Meyer H., Paululat A., 2013 The Conserved ADAMTS-like Protein Lonely heart Mediates Matrix Formation and Cardiac Tissue Integrity. PLoS Genet. 9: 16–18.

Duffy J. B., 2002 GAL4 system indrosophila: A fly geneticist's swiss army knife. Genesis 34: 1–15.

Eghbali M., Czaja M. J., Zeydel M., Weiner F. R., Zern M. A., *et al.*, 1988 Collagen chain mRNAs in isolated heart cells from young and adult rats. J. Mol. Cell. Cardiol. 20: 267–276.

Frantz C., Stewart K. M., Weaver V. M., 2010 The extracellular matrix at a glance. J. Cell Sci. 123: 4195–4200.

Glasheen B. M., Kabra A. T., Page-McCaw A., 2009 Distinct functions for the catalytic and hemopexin domains of a Drosophila matrix metalloproteinase. Proc. Natl. Acad. Sci. U. S. A. 106: 2659–2664.

Godenschwege T. A., Pohar N., Buchner S., Buchner E., 2000 Inflated wings, tissue autolysis and early death in tissue inhibitor of metalloproteinases mutants of Drosophila. Eur. J. Cell Biol. 79: 495–501.

Gu J. L., Gu J. L., Receive R., Receive R., Research G., *et al.*, 2005 The mouse genome. Genome Res.: 1729–1740.

Guha A., Lin L., Kornberg T. B., 2009 Regulation of Drosophila matrix metalloprotease Mmp2 is essential for wing imaginal disc:trachea association and air sac tubulogenesis. Dev. Biol. 335: 317–326.

Haack T., Schneider M., Schwendele B., Renault A. D., 2014 Drosophila heart cell movement to the midline occurs through both cell autonomous migration and dorsal closure. Dev. Biol. 396: 169–182.

Haag T. A., Haag N. P., Lekven A. C., Hartenstein V., 1999 The role of cell adhesion molecules in Drosophila heart morphogenesis: faint sausage, shotgun/DE-cadherin, and laminin A are required for discrete stages in heart development. Dev. Biol. 208: 56–69.

Han Z., Bodmer R., 2003 Myogenic cells fates are antagonized by Notch only in asymmetric lineages of the Drosophila heart, with or without cell division. Development 130: 3039–3051.

Harpaz N., Ordan E., Ocorr K., Bodmer R., Volk T., 2013 Multiplexin Promotes Heart but Not Aorta Morphogenesis by Polarized Enhancement of Slit/Robo Activity at the Heart Lumen. PLoS Genet. 9.

Hollfelder D., Frasch M., Reim I., 2014 Distinct functions of the laminin β LN domain and collagen IV during cardiac extracellular matrix formation and stabilization of alary muscle attachments revealed by EMS mutagenesis in Drosophila. BMC Dev. Biol. 14: 26.

Horn M. A., Graham H. K., Richards M. A., Clarke J. D., Greensmith D. J., *et al.*, 2012 Age-related divergent remodeling of the cardiac extracellular matrix in heart failure: Collagen accumulation in the young and loss in the aged. J. Mol. Cell. Cardiol. 53: 82–90.

Horn M. A., 2015 Cardiac physiology of aging: Extracellular considerations. Compr. Physiol. 5: 1069–1121.

Horn M. A., Trafford A. W., 2016 Aging and the cardiac collagen matrix: Novel mediators of fibrotic remodelling. J. Mol. Cell. Cardiol. 93: 175–185.

Huet E., Huet E., Gabison E., Vallee B., Mougenot N., *et al.*, 2015 Deletion of extracellular matrix metalloproteinase inducer/cd147 induces altered cardiac extracellular matrix remodeling in aging mice. J. Physiol. Pharmacol. 66: 355–366.

Hughes C. J. R., Jacobs J. R., 2017 Dissecting the Role of the Extracellular Matrix in Heart Disease: Lessons from the Drosophila Genetic Model. Vet. Sci. 4: 24.

Hynes R. O., 1987 Integrins: A family of cell surface receptors. Cell 48: 549–554.

Inanc S., Keles D., Oktay G., 2017 An improved collagen zymography approach for evaluating the collagenases MMP-1, MMP-8, and MMP-13. Biotechniques 63: 174–180.

Isabella A. J., Horne-Badovinac S., 2015 *Building from the Ground up: Basement Membranes in Drosophila Development*. Elsevier Ltd.

Jia Q., Liu Y., Liu H., Li S., 2015 Mmp1 and Mmp2 cooperatively induce Drosophila fat body cell dissociation with distinct roles. Sci. Rep. 4: 7535.

Kölsch V., Paululat A., 2002 The highly conserved cardiogenic bHLH factor Hand is specifically expressed in circular visceral muscle progenitor cells and in all cell types of the dorsal vessel during Drosophila embryogenesis. Dev. Genes Evol. 212: 473–485.

Kramer J. M., Staveley B. E., 2003 GAL4 causes developmental defects and apoptosis when expressed in the developing eye of Drosophila melanogaster. Genet. Mol. Res. 2: 43–47.

Kular J. K., Basu S., Sharma R. I., 2014 The extracellular matrix: Structure, composition, age-related differences, tools for analysis and applications for tissue engineering. J. Tissue Eng. 5: 204173141455711.

LaFever K. S., Wang X., Page-McCaw P., Bhave G., Page-McCaw A., 2017 Both Drosophila matrix metalloproteinases have released and membrane-tethered forms but have different substrates. Sci. Rep. 7: 44560.

Lee G., Park J. H., 2004 Hemolymph sugar homeostasis and starvation-induced hyperactivity affected by genetic manipulations of the adipokinetic hormone-encoding gene in Drosophila melanogaster. Genetics 167: 311–323.

Lee S., Park J., Kim Y., Chung H., Yoo M., 2012 Requirement of matrix metalloproteinase-1 for intestinal homeostasis in the adult Drosophila midgut. Exp. Cell Res. 318: 670–681.

Lehmacher C., Abeln B., Paululat A., 2012 The ultrastructure of Drosophila heart cells. Arthropod Struct. Dev. 41: 459–474.

Lemaître V., D'Armiento J., 2006 Matrix metalloproteinases in development and disease. Birth Defects Res. Part C - Embryo Today Rev. 78: 1–10.

Liu Y., Lehmann M., 2008 A genomic response to the yeast transcription factor GAl4 in Drosophila. Fly (Austin). 2: 92–98.

Llano E., Pendas A. M., Aza-Blanc P., Kornberg T. B., Lopez-Otin C., 2000 Dm1-MMP, a matrix metalloproteinase from Drosophila with a potential role in extracellular matrix remodeling during neural development. J. Biol. Chem. 275: 35978–35985.

Llano E., Adam G., Pendás A. M., Quesada V., Sánchez L. M., *et al.*, 2002 Structural and enzymatic characterization of Drosophila Dm2-MMP, a membrane-bound matrix metalloproteinase with tissue-specific expression. J. Biol. Chem. 277: 23321–23329.

Lo P. C. H., Frasch M., 2003 Establishing A-P polarity in the embryonic heart tube: A conserved function of Hox genes in Drosophila and vertebrates? Trends Cardiovasc. Med. 13: 182–187.

Lockhart M., Wirrig E., Phelps A., Wessells A., 2011 Extracellular Matrix and Heart Development. Birth Defects Res A Clin Mol Teratol 91: 535–550.

Mark D. Adams, Susan E. Celniker, Robert A. Holt, Cheryl A. Evans J. D. G., Peter G. Amanatides, Steven E. Scherer, Peter W. Li, Roger A. Hoskins, Richard F. Galle, Reed A. George, Suzanna E. Lewis, Stephen Richards, Michael Ashburner, Scott N. Henderson G. G. S., Jennifer R. Wortman, Mark D. Yandell, Qing Zhang, Lin X. Chen, Rhonda C. Brandon, Yu-Hui C. Rogers, Robert G. Blazej, Mark Champe, Barret D. Pfeiffer, Kenneth H. Wan, Clare Doyle, Evan G. Baxter, Gregg Helt, Catherine R. Nelson, George L. Gabor Miklos, Jo J. B., Leyla Bayraktaroglu, Ellen M. Beasley, Karen Y. Beeson, P. V. Benos, Benjamin P. Berman, Deepali Bhandari, Slava Bolshakov, Dana Borkova, Michael R. Botchan, John Bouck, Peter Brokstein, Phillipe Brottier, Kenneth C. Burtis, Dana A. Busam, Heather Butler, K. D., Lisa E. Doup, Michael Downes, Shannon Dugan-Rocha, Boris C. Dunkov, Patrick Dunn, Kenneth J. Durbin, Carlos C. Evangelista, Concepcion Ferraz, Steven Ferriera, Wolfgang Fleischmann, Carl Fosler, Andrei E. Gabrielian, Neha S. Garg, William M. Gelbart, Ken F. G., *et al.*, 2000 The genome sequence of Drosophila melanogaster. Science (80-.). 287: 2185—2195.

Martinek N., Shahab J., Saathoff M., Ringuette M., 2008 Haemocyte-derived SPARC is required for collagen-IV-dependent stability of basal laminae in Drosophila embryos.

J. Cell Sci. 121: 1671–1680.

Matveev L. A., Zaitsev V. Y., Gelikonov G. V, Matveyev A. L., Moiseev A. A., *et al.*, 2015 Hybrid M-mode-like OCT imaging of three-dimensional microvasculature in vivo using reference-free processing of complex valued B-scans. Opt. Lett. 40: 1472–1475.

Medioni C., Noselli S., 2005 Dynamics of the basement membrane in invasive epithelial clusters in Drosophila. Development 132: 3069–77.

Medioni C., Sénatore S., Salmand P. A., Lalevée N., Perrin L., *et al.*, 2009 The fabulous destiny of the Drosophila heart. Curr. Opin. Genet. Dev. 19: 518–525.

Meyer H., Panz M., Albrecht S., Drechsler M., Wang S., *et al.*, 2011 Drosophila metalloproteases in development and differentiation: The role of ADAM proteins and their relatives. Eur. J. Cell Biol. 90: 770–778.

Miller C. M., Page-McCaw A., Broihier H. T., 2008 Matrix metalloproteinases promote motor axon fasciculation in the Drosophila embryo. Development 135: 95–109.

Molina M. R., Cripps R. M., 2001 Ostia, the inflow tracts of the Drosophila heart, develop from a genetically distinct subset of cardial cells. Mech. Dev. 109: 51–59.

Myllyharju J., Kivirikko K. I., 2004 Collagens, modifying enzymes and their mutations in humans, flies and worms. Trends Genet. 20: 33–43.

Na J., Musselman L. P., Pendse J., Baranski T. J., Bodmer R., *et al.*, 2013 A Drosophila Model of High Sugar Diet-Induced Cardiomyopathy. PLoS Genet. 9.

Nagase H., Visse R., Murphy G., 2006 Structure and function of matrix metalloproteinases and TIMPs. Cardiovasc. Res. 69: 562–573.

Nienhaus U., Aegerter-Wilmsen T., Aegerter C. M., 2012 In-Vivo Imaging of the Drosophila Wing Imaginal Disc over Time: Novel Insights on Growth and Boundary Formation. PLoS One 7: e47594.

Nishimura M., Ocorr K., Bodmer R., Cartry J., 2011 Drosophila as a model to study cardiac aging. Exp. Gerontol. 46: 326–330.

Nishimura M., Kumsta C., Kaushik G., Diop S. B., Ding Y., *et al.*, 2014 A dual role for integrin-linked kinase and β1-integrin in modulating cardiac aging. Aging Cell 13: 431–440.

Ocorr K., Perrin L., Lim H.-Y. Y., Qian L., Wu X., *et al.*, 2007 Genetic control of heart function and aging in Drosophila. Trends Cardiovasc Med 17: 177–182.

Oh J., Takahashi R., Kondo S., Mizoguchi A., Adachi E., *et al.*, 2001 The membrane-

anchored MMP inhibitor RECK is a key regulator of extracellular matrix integrity and angiogenesis. Cell 107: 789–800.

Page-McCaw A., Serano J., Santé J. M., Rubin G. M., 2003 Drosophila matrix metalloproteinases are required for tissue remodeling, but not embryonic development. Dev. Cell 4: 95–106.

Page-McCaw A., Ewald A. J., Werb Z., 2007 Matrix metalloproteinases and the regulation of tissue remodelling. Nat. Rev. Mol. Cell Biol. 8: 221–233.

Pastor-Pareja J. C., Wu M., Xu T., 2008 An innate immune response of blood cells to tumors and tissue damage in Drosophila. Dis. Model. Mech. 1: 144–154.

Pastor-Pareja J. C., Xu T., 2011 Shaping Cells and Organs in Drosophila by Opposing Roles of Fat Body-Secreted Collagen IV and Perlecan. Dev. Cell 21: 245–256.

Paternostro G., Vignola C., Bartsch D., Omens J. H., D A., *et al.*, 2001 Integrative Physiology Age-Associated Cardiac Dysfunction in Drosophila melanogaster. Circ. Res.: 1053–1058.

Pelouch V., Dixon I. M., Golfman L., Beamish R. E., Dhalla N. S., 1993 Role of extracellular matrix proteins in heart function. Mol. Cell. Biochem. 129: 101–20.

Qian L., Liu J., Bodmer R., 2005 Slit and Robo control cardiac cell polarity and morphogenesis. Curr. Biol. 15: 2271–2278.

Raza Q., 2015 Collective Cell Migration During Heart Morphogenesis in Drosophila Requires Guidance Signaling and Extracellular Matrix Remodelling. PhD Thesis, McMaster Univ.

Raza Q., Jacobs J. R., 2016 Guidance signalling regulates leading edge behaviour during collective cell migration of cardiac cells in Drosophila. Dev. Biol. 419: 285–297.

Raza Q. S., Vanderploeg J. L., Jacobs J. R., 2017 Matrix Metalloproteinases are required for membrane motility and lumenogenesis during Drosophila heart development. PLoS One 12.

Reim I., Frasch M., 2005 The Dorsocross T-box genes are key components of the regulatory network controlling early cardiogenesis in Drosophila. Development 132: 4911–4925.

Rodriguez A., Zhou Z., Tang M. L., Meller S., Chen J., *et al.*, 1996 Immune System and Response Genes,. Genetics 143: 929–940.

Samakovlis C., Hacohen N., Manning G., Sutherland D. C., Guillemin K., *et al.*, 1996 Development of the Drosophila tracheal system occurs by a series of morphologically

distinct but genetically coupled branching events. Development 122: 1395–1407.

Santiago-Martínez E., Soplop N. H., Patel R., Kramer S. G., 2008 Repulsion by Slit and Roundabout prevents Shotgun/E-cadherin-mediated cell adhesion during Drosophila heart tube lumen formation. J. Cell Biol. 182: 241–248.

Segura A. M., Frazier O. H., Buja L. M., 2014 Fibrosis and heart failure. Heart Fail. Rev. 19: 173–185.

Sellin J., Albrecht S., Kölsch V., Paululat A., 2006 Dynamics of heart differentiation, visualized utilizing heart enhancer elements of the Drosophila melanogaster bHLH transcription factor Hand. Gene Expr. Patterns 6: 360–375.

Sessions A. O., Engler A. J., 2016 Mechanical Regulation of Cardiac Aging in Model Systems. Circ. Res. 118: 1553–1562.

Sessions A. O., Kaushik G., Parker S., Raedschelders K., Bodmer R., *et al.*, 2017 Extracellular matrix downregulation in the Drosophila heart preserves contractile function and improves lifespan. Matrix Biol. 62: 15–27.

Shah A. P., Nongthomba U., Kelly Tanaka K. K., Denton M. L. B., Meadows S. M., *et al.*, 2011 Cardiac remodeling in Drosophila arises from changes in actin gene expression and from a contribution of lymph gland-like cells to the heart musculature. Mech. Dev. 128: 222–233.

Snoek-van Beurden P. A., den Hoff J. W. Von, 2005 Zymographic techniques for the analysis of matrix metalloproteinases and their inhibitors. Biotechniques 38: 73–83.

Spinale F. G., 2002 Matrix metalloproteinases: Regulation and dysregulation in the failing heart. Circ. Res. 90: 520–530.

Srivastava A., Pastor-Pareja J. C., Igaki T., Pagliarini R., Xu T., 2007 Basement membrane remodeling is essential for Drosophila disc eversion and tumor invasion. Proc. Natl. Acad. Sci. U. S. A. 104: 2721–6.

Stamenkovic I., 2003 Extracellular matrix remodelling: The role of matrix metalloproteinases. J. Pathol. 200: 448–464.

Stark K. A., Yee G. H., Roote C. E., Williams E. L., Zusman S., *et al.*, 1997 A novel alpha integrin subunit associates with betaPS and functions in tissue morphogenesis and movement during Drosophila development. Development 124: 4583–94.

Sternlicht M., Werb Z., 2009 How Matrix metalloproteinases regulate cell behavior. Annu REv Cell Biol: 463–516.

Streuli C., 1999 Extracellular matrix remodelling and cellular differentiation. Curr. Opin.

Cell Biol. 11: 634–640.

Suster M. L., Seugnet L., Bate M., Sokolowski M. B., 2004 Refining GAL4-driven transgene expression in Drosophila with a GAL80 enhancer-trap. Genesis 39: 240–245.

Tao Y., Schulz R. A., 2007 Heart development in Drosophila. Semin. Cell Dev. Biol. 18: 3–15.

Tögel M., Meyer H., Lehmacher C., Heinisch J. J., Pass G., *et al.*, 2013 The bHLH transcription factor hand is required for proper wing heart formation in Drosophila. Dev. Biol. 381: 446–459.

Urbano J. M., Torgler C. N., Molnar C., Tepass U., Lopez-Varea A., *et al.*, 2009 Drosophila laminins act as key regulators of basement membrane assembly and morphogenesis. Development 136: 4165–4176.

Valle Rodríguez A. del, Didiano D., Desplan C., 2011 Power tools for gene expression and clonal analysis in Drosophila. Nat. Methods 9: 47–55.

Vanderploeg J., Vazquez Paz L. L., MacMullin A., Jacobs J. R., 2012 Integrins are required for cardioblast polarisation in Drosophila. BMC Dev. Biol. 12: 8.

Vaughan L., Marley R., Miellet S., Hartley P. S., 2017 The impact of SPARC on age-related cardiac dysfunction and fibrosis in Drosophila. Exp. Gerontol.: Under Review.

Visse R., Nagase H., 2003 Matrix metalloproteinases and tissue inhibitors of metalloproteinases: Structure, function, and biochemistry. Circ. Res. 92: 827–839.

Volk T., Wang S., Rotstein B., Paululat A., 2014 Matricellular proteins in development: Perspectives from the Drosophila heart. Matrix Biol. 37: 162–166.

Wart H. E. Van, Birkedal-Hansen H., 1990 The cysteine switch: a principle of regulation of metalloproteinase activity with potential applicability to the entire matrix metalloproteinase gene family. Proc. Natl. Acad. Sci. U. S. A. 87: 5578–5582.

Weavers H., Prieto-Sánchez S., Grawe F., Garcia-López A., Artero R., *et al.*, 2009 The insect nephrocyte is a podocyte-like cell with a filtration slit diaphragm. Nature 457: 322–326.

Wei S., Xie Z., Filenova E., Brew K., 2003 Drosophila TIMP Is a Potent Inhibitor of MMPs and TACE: Similarities in Structure and Function to TIMP-3. Biochemistry 42: 12200–12207.

Wolfstetter G., Holz A., 2012 The role of LamininB2 (LanB2) during mesoderm differentiation in Drosophila. Cell. Mol. Life Sci. 69: 267–282.

Yamamoto K., Murphy G., Troeberg L., 2015 Extracellular regulation of metalloproteinases. Matrix Biol. 44–46: 255–263.

Yarnitzky T., Volk T., 1995 Laminin is required for heart, somatic muscles, and gut development in the Drosophila embryo. Dev. Biol. 169: 609–18.

Yurchenco P. D., Lu P., Takai K., Weaver V. M., Hynes R. O., *et al.*, 2012 Basement Membranes : Cell Scaffoldings and Signaling Platforms. : 1–28.

Zang Y., Wan M., Liu M., Ke H., Ma S., *et al.*, 2015 Plasma membrane overgrowth causes fibrotic collagen accumulation and immune activation in Drosophila adipocytes. Elife 4: 1–23.

Zhou Y., Chan K. K. H., Lai T., Tang S., 2013 Characterizing refractive index and thickness of biological tissues using combined multiphoton microscopy and optical coherence tomography. Biomed. Opt. Express 4: 38.

Appendix A: Supplementary Figures

Genotype	Temperature (Degrees C)	Embryos Hatched	*n*	Survival to EL3	Survival to LL3	Survival to Pupariation	Survival to Adulthood
+/+	25	90/90	90	93%	87%	87%	82%
mmp1^{Q112}/+	25	92/93	92	99%	96%	96%	96%
mmp1^{Q112}/ mmp1^{Q112}	25	72/73	72	64%	25%	16%	0%
mmp2^{W307}/+	25	102/102	102	92%	89%	89%	61%
mmp2^{W307}/ mmp2^{W307}	25	82/89	82	87%	84%	79%	0%
vkg-GFP/+	29	129/129	129	95%	91%	91%	87%
	18	65/65	65	89%	83%	83%	80%
UAS-TIMP/+	29	129/130	129	97%	88%	87%	79%
	29 to 18	N/A	54	80%	78%	78%	44%
	18 to 29	N/A	119	93%	84%	83%	46%
	18	99/100	99	95%	80%	80%	73%
UAS-TIMP/HandGal4	29	92/94	92	92%	87%	86%	77%
UAS-TIMP/daGal80	29	94/96	94	84%	59%	27%	1%
	29 to 18	N/A	94	43%	38%	37%	32%
	18 to 29	N/A	109	78%	51%	32%	0%
	18	45/46	45	93%	91%	87%	82%
mmp2RNAi II/+	29	34/35	87	97%	89%	83%	83%
	18 to 29	N/A	107	90%	87%	85%	80%
	18	N/A	90	81%	73%	73%	62%
mmp2RNAi II/HandGal4	29	64/64	73	86%	85%	85%	79%
mmp2RNAi II/daGal80	29	115/116	115	64%	39%	23%	3%
	29 to 18	N/A	63	78%	60%	59%	37%
	18 to 29	N/A	94	88%	87%	85%	0%
	18	113/120	113	83%	76%	75%	72%
mmp2RNAi III/+	29	N/A	60	93%	90%	88%	88%
mmp2RNAi III/daGal80	29	N/A	74	88%	84%	82%	12%
UAS-mmp2/+	29	65/65	90	91%	86%	84%	83%
	18	118/118	90	93%	89%	88%	83%
UAS-mmp2/HandGal4	29	38/40	68	32%	5%	1%	0%
UAS-mmp2/daGal80	29	22/109	22	0%	0%	0%	0%
	18 to 29	N/A	54	0%	0%	0%	0%
	18	N/A	75	85%	79%	77%	63%

Figure S1: Loss of MMP function results in larval and pupal lethality but not embryonic lethality. Amongst *mmp* mutants, embryonic lethality is not more than 7.8% for any genotype. Embryonic survivorship is lowest for homozygous *mmp2* mutants at 92.12% (*n*=89 with 7 dead eggs). Homozygous *mmp1* mutants show a hatching success of 98.6% (*n*=73 with one dead egg), compared to 100% for the wildtype (*n*=90). Embryonic lethality is low amongst specimens over-expressing *Timp* or expressing *Mmp2* dsRNA, and hatching success is not affected by temperature. Embryonic over-expression of *Mmp2* does not affect hatching success when constrained to cardiac cells. However, ubiquitous over-expression of *Mmp2* is correlated with a severe drop in embryonic survivorship (22% of embryos successfully hatch). Percent survival to each larval stage is measured by comparison to the number of hatched individuals. EL3: Early third instar larva; LL3: late third instar larva.

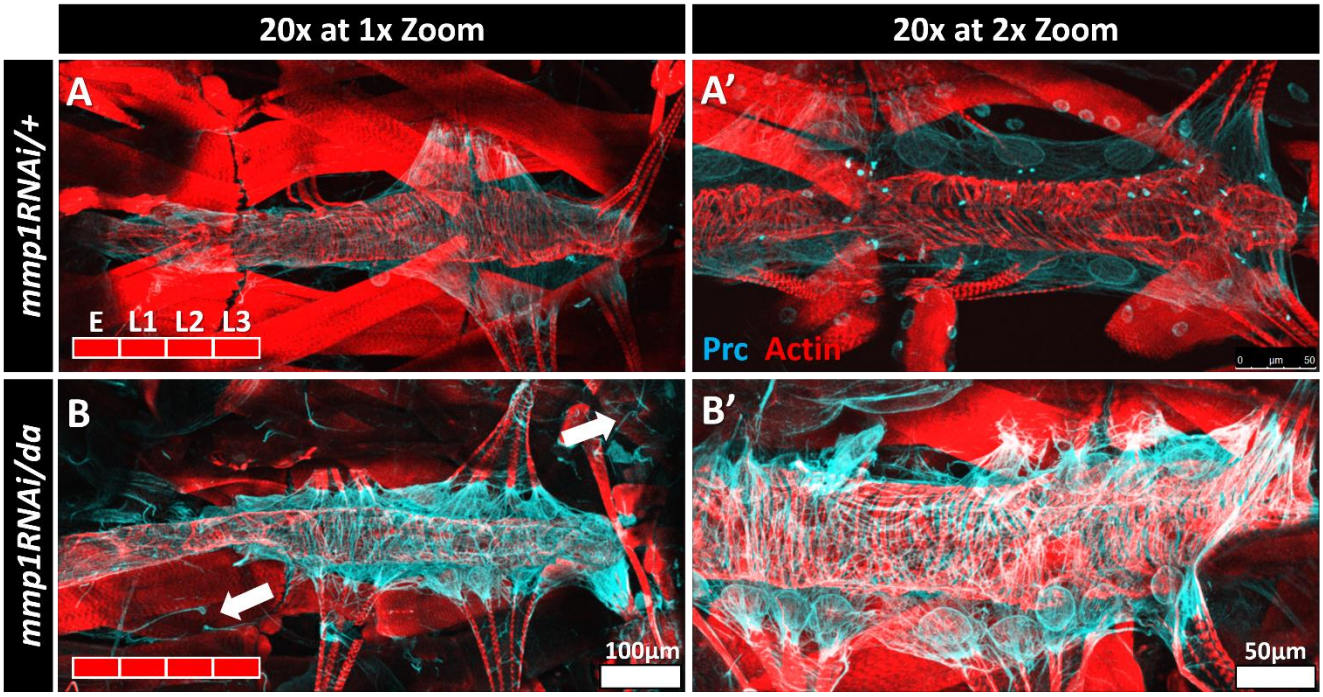

Figure S2: Ubiquitous reduction of *Mmp1* does not result in aberrant cardiac structure but does correlate with ectopic Pericardin in early third instar larvae. DV segments A6 and A7. **(A-A')** Late early instar dsRNA controls reared at 29°C have a uniform network of Prc bundles, though a small number of ectopic fibres are present beyond the heart perimeter. Myofibrils are circumferentially arrayed in parallel along the length of the vessel. **(B-B')** Ubiquitous expression of *Mmp1* dsRNA with *daGal4* throughout embryonic and larval development does not result in conspicuous morphological defects. Ectopic Prc fibres are visible beyond the DV perimeter (arrows) and signal intensity appears elevated.

Genotype	L3 Stage	Temperature (Degrees C)	*n*	# w/ Cardia Bifida	# w/ Incomplete Vessel
UAS-TIMP/+	Early	29	19	0	0
	Late	29	19	0	0
UAS-TIMP/Hand	Early	29	15	0	1
	Late	29	35	1	7
	Late	29 to 18	9	3	1
	Late	18 to 29	12	0	2
	Late	18	8	0	0
UAS-TIMP/R4	Late	29	20	0	0
UAS-TIMP/da	Early	29	20	4	12
	Early	29 to 18	7	2	2
	Early	18 to 29	25	0	4
	Early	18	22	0	4*
	Late	29	26	2	6
	Late	29 to 18	13	4	10
	Late	18 to 29	24	0	6
	Late	18	15	0	2
mmp1RNAi/+	Early	29	8	0	0
mmp1RNAi/da	Early	29	10	0	0
mmp2RNAi II/+	Early	29	10	0	1
	Late	29	13	0	0
mmp2RNAi II/Hand	Late	29	29	4	5
mmp2RNAi II/da	Late	29	26	0	0
	Late	18 to 29	22	0	2
	Late	18	8	0	0

Figure S3: Penetrance of aberrant cardiac morphology in larvae over-expressing *Timp* or expressing *Mmp2* dsRNA. Cardiac morphology is analysed by cross-section along DV segments A6 and A7. Larvae are considered to exhibit cardia bifida if an extracellular gap is observed between the divergent vessels. Torn or incomplete lumens correspond to lumenal cavities that are not completely enclosed along a portion of the vessel length. Features are not mutually exclusive and larvae may exhibit one or all of the listed abnormalities. Each abnormality is scored only once per individual. Asterisks denote that the observed aberration is likely the result of damage incurred during dissection or handling.

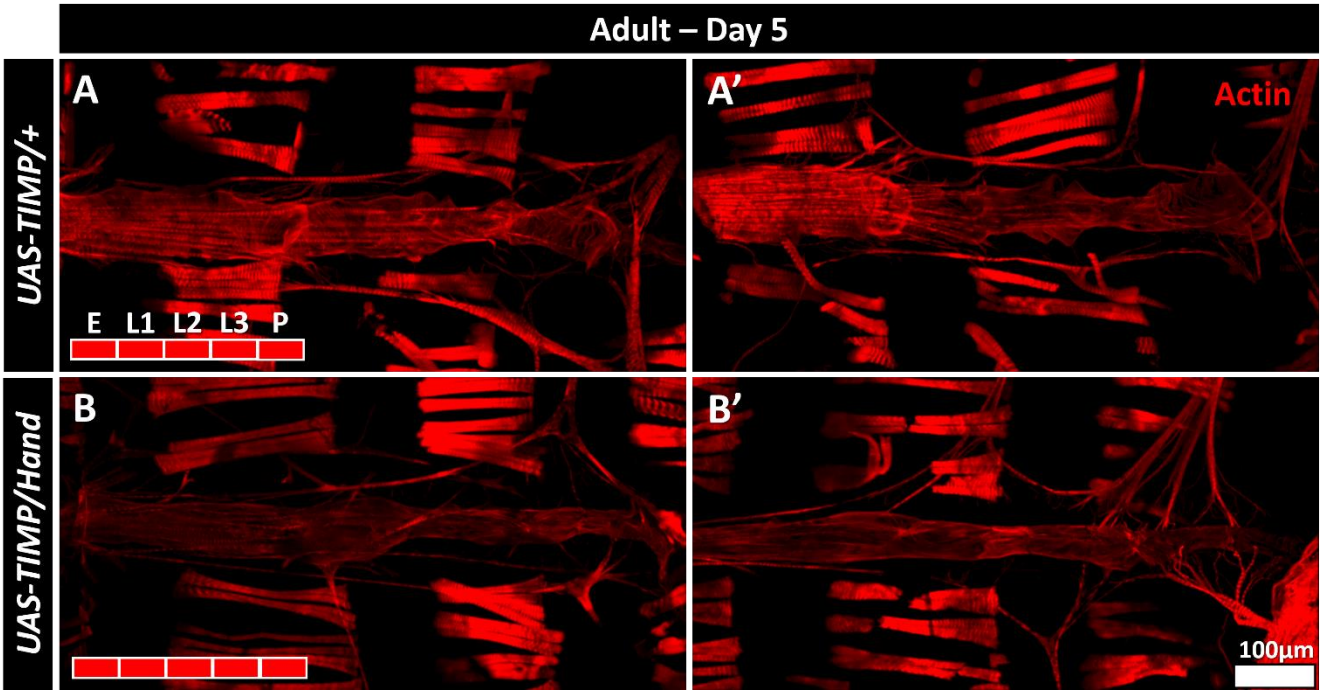

Figure S4: Localised over-expression of *Timp* within cardiac cells does not result in a discernible cardiac phenotype amongst surviving adults. DV segments A4 and A5 **(A-A')** Two five-day-old adult *UAS-TIMP* controls reared at 29°C. Myofibrils are longitudinally arrayed along the ventral side of the vessel. Alary muscles also show longitudinal arrangement along the vessel between primary sites of attachment **(B-B')** Over-expression of *Timp* in cardiac cells with *HandGal4* throughout embryonic and larval development does not result in conspicuous defects; arrangement of Actin myofibrils and alary muscles are not different from controls.

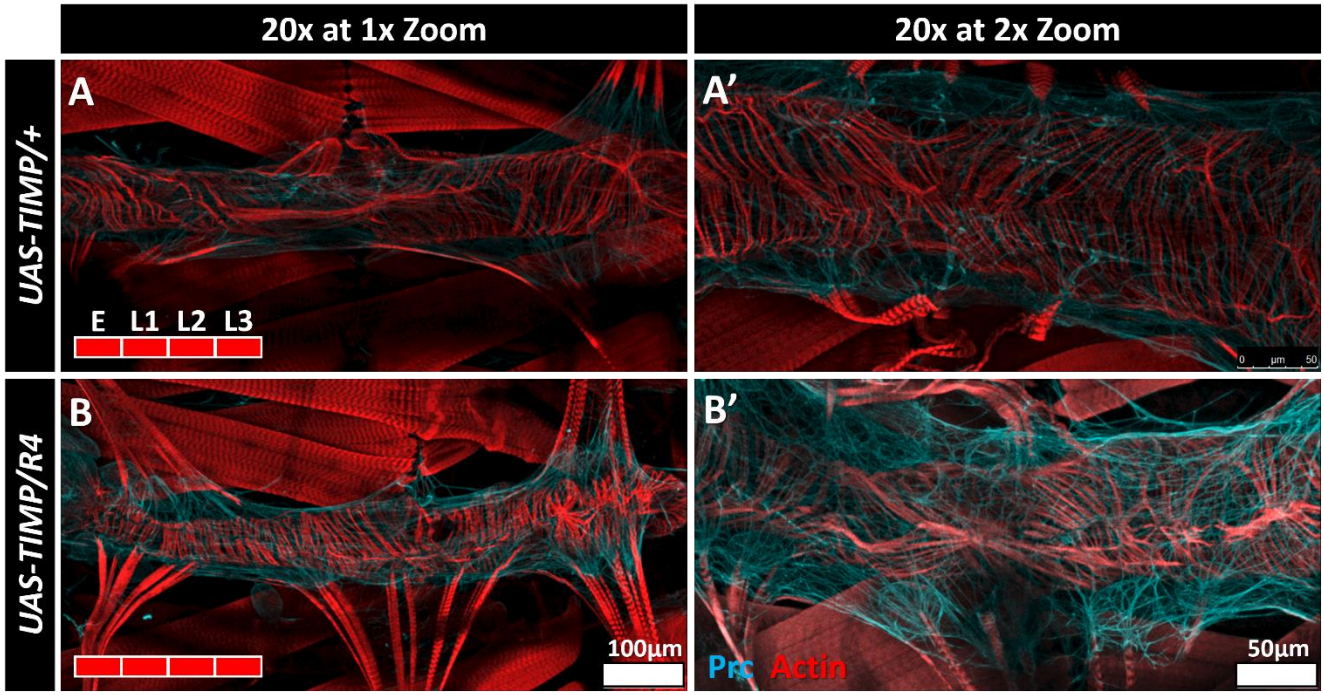

Figure S5: Localised over-expression of *Timp* in the fat body does not result in a discernible cardiac phenotype in late third instar larvae. DV segments A6 and A7. **(A-A')** Late third instar *UAS-TIMP* controls reared at 29°C have a uniform network of Prc bundles, though a small number of ectopic fibres are present beyond the heart perimeter. Myofibrils are circumferentially arrayed in parallel along the length of the vessel. **(B-B')** Over-expression of *Timp* in the fat body with *R4Gal4* throughout embryonic and larval development does not result in conspicuous defects; Actin myofibrils and Prc networks are not obviously different from controls.

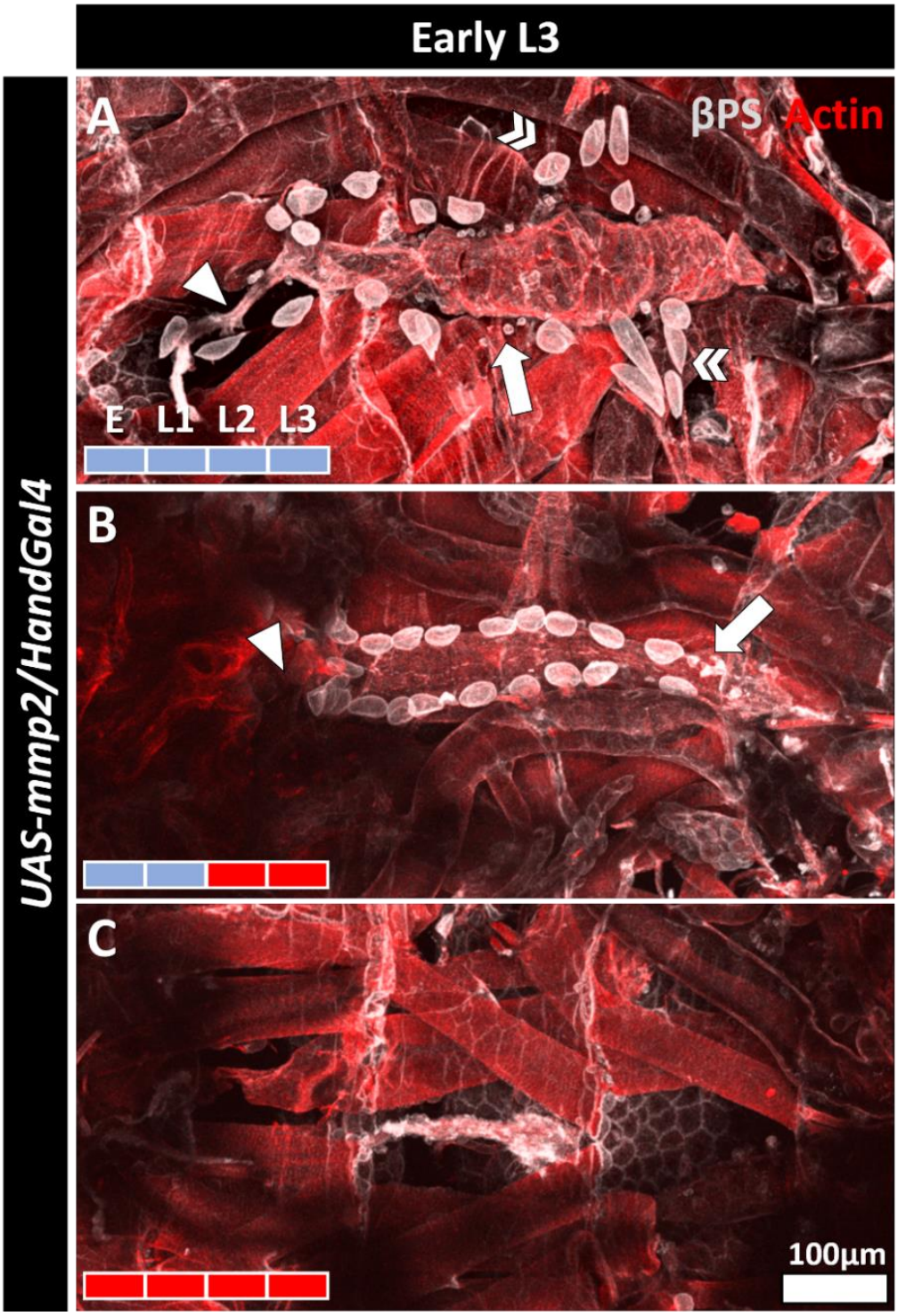
Early L3
UAS-mmp2/HandGal4
A
βPS Actin
E L1 L2 L3
B
C
100µm

Figure S6: Localised over-expression of *Mmp2* in the heart results in aortal defects and the loss of pericardial cells. DV segments A6 and A7. Monoclonal βPS antibody (**grey**) is used to visualise Integrin. βPS intensity is manipulated to ease viewing. Conjugated Phalloidin (**red**) is used to visualise the dorsal vessel muscle fibres. **(A-C)** Early third instar larvae with reduced or full expression of *UAS-MMP2* in cardiac cells under the control of the *HandGal4* driver. **(A)** Dampened over-expression of MMP2 throughout embryonic and larval development (18°C). Third instar larvae show only a remnant of the aorta that is anteriorly detached (arrowhead). Pericardial cells (PCs) are still present, although some loss in numbers is observed. PCs are surrounded by smaller cells that may be hemocytes (arrow). In some instances, alary muscles and associated PCs are tearing away from the vessel (double chevrons) **(B)** Dampened over-expression of MMP2 throughout embryogenesis (18 to 29°C). Third instar larvae resemble those raised entirely at 18°C. **(C)** Over-expression of MMP2 throughout embryonic and larval development (29°C). The DV of third instar larvae is reduced and lacks an aorta. No alary muscles or PCs are evident at the perimeter of the vessel.